Functional characterization of the microRNA-26 family in zebrafish neurogenesis

Dissertation zur Erlangung des naturwissenschaftlichen Doktorgrades
der
Julius-Maximilians-Universität Würzburg

vorgelegt von
Holger Dill

aus Hammelburg

Würzburg 2012

Eingereicht bei der Fakultät für Chemie
und Pharmazie am:

Gutachter der schriftlichen Arbeit:
1.Gutachter: Prof. Dr. U. Fischer
2. Gutachter: Prof. Dr. Dr. M. Schartl

Prüfer des öffentlichen Promotionskolloquiums:
1. Prüfer: Prof. Dr. U. Fischer
2. Prüfer: Prof. Dr. Dr. M. Schartl
3. Prüfer: Prof. Dr. A. Buchberger

Datum des öffentlichen Promotionskolloquiums:

Doktorurkunde ausgehändigt am:

Diese Dissertation wurde in der Arbeitsgruppe von Prof. Dr. U. Fischer am Institute für Biochemie der Julius-Maximilians-Universität Würzburg angefertigt.

CONTENTS

Figures

Tables

1 SUMMARY

Formation oft the central nervous system (CNS) from multipotent neuronal stem cells (NSCs) requires a tightly controlled, step-wise activation of the neuronal gene expression program. Expression of neuronal genes at the transition from neural stem cell to mature neuron (i. e. neuronal cell differentiation) is controlled by the Repressor element 1 (RE1) silencing transcription factor (REST) complex. As a master transcriptional regulator, the REST-complex specifically inhibits expression of neuronal genes in non-neuronal tissues and neuronal progenitor cells.
Differentiation of NSCs to mature neurons requires the activation of genes controlled by the REST-complex, but how abrogation of REST-complex mediated repression is achieved during neurogenesis is only poorly understood.
MicroRNAs (miRNAs) are a class of small regulatory RNAs that posttranscriptionally control target gene expression. Binding of miRNAs to target sequences in the 3'UTR of mRNAs, leads either to degradation or translational inhibition of the mRNA. Distinct neuronal miRNAs (e.g. miR-124) were shown to modulate REST-complex activity by silencing expression of REST-complex components. Interestingly, these miRNAs are also under transcriptional control of the REST-complex and inactivation of the REST-complex precedes their expression. Hence, additional factors are required for derepression of neuronal genes at the onset of neurogenesis.
In this study function of the miR-26 family during neurogenesis of the zebrafish (*Danio rerio*) was analyzed. Computational target prediction revealed a number of REST-complex components as putative miR-26 targets. One of these predicted target genes, the C-terminal domain small phosphatase 2 (Ctdsp2) was validated as an *in vivo* target for miR-26b. Ctdsps are important cofactors of REST and suppress neuronal gene expression by dephosphorylating the C-terminal domain (CTD) of RNA polymerase II (Pol II). Interestingly, miR-26b is encoded in an intron of the *ctdsp2* primary transcript and is cotranscribed together with its host gene. Hence, miR-26b modulates expression of its host gene ctdsp2 in an intrinsic negative autoregulatory loop. This negative autoregulatory loop is inactive in NSCs because miR-26b biogenesis is inhibited at the precursor level. Generation of mature miR-26b is activated during neurogenesis, where it suppresses Ctdsp2 protein expression and is required for neuronal cell differentiation *in vivo*. Strikingly, miR-26b is expressed prior to miR-124 during neuronal cell differentiation. Thus, it is reasonable to speculate about a function of miR-26b in early events of neurogenesis. In line with this assumption, knockdown of miR-26b in zebrafish embryos results in downregulation of REST-complex controlled neuronal genes and a block in neuronal cell differentiation, most likely due to aberrant regulation of Ctdsp2 expression. This is evident by reduced numbers of secondary motor neurons compared to control siblings. In contrast, motor neuron progenitor cells and glia cells were not affected by depletion of miR-26b.This study identifies the *ctdsp2*/miR-26b autoregulatory loop as the first experimentally validated interaction between an intronic miRNA and its host gene transcript. Silencing of *ctdsp2* by miR-26b in neurons is possible because biogenesis of the *ctdsp2* mRNA and mature mir-26b is uncoupled at the posttranscriptional level. Furthermore the obtained data indicate a cell type specific role for miR-26b in vertebrate neurogenesis and CNS development.

2 ZUSAMMENFASSUNG

Die Entwicklung des Zentralen Nervensystems (ZNS) aus multipotenten neuronalen Stammzellen erfordert eine stufenweise und genau regulierte Aktivierung der neuronalen Genexpression. Bei der Differenzierung neuronaler Stammzellen zu Neuronen wird die Expression neuronaler Gene durch den sogenannten „Repressor element 1 (RE1) silencing transcription factor (REST)"-Komplex gesteuert. Der REST-Komplex unterdrückt spezifisch in proliferierenden neuronalen Vorläuferzellen die Expression neuronaler Gene. Während der neuronalen Zelldifferenzierung wird die Expression dieser Gene jedoch benötigt. Wie die Inaktivierung neuronaler Gene durch den REST-Komplex während des Prozesses der Neurogenese aufgehoben wird ist bislang nicht genau bekannt.

MicroRNAs (miRNAs) sind kleine regulatorische RNAs, die die Expression ihrer Zielgene auf posttranskriptioneller Ebene regulieren. Dazu binden miRNAs an Zielsequenzen in 3'UTRs von mRNAs, was zu einer Inhibition der Translation oder Abbau der mRNA führt. Auch Komponenten des REST-Komplexes stehen unter Kontrolle bestimmter neuronaler miRNAs (z.B. miR-124). Erstaunlicherweise stehen diese miRNAs selber wiederum unter der transkriptionellen Inhibition des REST-Komplexes und können daher nicht für die Inaktivierung des REST-Komplexes zu Beginn der Neurogenese verantwortlich sein. Übereinstimmend damit konnte beobachtet werden, dass der REST-Komplex aus differenzierenden Zellen entfernt wird, bevor die genannten neuronalen miRNAs exprimiert werden. Diese Umstände legen die Existenz weiterer, bis jetzt unbekannter Faktoren nahe, die die Expression des REST-Komplexes selber inhibieren und so die Neurogenese erlauben

Im Rahmen dieser Dissertation wurde die Funktion der miR-26 Familie während der Neurogenese des Zebrafisches (*Danio rerio*) untersucht. Eine bioinformatische Zielgenvorhersage für die miR-26 Familie ergab, dass unter anderem zahlreiche bekannte Komponenten des REST-Komplexes unter den Kandidatengenen sind. Für eines dieser vorhergesagten Zielgene, die sogenannte „C-terminal domain small phosphatase 2 (Ctdsp2)" wurde daraufhin gezeigt, dass seine Expression in der Tat durch die miR-26b inhibiert wird. Ctdsps sind wichtige Kofaktoren des REST-Komplexes und unterdrücken die Expression neuronaler Gene, indem die die C-terminale Domäne (CTD) der RNA Polymerase II dephosphorylieren und diese dadurch inaktivieren. In diesem Zusammenhang von besonderer Bedeutung ist die Tatsache, dass die miR-26b in einem Intron des *ctdsp2* Gens kodiert ist und mit *ctdsp2* zusammen transkribiert wird. Folglich beeinflusst die miR-26b die Expression ihres eigenen „Host genes" in einer Art autoregulativer Rückkopplungsschleife. Die beschriebene negative Regulation ist in neuronalen Stammzellen nicht aktiv, da dort die Biogenese der miR-26b auf Vorläuferebene angehalten wird. Reife miR-26b wird erst während der Neurogenese produziert, wo sie daraufhin die Expression von Ctdsp2 Protein verhindert. Während der neuronalen Zelldifferenzierung wird die miR-26b deutlich früher exprimiert als zum Beispiel die miR-124. Daher liegt es nahe eine Funktion der miR-26b während früher Prozesse in der Neurogenese anzunehmen. In Übereinstimmung mit dieser Annahme führt ein „Knockdown" der miR-26b zu einer schwächeren Expression von neuronalen Genen, die unter der Kontrolle des REST-Komplex stehen. Weiterhin führt ein reduziertes Maß an miR-26b zu fehlerhafter oder gänzlich ausbleibender neuronaler

Zelldifferenzierung. Dies konnte anhand einer verringerten Anzahl differenzierter spinaler Motorneuronen aufgezeigt werden. Die Vorläufer dieser Motorneuronen und Gliazellen waren hingegen vom miR-26b-„Knockdown“ nicht beeinflusst.

Die hier präsentierte Studie zeigt erstmals in experimenteller Weise das Vorhandensein einer direkten Interaktion zwischen einer intronischen miRNA und ihrem eigenen Primärtranskript. Die negative Regulation der Ctdsp2 Expression in Neuronen wird erst dadurch möglich, dass die Biogenese der *ctdsp2* mRNA und der reifen miR-26b durch einen posttranskriptionellen Mechanismus voneinander getrennt werden. Weiterhin legen die Daten aus dieser Studie nahe, dass die miR-26b in der Tat eine spezifische Funktion in der Entwicklung des ZNS von Vertebraten hat.

3 INTRODUCTION

3.1 MicroRNAs

3.1.1 MicroRNA function

The central dogma of molecular biology is that genomic DNA is transcribed into messenger RNA (mRNA) which is exported to the cytoplasm and translated into proteins (Figure 1). Gene expression was assumed as being mainly controlled by the influence of transcriptional regulators on protein coding gene loci [1]. This view began to crumble with discovery of RNA interference (RNAi) [2] and the first microRNA (miRNA) lin-4, as a regulator of *Caenorhabditis elegans* developmental timing ([3] and [4]). MiRNAs turned out to be an evolutionary conserved species of short (~22 nucleotide; nt) non-coding RNAs, which posttranscriptionally silence protein synthesis from target genes (Figure 1). To repress target gene expression, miRNAs guide a ribonucleoprotein particle (RNP) with silencing activity, the so called miRNA induced silencing complex (miRISC), to 3'-untranslated regions (3'UTRs) of target transcripts (see 3.1.2 and Figure 2). As each individual miRNA has up to several hundreds of potential targets [5], discovery of miRNAs as gene regulatory molecules from plants, fungi, animals and even viruses opened up a new level of gene expression control ([6] and Figure 1).

Specific functions of distinct miRNAs could be shown in a number of developmental processes including early events like clearance of maternal mRNAs [7], gastrulation [8] or patterning of the anterior-posterior ([9] and [10]) and left-right body axis [11]. Furthermore target regulation by miRNAs is necessary for CNS formation ([8], [12] and [13]), development of skeletal muscles ([8] and [14]), the cardiovascular system ([8], [15], [16], [17] and [18]) and germline ([19] and [20]) or cell migration ([21] and [22]). Hence, it is predicted that many, probably all developmental processes require target silencing my miRNAs.

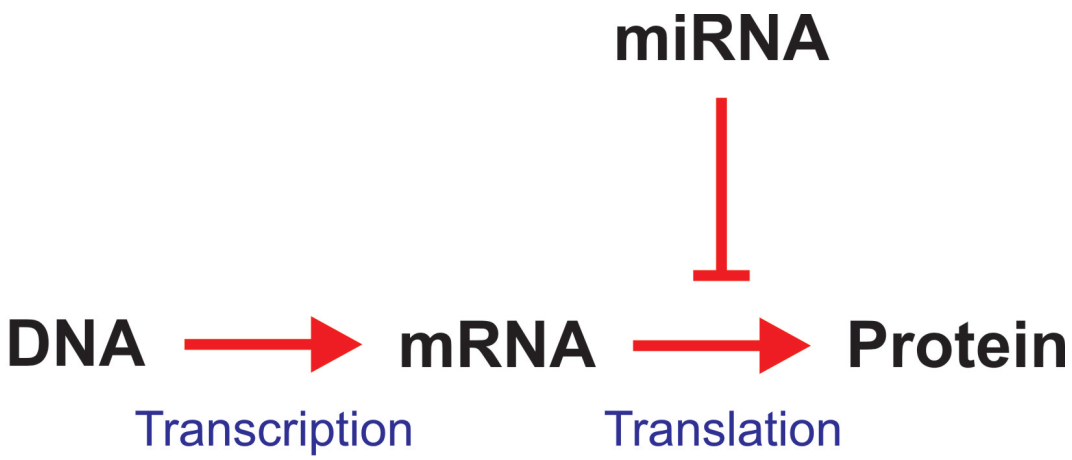

Figure 1: MiRNAs and the central dogma of molecular biology
The central dogma of classical molecular biology is that genes are transcribed into mRNA which is translated into proteins. MiRNAs inhibit protein synthesis from mRNAs and interrupt the flow of genetic information.

3.1.2 Mechanistic aspects of miRNA mediated target silencing

To silence target gene expression, miRNAs cooperate with a macromolecular complex, the miRISC (see 3.1.1). Although exact protein composition of the miRISC varies between different eukaryotic species and precise functions of most components within the miRISC are not fully understood, some factors are commonly found in purified miRISCs (Figure 2). For example, members of the Argonaute (Ago) protein family and GW182 seem to be core components of the miRISC and responsible for its silencing activity ([6], [23], [24] and [25]; Figure 2). MiRNAs guide the miRISC (see 3.1.1 and Figure 2) sequence specifically to target transcripts in order to downregulate target gene expression by two posttranscriptional effector mechanisms: mRNA cleavage and translational inhibition ([26]; Figure 2). The mode of miRNA action depends on miRNA/target-complementarity, as a high degree of complementarity leads to target mRNA cleavage, whereas miRNAs with low sequence complementarity block translation ([26]; Figure 2).

In case of target mRNA cleavage, the cleavage reaction is accomplished by Ago2 as endonucleolytic component of the miRISC [27]. During cleavage, the RISC loaded miRNA stays intact and is available for additional rounds of target silencing [26]. Thus, the mechanism of miRNA mediated target cleavage occurs in a way very similar to that of small interfering RNAs (siRNAs; [28]). In general, metazoan miRNAs pair imperfectly and thus act via translational repression rather than mRNA cleavage [26]. As target mRNA characteristics required for translational inhibition by the miRISC, a 7-methyl-guanine (m^7G) cap and the poly(A)-tail were identified ([25] and [29]). Interaction of the miRISC with a target mRNA interferes with ribosome recruitment and results in incorporation of miRNA and target mRNA into pseudo-polysomes [25]. Silenced mRNAs often localize to processing bodies (P-bodies) but whether localization to P-bodies is causal for inhibition of protein synthesis or is a consequence of the same remains unclear [30]. Inhibition of translation is often accompanied by deadenylation and consequently destabilization of target mRNA ([7] and [25]). For this, the miRISC interacts with the Poly(A)-binding protein (PABP) to recruit the deadenylase complex CAF1-CCR4-NOT1. This interaction is mediated by the miRISC component GW182. In this scenario deadenylation follows the initial step of cap-dependent translational repression and triggers degradation of the mRNA ([31] and [32]). Destabilization of poly(A)-lacking target mRNAs might secondarily contribute to the observed reduction of target mRNA levels by miRNAs. Another mechanism of miRNA mediated target mRNA degradation implicates decapping by the DCP1:DCP2 decapping complex ([33] and [34]).

In the past few years bioinformatical and biochemical studies have focused on the questions: (1) how miRNA target specificity is achieved and (2) what typical characteristics of an active miRNA target site are. Perfect complementarity of a target sequence and 5'-residues 2 – 8, the so called seed region, of miRNAs turned out to be predominantly responsible for target silencing ([26] and [35]). One explanation for the importance of the seed region for target recognition is that these nucleotides are conformationaly rearranged and presented to the target 3'UTR by the miRISC [36]. Base pairing of 3'-portions of the miRNA to its target can enhance specificity and target silencing. These so-called 3'-supplementary sites allow 3'-base pairing between nucleotides 13 – 16 of the miRNA and target mRNA sequences. [36]. Positioning of target sites within the mRNA have also been shown to have impact on biological activity. Most validated miRNA target sites are located within 3'UTRs, but also target

sites in open reading frames (ORFs) or 5'UTRs turned out to be functional [35]. Not all aspects of miRNA annealing to target mRNAs are fully understood and unmistakable characteristics to distinguish between functional and non-functional target sites without *in vivo* validation experiments are still missing. Nevertheless, miRNA target sites are under evolutionary pressure and therefore often conserved across species [36], a fact that underlines the importance of miRNA mediated gene expression control.

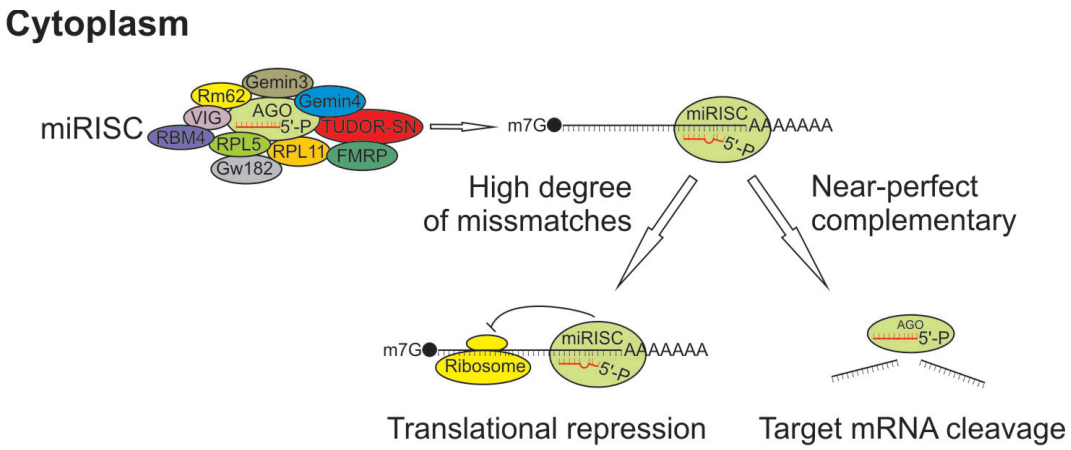

Figure 2: Mechanisms of miRNA target silencing.
Annealing of miRNAs to their corresponding mRNA targets leads to target cleavage or inhibition of translation depending on miRNA/target-3'UTR complementarity. Both, repression of protein synthesis and target degradation are conducted by the miRISC. Note that graphical arrangement of miRISC components does not represent validated protein interactions.

3.2 MicroRNA biogenesis

3.2.1 Genomic organisation of microRNA coding genes

Since the first miRNAs were identified, numbers of known miRNAs have tremendously increased ([37], [38] and [39]). 695 miRNAs were identified in the human, 145 in the *Caenorhabditis elegans*, 104 in the *Drosophila melanogaster* and 337 the *Danio rerio* genomes ([23], [26] and [40]). MiRNA precursor molecules can either be encoded intergenic, as independent transcriptional units, or within introns of protein coding genes. At least 25% of human miRNAs are intron encoded, preferentially in sense orientation with their harbouring host gene. Until recently, most sense orientated intronic miRNAs were thought to be coexpressed with their host genes. However, novel studies revealed independent promoter sequences for some intronic miRNAs, producing non-overlapping expression patterns of miRNA and host gene [41]. MiRNA primary transcripts (pri-miRNAs), derived from either spliced introns or independent transcription units, can contain one (monocistronic) or multiple (polycistronic) miRNA precursors. These precursors need to be extensively processed before they become functional miRNAs ([26]; see 3.2.2 and Figure 3).

3.2.2 The microRNA processing pathway

Most miRNA genes, irrespective if intronic or intergenic, are transcribed by RNA polymerase II (Pol II) resulting in 5'-capped and poly(A)-tailed transcripts ([42], [43] and [44]) with local hairpin structures. Mature miRNAs are processed from these longer pri-miRNAs in a stepwise and compartmentalized manner ([45] and Figure 3). The RNase III Drosha executes the initial step to produce a highly structured ~70 nt hairpin precursor microRNA (pre-miRNA; Figure 3). For this purpose, Drosha cooperates with Pasha (Partner of drosha) to build a complex called microprocessor. *Cis*-acting sequence elements within 20 nt upstream and 25 nt downstream from cleavage sites, including single stranded regions of the pri-miRNA and the stem loop, are required to specify Drosha cleavage sites ([46] and [47]). As a result of this processing step, the pri-miRNA is converted into a pre-miRNA, which contains a 2 nt overhang at its 3'-end, characteristic for RNase III mediated cleavage ([48] and [49]; Figure 3). An exceptional subclass of intronic miRNAs can overleap Drosha processing. These miRNAs are located within ultra short introns, called mirtrons. In this scenario, pre-mRNA splicing substitutes for Drosha cleavage [50]. Debranched mirtrons exhibit a pre-miRNA like secondary structure and directly serve as pre-miRNAs after splicing reaction ([23], [51] and [52]).

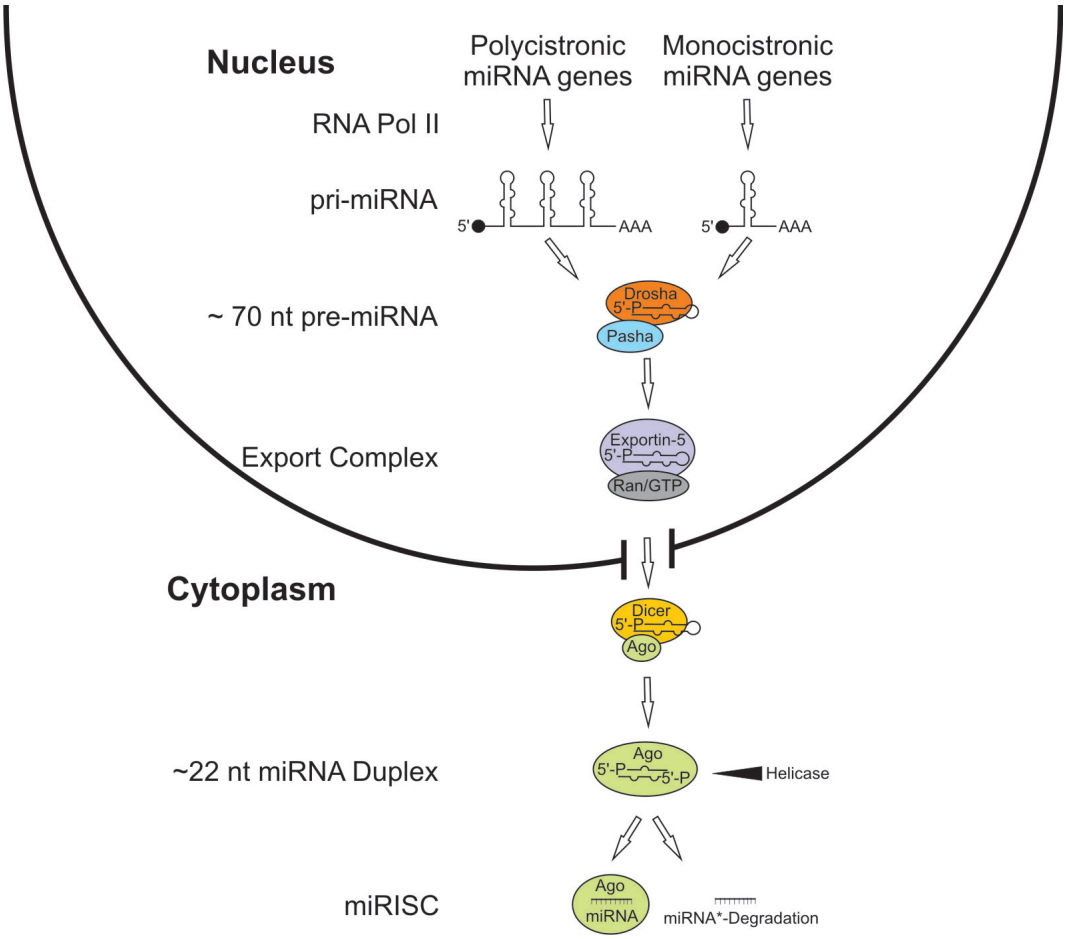

Figure 3: Canonical microRNA maturation pathway in animals.
Pri-miRNAs are transcribed by RNA-Polymerase II (RNA Pol II) in the cell nucleus. The canonical miRNA processing cascade includes RNase III cleavage of the precursor intermediates by Drosha and Dicer as well as nuclear export by Exportin-5. Mature miRNAs are incorporated into the miRNA induced silencing complex (miRISC).

All pre-miRNAs are exported from the nucleus by the Exportin-5/Ran guanosine triphosphate (RanGTP) complex for further processing [53]. In the cytoplasm, Dicer, another member of the RNase III family, converts pre-miRNAs into mature miRNA duplices [54]. In this processing step Dicer cuts the stem-loop pre-miRNAs about 22nt away from the bottom of the stem to remove the loop structure. So, 5'- and 3'-termini of pre-miRNAs predetermine one end of the mature miRNA and its antisense counterpart, the so called microRNA* or passenger strand ([26], [55] and [56]; Figure 3).

Dependent on thermodynamical features of the intermediate miRNA duplex, one strand is incorporated into the miRNA induced silencing complex (miRISC; Figure 3). The strand showing less tight base pairing at its 5'-end will be loaded onto the miRISC, whereas the miRNA* is degraded (Figure 3). In some rare cases, both miRNA strands are incorporated into the miRISC and hence can regulate individual targets ([57] and [58]). This asymmetric loading onto the miRISC is supported by a so far unknown RNA helicase (Figure 3) and depends on coordinated Dicing and Ago loading. Specific functions of miRNA sorting (loading of mature miRNA on one distinct Ago partner) are still elusive, but different Ago proteins show defined expression patterns, indicating tissue specific functions ([6] and [44]).

Maturation of miRNAs and Ago loading are therefore clearly separated from the miRISC-mediated targeting of mRNAs. The cytoplasmic steps of miRNA maturation and target regulation can consequently be divided into two distinct steps, which are Dicer processing/Ago loading and miRISC regulatory activity ([55] and [56]).

3.2.3 Posttranscriptional regulation of microRNA expression and function

Precise regulation of mature miRNA expression is crucial for proper cellular function. This regulation occurs not exclusively at the transcriptional level but also by modulation of pri- and pre-miRNA processing. Defects in the responsible regulatory networks can result in human diseases, for instance cancer ([23], [59] and [60]). All four cardinal steps in the miRNA processing cascade (see 3.2.2), Drosha cropping, nuclear export, Dicer processing and turnover of mature miRNAs are specifically regulated. The following posttranscriptional mechanisms appear to regulate miRNA abundance:

Drosha cleavage: Pri-mir-18a and pri-let-7a processing is influenced by the heterogeneous ribonucleoprotein particle A1 (hnRNPA1; [23], [61] and [62]). Whereas hnRNPA1 enhances Drosha processing of pri-mir-18a ([61] and [63]). It inhibits Drosha cleavage of pri-let-7a [62]. Both regulations depend on hnRNPA1 binding sites in the stem-loop structures of respective pri-miRNAs. This clearly shows how stem loop precursor sequences contribute to the regulation of miRNA maturation and that the same protein factor can regulate the processing of two distinct miRNAs in opposite ways (Figure 4).

MiRNA transport: MiRNA maturation is also regulated at the level of pre-miRNA export from the nucleus (Figure 4). Pre-mir-31, -mir-128, -mir-105 are retained in the nucleus of some cell types preventing cytoplasmic Dicer processing [23]. Transport of pre-miRNAs to the cytoplasm – and hence their maturation - is stimulated by DNA damage ([64] and [65]), but underlying molecular mechanisms are still poorly understood.

Dicer processing: Presumably, Dicer cleavage of pre-miRNAs is the most frequently regulated step in miRNA maturation. The RNA binding protein Lin-28 is implicated in suppression of let-7 biogenesis by interfering with

pre-let-7 Dicing ([23], [66] and [67]; Figure 4). To this end, Lin-28 acts in two biochemically distinct mechanisms. First, Lin-28 binds to pre-let-7, thus covering the Dicer cleavage site [67]. Second, Lin-28 recruits the Terminal uridyl transferase 4 (TUT4) to pre-let-7. Thereupon, TUT4 adds untemplated uridyl-residues to the 3'-end of pre-let-7, which efficiently inhibits Dicer processing (Figure 4). Both mechanisms specifically depend on conserved nucleotide motifs in the loop region of pre-let-7 [68]. In addition to the inhibitory Lin-28/TUT4-system, also Dicer-promoting factors were discovered. The KH-type splicing regulatory protein (KSRP) was identified as a component of the Dicer complex, indicating a function in miRNA maturation. KSRP directly interacts with human pre-let-7a and miR-26b to support Dicer processing of this particular miRNAs. High affinity binding of KSRP is mediated by G-stretches in the terminal loops of pre-miRNAs [69]. Together, above mentioned studies suggest the terminal loop of miRNA precursors (pri- or pre-miRNAs) as a platform for coordinating miRNA maturation.

MiRNA turnover: Mature miRNAs are biologically active in the cytoplasm (see 3.1.2 and 3.2.2) and silencing activity as well as stability of the miRNA is also regulated at this level (Figure 4). Untemplated elongation of mature miRNA 3'-ends appears to be a common instrument to accomplish negative as well as positive effects on miRNA function and stability. During inflammatory response, expression of cytokines has to be accurately regulated. In this process, miR-26b targets Interleukin-6 (*il-6*; [70]). Adding uridines to its 3'-end abrogates the potential of miR-26b to silence translation of *il-6* mRNA, whereas stability of mature miR-26b is not affected. Terminal uridylation of mature miR-26b is performed by TUT4 (Figure 4), the same nucleotidyltransferase which is responsible for inhibition of pre-let-7 Dicer processing ([68] and [70]). MiR-122 is 3'-mono-adenylated by the cytoplasmic poly(A) polymerase GLD-2 (Figure 4). Adenylation of miR-122 stabilizes its mature form and helps to maintain regulatory function of this particular miRNA [71]. In summary, 3'-adenylation stabilizes activity of mature miRNAs in the cytoplasm, in clear contrast to poly-uridylation. The findings mentioned above suggest regulation of miRNA turnover as another mechanism to modulate miRNA activity.

In summary, maturation and silencing activity of many miRNAs are posttranscriptionally regulated. Regulation of individual miRNAs seems to be achieved by the combined action of enzymatic factors like TUT4 with miRNA sequence specific adaptors like Lin-28 or KSRP. By modulating miRNA abundance in a cell type specific manner, these events might have strong impact on basic functions like cell differentiation or cell fate maintenance. As posttranscriptional regulation of miRNA expression seems to be a widespread phenomenon, it is tempting to speculate that there is a function for it in embryonic development and organogenesis.

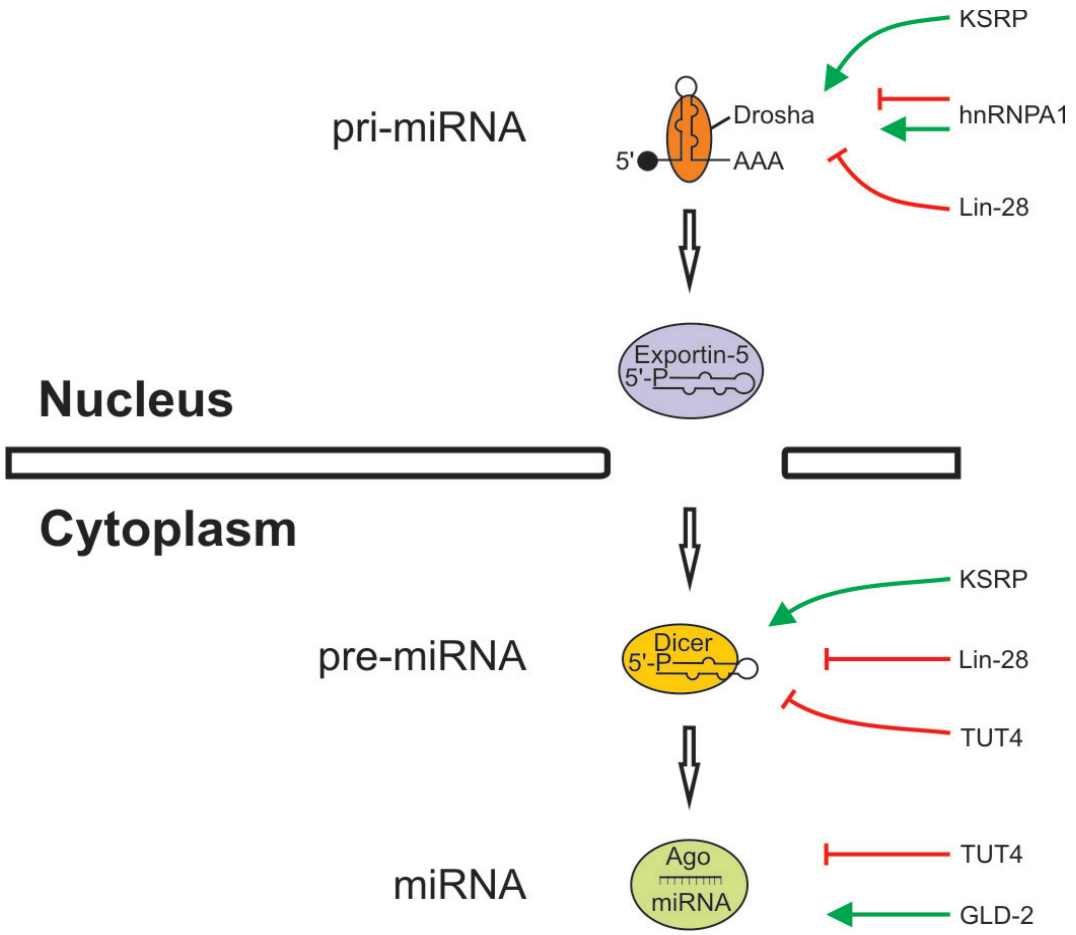

Figure 4: Posttranscriptional regulation of miRNA processing
MiRNA expression is controlled at the level of Drosha cropping, Dicer cleavage and function/stability in the cytoplasm. Production of intermediates can be stimulated (e.g. by KSRP) or inhibited (e.g. by Lin-28). Negative or positive regulatory function of other factors (e.g. hnRNPA1) depends on the particular stem loop structure. Regulatory factors are indicated at the right.

3.3 Zebrafish neural tube formation and neurogenesis

The process of vertebrate neurogenesis follows a generally accepted schedule: neural induction of the ectoderm followed by regionalization of the CNS, neurulation, and establishment of connections between neurons in the CNS and the peripheral nervous system (PNS; [72]). Zebrafish neurulation and neurogenesis is characteristic of teleosts. During gastrulation a cell layer termed epiblast is formed which will give rise to the neuroectoderm. Subsequently, the neural plate epithelium is induced by the BMP-antagonists *follistatin*, *noggin* and *chordin* and becomes distinguishable from the surrounding ectoderm by end of gastrulation. A massive neural keel is formed, which successively detaches from the surface and forms a central lumen to build the neural tube. By this stage, all major subdivisions of the CNS have emerged and first neurons became postmitotic. The neural tube is patterned along the anterior-posterior and dorso-ventral axis. Fibroblast Growth Factor (FGF), Bone Morphogenic Protein (BMP), Wnt and retinoic acid (RA) signalling are implicated in the process of anterior-posterior specification. An important organizing centre for dorsal-ventral patterning is the axial mesoderm. A gradient of Sonic hedgehog (Shh), secreted from notochord and ventral floor plate, provides positional information to prospective neurons in the neural tube and thereby induces distinct precursor domains. Shh concentrations along

this gradient are integrated and converted into expression of homeodomain proteins like NK2 homeobox 2 (Nkx2.2) or Paired box 6 (Pax6) in distinct areas of the neural tube. Dorsal domains of the neural tube will form Rohon-Beard primary sensory neurons while motor neurons will arise from more ventral positions, both separated by an intermediate region containing interneurons ([72], [73], [74], [75], [76], [77] and [78]).

The basic helix-loop-helix transcription factors of the Oligodendrocyte lineage transcription factor (*olig)* gene family are central players in neural cell type specification [79]. Especially *olig1* and *olig2* are essential for cell fate acquisition of motor neurons and oligodendrocytes, the myelinating cells of the vertebrate CNS [80]. Both, motor neurons and oligodendrocytes are sequentially generated from a common population of neuroglial precursor cells ([80], [81] and [82]). These proliferative progenitor cells in the prospective ventral spinal cord express *olig2* ([79], [83] and [84]) and divide asymmetrically to produce motor neurons and oligodendrocyte precursor cells ([81]; Figure 5).

Precursor cells that coexpress *olig2* and Neurogenin 2 (*ngn2*) are predetermined to develop into motor neurons [82]. There are two classes of motor neurons in zebrafish: Primary (PMNs) and Secondary Motor Neurons (SMNs). During differentiation of PMNs *olig2* is downregulated ([79], [81] and [83]). After their final mitotic division, the entire population of PMNs initially begins to express the ISL LIM homeobox 1 (*islet1*) gene, the earliest marker for developing motor neurons ([77], [85] and [86]). Later on, different subtypes of PMNs can be determined according to their axonal projection pathways and expression of *islet* genes ([86] and [87]). Middle PMNs (MiPs) and Rostral PMNs (RoPs) still express *islet1*, whereas Caudal PMNs (CaPs) express *islet2* ([87], [88] and [89]). Together MiPs, RoPs and CaPs innervate each myotome of the developing embryo. All PMN axons exit the spinal cord at a single exit point before they grow towards their appropriate destinations. MiPs develop dorsally projecting axons, CaPs ventrally projecting axons and axons of RoPs grow along the myoseptum in rostral direction [85]. SMNs arise later in development, but are specified by Shh signalling as PMNs are. Their axons use the same exit points as PMN axons and follow similar paths ([85], [89] and [90]; Figure 5).

The second cell type arising from *olig2*$^{+}$ neurogliablasts are oligodendrocytes. Oligodendrocyte differentiation and acquisition of their function in conduction of action potentials depends on serial activation of different transcription factors and consequently expression of genes encoding for specific structural components [91]. Nerve/glial antigen-2 (*ng2*) and SRY-box 10 (*Sox10*) are among the earliest marker genes for cycling oligodendroblast in the ventral neural tube ([92] and [93]). Olig1 is expressed in premyelinating oligodendrocytes where it forms a transcriptional activating complex with Sox10 to stimulate expression of the Myelin basic protein (*mbp*) gene in myelinating oligodendrocytes [94]. In contrast to motor neurons, oligodendrocytes maintain expression of *olig2* in their mature form ([79], [83] and [84]; Figure 5). Subsequently mature oligodendrocytes in the neural tube migrate dorsally and reach their final position [92].

As probably the most complex organ, regular formation of the CNS from embryonic stem cells (ESCs) depends on concerted repression of pluripotency genes and activation of neuronal genes [95]. Transcription factors underlying the switch from the pluripotency to the neuronal gene expression program are insufficiently explored but mechanisms are more and more elucidated (see 3.4).

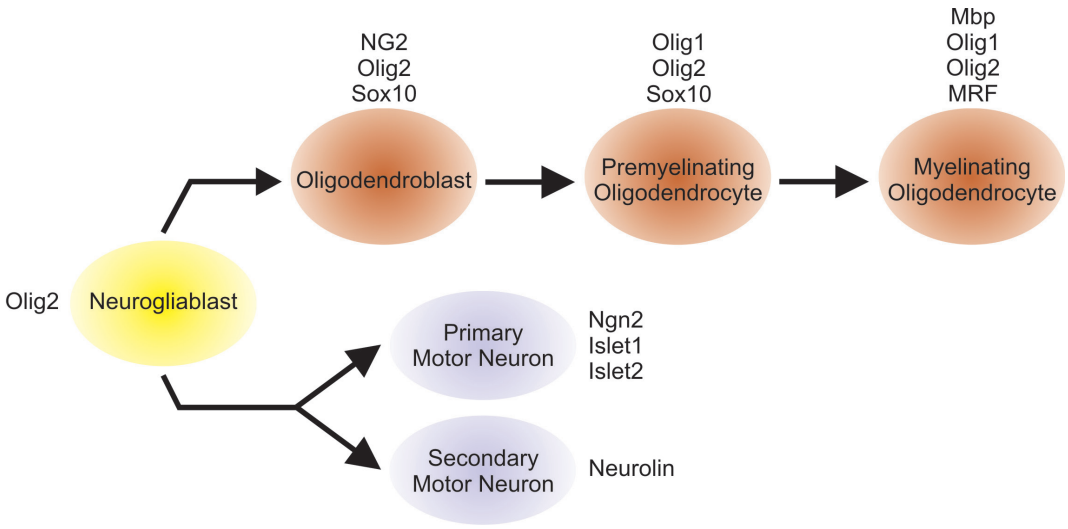

Figure 5: The neuroglial cell lineage.
Schematic of the motor neuron and oligodendrocyte lineage showing examples of characteristic marker genes. Motor neurons and oligodendrocytes develop from a common precursor cell population. Differentiation of both cell types requires expression of specific transcription factors and structural components.

3.4 The REST-complex

3.4.1 Regulation of neuronal gene expression by the REST-complex

Development and proper function of the central nervous system (CNS) requires a tightly regulated gene expression program in neuronal precursor cells and neurons as well as in surrounding non-neuronal tissues (see 3.3). Cell fate determination is achieved by transcriptional activation of neuronal genes in neurons and differential silencing of these genes in non-neuronal tissues [96]. Derepression of neuronal genes at the transition from neuronal progenitor to a terminally differentiated neuron is essential for neurogenesis. Studies of transcriptional control of neuronal genes identified a conserved ~24 bp *cis*-acting DNA silencer element found in regulatory regions of these genes, termed Repressor Element 1 (RE1; also called Neural-Restrictive Silencer Element, NRSE). The RE1 specifically attracts the *trans*-acting Repressor Element 1 Silencing Transcription factor (REST; also called Neural-Restrictive Silencer Factor, NRSF), present only in non-neuronal cells and undifferentiated neuronal progenitors. REST switches off transcription of neuronal genes, including neuronal transcription factors ([96], [97], [98], [99], [100], [101] and [102]; Figure 6). Hence REST is part of a complex regulatory cascade controlling expression of neuronal genes.

To silence transcription, REST nucleates a multiprotein complex on RE1 sequences. Inactivation of RE1 containing genes occurs by two distinct mechanisms: Epigenetic silencing by heterochromatin formation and prevention of efficient transcription by posttranslational inhibition of Pol II activity (Figure 6). In both mechanisms, REST serves as a RE1 specific factor and silencing is conducted rather by corepressors than REST itself.

For long term gene silencing, REST recruits corepressors like Sin3A/B [103], BRAF35 [104], Methyl-CpG-binding protein (MeCP2; [105], [106] and [107]) and REST corepressor (CoREST; [108]) to its target genes. These corepressors tether Histone deacetylases 1 - 3 (HDAC1/2/3; [105]) and the lysine specific histone demethylase 1

(LSD1; [109]) to target gene loci. Subsequently, these factors alter acetylation and methylation states of nearby histones, leading to formation of condensed, inactive chromatin ([103], [104], [106] and [109]; Figure 6). The second mechanism of transcriptional silencing by the REST complex is the direct modification of Pol II activity at RE1 containing genes [110]. Regulation of the transcription cycle depends on de-/phosphorylation of consensus heptapeptide repeats within the carboxyl-terminal domain (CTD) of the largest Pol II subunit [111]. Combination of different modified amino acids in the CTD creates a code influencing its interaction with cofactors and consequently transcriptional activity. This process is not fully understood, but it becomes apparent that the unphosphorylated form of Pol II is recruited by the pre-initiation complex to promoter sequences and transcript elongation and capping are mediated by the phosphorylated forms. Dephosphorylation leads to termination of transcription and is essential for Pol II recycling ([111], [112] and [113]). The REST-complex exploits the phosphatase activity of so called C-terminal domain small phosphatases (Ctdsps) to dephosphorylate Pol II CTD and inactivate transcription [110]. The Ctdsp gene family comprises four annotated (Release Zv9, zebrafish genome project) homologues in the zebrafish genome (*ctdsp1*, *2* and *ctdsp-like a* and *b*). Ctdsps belong to the class C phosphatases and regulate transcription and processing of pre-mRNAs in eukaryotic cells by dephosphorylating preferentially Ser^5 in the Pol II CTD ([114]).

By combining these two silencing mechanisms, the REST-complex functions in both, establishing and maintaining repression of neuronal genes and consequently non-neuronal cell identity (Figure 6). For neurogenesis, REST mediated repression of neuronal genes has to be interrupted to allow transition from neural progenitor cell to neuron (see 3.4.2).

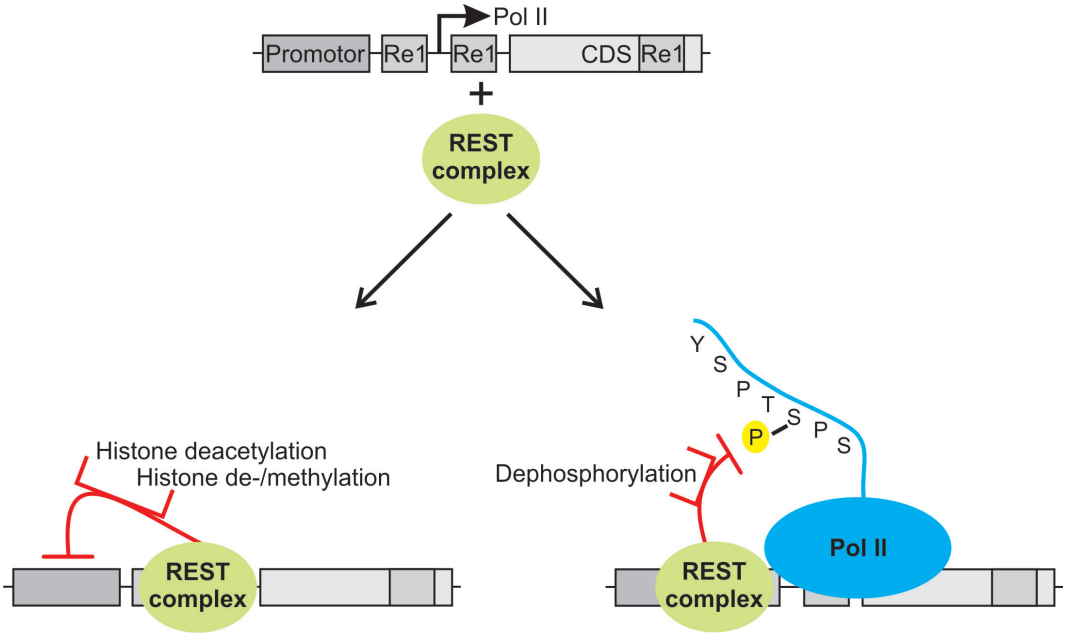

Figure 6: Target gene silencing by the REST complex.
The REST complex inhibits transcription of RE1 containing target genes by heterochromatin formation or inactivation of RNA Polymerase II C-terminal domain. To silence its neuronal target genes the REST-complex recruits corepressors to RE1 containing gene loci. As REST protein is absent from neuronal tissues, it probably acts as a cell type and RE1-sequence specific scaffold molecule for more widespread expressed coregulatory proteins. RE1s are located in promotor regions, 5'UTRs, exons and introns. RE1: Repressor Element 1, CDS: Coding Sequence, REST: Repressor Element 1 Silencing Transcription factor, Y: tyrosine, S: serine, P: proline, T: threonine.

3.4.2 Control of embryonic neurogenesis by the REST/Ctdsp/miR-124 pathway

For embryonic development of the CNS, the neuronal gene expression program has to be tightly regulated in a spatio-temporal manner (see 3.3). It is fundamental to switch on neuronal genes for transition from pluripotent stem cell to terminally differentiated neuron, and to suppress them in non-neuronal cell types. Inhibition of these critical genes is in part accomplished by the REST-complex (see 3.4.1 and Figure 7).

Function of the REST/Ctdsp-complex in silencing neuronal genes was initially described *in vitro*, using reporter gene constructs [114]. Recently, several studies elucidated the function of the REST-complex in the context of developing embryos. In vertebrate embryos, expression of *rest* as well as *ctdsp* mRNAs is restricted to non-neuronal tissues and proliferating neuroepithelial cells ([101], [110], [115] and [116]; Figure 7). This expression pattern seems not to be determined by cell proliferation, as *ctdsp* mRNAs were also found to be expressed in non-proliferating muscle cells [115]. Differentiation of neuronal progenitor cells into neurons is accompanied by downregulation of Ctdsp and REST ([110] and [117]). For this, REST protein is degraded by the proteasome ([118] and [119]) and miRNAs inhibit *de novo* synthesis of REST protein [57].

A generally accepted model of REST-complex regulated neurogenesis includes a step-wise elimination of REST during transition from pluripotent stem cell to neural stem cell (NSC) and further to mature neuron (Figure 7). When cells descend from pluripotent stem cell to neural progenitor, REST protein concentration is decreased. As RE1s with slightly different sequences also show variable affinity for REST, reduced REST levels in NSCs allow basal expression of some neuronal genes, whereas other RE1s with higher affinity to REST are still occupied and repressed [120]. This poised transition state makes rapid derepression of neuronal genes possible to allow neuronal cell differentiation. During differentiation into postmitotic neurons, expression of REST is further decreased and its own transcription is finally silenced ([116] and [118]; Figure 7). Therefore, in context of the REST-complex, Ctdsps avoid expression of neuronal genes in non-neuronal tissues and help to maintain stem cell properties of proliferating neuronal precursor cells ([110]; Figure 7). But how REST/Ctdsp mediated repression is abrogated to allow neurogenesis *in vivo* is only poorly understood.

Among genes directly silenced by the REST-complex, neuronal miR-9, miR-132 and miR-124 take prominent positions [117]. In multiple double negative feedback loops, these miRNAs silence REST-complex components, as bifunctional miR-9/9* represses REST and CoREST ([57] and [121]), miR-132 targets MeCP2 [122] and miR-124 silences Ctdsp1/2 ([5], [115], [123] and [124]; Figure 7), respectively. In the developing neural tube anti-neural respectively pro-neural functions of Ctdsps and miR-124 counteract each other. This becomes evident by similar effects of Ctdsp1 overexpression and miR-124 inactivation on expression of markers for postmitotic neurons [115]. These negative feedback loops might provide stability of gene expression and prevent disturbance of cell homeostasis, as changes in this tight regulatory network lead to severe neurological disorders ([57], [122] and [125]).

Hence, neuronal miRNAs and REST-complex components inhibit their expression reciprocally. Target silencing by these particular miRNAs is essential for expression of other neuronal genes and therefore neurogenesis ([5] and [123]). Which events destabilize REST-complex mediated repression to allow expression of neuronal genes is currently unknown, but the described miRNAs (e.g. miR-124) might contribute to this process.

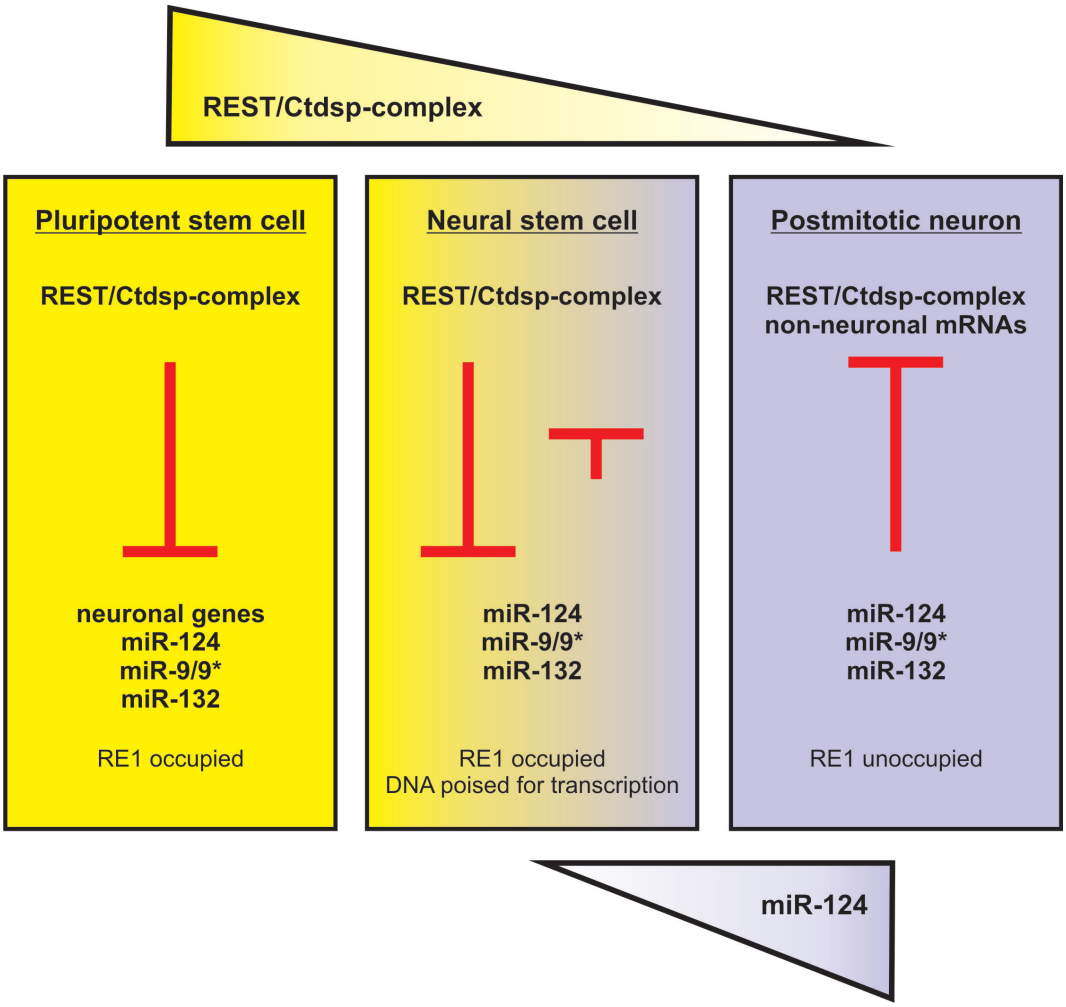

Figure 7: Control of neuronal cell differentiation by the REST/Ctdsp/miR-124 pathway.
Transition from pluripotent stem cell to mature neuron is controlled by antagonistic functions of the REST/Ctdsp-complex and neuronal miRNAs. During the course of neuronal cell differentiation REST is removed from the cell, what allows transcription of neuronal genes. Inactivation of the REST/Ctdsp-complex is in part facilitated by miRNAs which are under transcriptional control of the REST/Ctdsp-complex.

3.5 The miRNA-26 family

3.5.1 Processing and expression pattern of intronic miRNA-26

MiRNAs are encoded either by independent miRNA genes or in introns of protein coding genes (see 3.2.1). The miR-26 family is part of the second miRNA subclass, intronic miRNAs ([126], [127] and [128]; see also 6.1.1). Monteys *et al.* describe miR-26a and miR-26b as devoid of any own promoter sequences [129]. Hence, miR-26 family members are co-expressed as one transcript together with their host genes ([126], [130] and [131]). The biogenesis of miR-26b was biochemically analysed in detail [126]. Obtained data strongly suggest that Drosha cleavage of pri-mir-26b occurs between the splicing commitment step and the excision of the intron from the host pre-mRNA, finally resulting in equimolar production of pre-mir-26b and correctly spliced host mRNA [126].

The expression pattern of the miR-26 family was so far not analysed in detail. As most other miRNAs, miR-26a and miR-26b are not expressed in embryonic stem cells (ESCs), but are upregulated during differentiation processes ([132], [133] and [134]), including neurogenesis [135]. Upregulation of miR-26 during cell differentiation

results in strong expression in terminally differentiated neuronal cell types, as it is expressed in cultured mouse motor neurons [136], cortical neurons and astrocytes [137] but not in proliferating human retinoblastoma cells [136]. In vertebrate organisms not much is known about the spatio-temporal expression pattern of miR-26 family members. MiRNA expression profiling in *Xenopus laevis* embryos revealed miR-26a expression in neurula, tailbud and tadpole stages [138]. During mouse embryonic brain development miR-26 is expressed in primary neurons as well as primary astrocytes [137]. In developing zebrafish embryos miR-26a and miR-26b were shown to be first detectable 24 and 48hpf (hours post fertilization), respectively ([139], [140] and [141]). *In situ* hybridization shows ubiquitous expression patterns for both, with higher levels in head, spinal cord and neuromasts [139]. Likewise, in adult mouse tissues miR-26 is expressed ubiquitously, but miR-26a is enriched in hippocampus, cerebellum and midbrain ([130] and [142]), whereas miR-26b is highly expressed in liver, pituitary, cortex and cerebellum ([142] and [143]).

Taken together, the available data indicate that members of the miR-26 family are upregulated during neuronal cell differentiation and are expressed predominantly in brain astrocytes and neurons.

3.5.2 MiRNA-26 target genes

Like most miRNAs, also the miR-26 family has hundreds of *in silico* predicted targets (in the zebrafish genome there are 828 predicted targets for miR-26a and 782 for miR-26b, as registered in the miRBase Target Database). However, only few of these predicted targets were experimentally validated so far.

In vivo validated miR-26 target genes can roughly be divided into three groups, according to the cellular function of their gene products. The first group comprises negative regulators of terminal cell differentiation and oncogenes like the Polycomb group protein Enhancer of zeste homolog 2 (Ezh2; [144], [145] and [146]), Cyclins D2 and E2 ([145] and [147]), Cyclooxygenase-2 (COX-2; [148]) or Lymphoid enhancer factor 1 (Lef-1; [143]). The second group consists of proteins overrepresented in various cancer types, but with unknown functions. SERPINE1 mRNA binding protein 1 (Serbp1) is overexpressed in ovarian cancer ([149] and [150]), Metadherin (MTDH) and Solute carrier family seven member 11 (SLC7A11) in breast cancer ([151] ,[152] and [153]). For these proteins, there are speculative roles in tumorigenesis, metastasis and chemoresistence ([150], [152] and [153]). The third group are positive regulators of cell differentiation and hence tumor suppressor molecules. For example Phosphatase and tensin homolog (PTEN) is a well characterized tumor suppressor [154]. SMAD family members 1 (SMAD-1) and 4 ([155] and [156]), are a components oft the (BMP) signalling cascade triggering differentiation of osteoblastic cells [157] and regulating smooth muscle cell plasticity [156]. Ring finger protein 6 (RNF6; [151]) has a described function within gene expression control in germinal differentiation [158].

Hence, most miR-26 targets are regulators of cell proliferation and silencing of these targets by miR-26 is essential for myogenesis [144], gliomagenesis [154] and pituitary formation [143]. Together with the previously described upregulation of miR-26 family members during cell differentiation (see 3.5.1) this makes miR-26 an attractive candidate to study the impact of miRNA mediated gene silencing on cell differentiation and organogenesis in vertebrate embryos.

3.6 Aim of the study

MicroRNAs have highly specific expression patterns and fundamental functions in embryonic development. In previous studies, the miRNA-26 family has been reported to be enriched in neuronal tissues and cell lines (see 3.5.1). Expression pattern and published target genes of miR-26 imply a role in cell differentiation for this particular miRNA family (see 3.5.1 and 3.5.2). However, so far not much is known about the role of miR-26 during cell fate determination and vertebrate embryonic development.

The main goal of this study was to analyze functions of miR-26 in differentiation of neuronal cell types *in vivo*. To this end, the zebrafish (*Danio rerio*) was used as a vertebrate model system as it allows rapid embryological, histological and biochemical analysis of miRNA function. To gain more insight into the functions of miR-26 in zebrafish neurogenesis this study focused on the following experimental attempts:

- Analysis of the spatio-temporal expression pattern of miR-26 in zebrafish.
- Bioinformatical prediction of putative target genes of miR-26 in zebrafish.
- *In vivo* validation of predicted targets in developing zebrafish embryos.
- Phenotypical analysis of miR-26 depleted zebrafish embryos.

The miR-26 family is subject to posttranscriptional regulation of its maturation pathway (see 3.2.3). KSRP supports Dicer cleavage of pre-mir-26 and regulatory activity of mature miR-26 is negatively controlled via 3'-uridylation by TUT4. For this reasons, the miR-26 family is especially applicable for studying regulation of miRNA expression *in vivo*. For other miRNAs, regulated processing was already described during embryogenesis, but not analyzed in detail. Hence, the second focus of this study was to find out more about the impact of posttranscriptional regulation of miRNA processing on vertebrate embryonic development. Possible factors and miRNA sequence motifs, which influence miR-26 biogenesis and their role in embryonic development should be analyzed in zebrafish.

Together the obtained data should give an idea about how miR-26 acts in neuronal cell differentiation and if posttranscriptional regulation of miR-26 processing has any relevance for its biological function.

4 MATERIAL

4.1 Zebrafish maintenance and breeding

For this study only zebrafish (*Danio rerio*) lines Tu and gata2:GFP [159] were used. Adult zebrafish were kept at 28°C, with a light-dark cycle of 14 h light and 10 h darkness and fed three times a day with dry food or Artemia. To obtain embryos for experiments, one male and one female were put into a mating container in the late evening. The male and the female were separated by a sieve. At the beginning of the light period, the fish were put together. Fertilized eggs were collected and stored in 30% Danieau's medium. Embryos were raised in an incubator at 28.5°C and developmental stages were determined according to [160]. To inhibit pigmentation, embryos can be treated with 0.2 mM PTU after gastrulation.

4.2 Bacterial strains

For transformations with plasmid DNA, heat shock competent Escherichia Coli DH5α were used.

4.3 Plasmids

According to experimental demands, DNA fragments were cloned into the pCRII (Invitrogen) or pCS2+ [161] vectors (see 8.2).

4.4 DNA-Oligonucleotides

DNA-Oligonucleotides were ordered from biomers.net GmbH.

Oligo	**Sequence**
PCR-Primer	
dre-gapdhUP	TCGGTCGCATTGGCCGTCTG
dre-gapdhDOWN	ACCACGGCCATCCCTCCACA
GFP-UP	CTACCTGTTCCATGGCCAAC
GFP-DOWN	CATGCCATGTGTAATCCCAG
zfaactinUP	GATGCTGGTGATGGTGTGAC
zfaactinDOWN	CTTCTGCATACGGTCAGCAA
zfzgc:77714UP	ACCAGGGGAAGATCTGTGTG
zfzgc:77714DOWN	TTTGCGTTGCTGTTTGAGTC
zf-CTDSP1-UP	GACAGAGGTACCCCTCCACA
zf-CTDSP1-DOWN	GCGAGTTGTCCACAATGATG
zf-CTDSPL1-UP	GCCTGGCTAAGTACGCTGAC
zf-CTDSPL1-DOWN	AAAGTGTTTACACGCCGGTC
zf-CTDSPL2-UP	CAGAACTCGCTGGAAAAAGG
zf-CTDSPL2-DOWN	AAGCCGACTCAGGTCTTTGA
zfCD146UP	ATGCACAAGGCTACCCAATC

zfCD146DOWN	TCTTCGGGATTGGATTTGAG
zfCTDSP2intron4UP	TTCATGCATGTGCCAATTTT
zfCTDSP2intron4DOWN	TCCTGTAGTGCTGTTGCTCG
zfKSRPUP	TGGTCCGCCTGGCAGTGAGA
zfKSRPDOWN	GCTGCAGGCGTCTGTCCAGG
zfmyf5UP	TCTCCAACCGGAAGTGATTC
zfmyf5DOWN	ATGGCCTTGGCCTTTATTCT
zfmyoDUP	ACCCTTGCTTCAACACCAAC
zfmyoDDOWN	CATGCAGGAGTCTCTGTGGA
zfpax2aUP	CCGGCAGTATTAAACCTGGA
zfpax2aDOWN	TGCTCTGGCTTGATGTGTTC
zfpcnaUP	GGCACTGGTCTTTGAAGCTC
zfpcnaDOWN	TGCAGAATGAAAATCCCACA
zftubb5UP	CAGCTGGTGGAGAACACAGA
zftubb5DOWN	GCTCGGAGATACGCTTGAAC
zfbactin13UTRUP	ACGACCAACCTAAACCTCTCG
zfbactin13UTRDOWN	GGTTTTACATGTGCACGTTTTATT
zgc:777143UTRUP	GCGATCTCGAGCCATACGCTAAACCTCCATGT
zgc:777143UTRDOWN	GCGATCTCGAGAGGCCTTATCAGGGCACATT
BamHI-dre-RhoUP	GCGCGGGATCCATGAACGGTACAGAGGGACC
XhoI-dre-RhoDOWN2	GCGCGCTCGAGTTACGCCGGAGACACGGAGC
oligo(dT) anchor	GCGAGCTCCGCGGCCGCGTTTTTTTTTTTT
oligo(dT)	TTTTTTTTTTTTTTTTT
pCS2MCSsense	AGGCCTCTCGAGCCTCTAGA
SP6 Promoter Primer	ATTTAGGTGACACTATAGAA
T7 Promoter Primer	TAATACGACTCACTATAGGG
Mutagenesis Primer	
dre-sp2-3'UTRmutfor	GCTTCAAGTGTACGCGATGGGAAGCAG
dre-sp2-3'UTRmutrev	CTGCTTCCCATCGCGTACACTTGAAGC
T7 runoff templates	
T7 runoff primer	AATTTAATACGACTCACTATAGG
pre-dre-mir-430b AS+T7+GG	CTACCCCAACTTGATAGCACTTTCTACTTTGCTTAA AAGAAAGATGCTAAAGTTAGACCTATAGTGAGTCG TATTAAATT
pre-dre-mir26b AS+T7+GG	GAAACAAGTAACCAAGAATAGGCCGTACTAGTGGG AACTAACCTATCCTGGATTACTTGCCTATAGTGAGT CGTATTAAATT
Northern blot probes	
dre-mir-124 SL NB	GAAATACAATAAATCAAGGTCCACTGTGAA

NBdre-miR-124	GTTGGCATTCACCGCGTGCCTTA
dre-mir-26b-stemNB	GTAACCAAGAATAGGCCGTACTAGTGGGAACT
NBanti-dre-mir-26b	GAACCTATCCTGGATTACTTGAA
dre-mir-430b SL NB	GCTTAAAAGAAAGATGCTAAAGTTAGAGTT
dre-mir-430b NB	GCTACCCCAACTTGATAGCACTTT
mmu-mir-26bstemNB	GTAATGGAGAACAGGCTGGTCAGCACCACA
NBmmu-mir-26b	ACCTATCCTGAATTACTTGAA
NBmmu-miR-124-2SL	GACATTAAATCAAGGTCCGCTGTGAACACG
NBmmu-124	GGCATTCACCGCGTGCCTTA
NBdre-mir-206	GCCACACACTTCCTTACATTCCA
NB5srRNA	GTCTCCCATCCAAGTACTAACCAAGCCCGACCCTGCTTA
tRNANB	GTGGTGTTTCCGCCCGGTTT
zfU6 NB	GCTAATCTTCTCTGTATCGATCCAATTTTAGTA

4.5 Morpholinos

Morpholino oligos were ordered from Gene Tools, LLC.

Oligo	**Sequence**
DRprp31	CAAGCAGCTCGTCTGCCAAAGACAT
snrpc/U1-C	CATCTTCACAGCGGAACAGCGCGGG
SMNMO	CGACATCTTCTGCACCATTGGC
miR-26bMo	AACCTATCCTGGATTACTTGAA
KSRPMo	GCACCGCGCTGTACTCAGACATGCT
lin-28Mo	CTGCTTTTTCTGTGGTGTAATCAAC
TUT4Mo	GGATCTGTGTTTGTTCTGTAATGCT
ctdsp2Mo	AGAACTTTCCATCTAACAAACGCAC
Standard Control	CCTCTTACCTCAGTTACAATTTATA

4.6 Locked nucleic acid (LNA) probes

LNA probes were ordered from Exiqon.

Oligo	**Sequence**
dre-miR-26b	AACCTATCCTGGATTACTTGAA
Sense miR-159	AGAGCTCCCTTCAATCCAAA

4.7 Synthetic microRNA duplexes

MicroRNA duplexes were ordered from Ambion.

Duplex	Resulting microRNA sequence
dre-miR-26b	UUCAAGUAAUCCAGGAUAGGUU
Negative Control #1	Random sequence (Ambion patent licence)

4.8 Enzymes

2xPCR Master Mix	Promega
KAPAHiFi DNA-Polymerase (1 U/µl)	Peqlab
Pfu DNA-Polymerase	Department of Biochemistry, University of Wuerzburg
Sp6 RNA-Polymerase (20 U/µl)	Fermentas
T7 RNA-Polymerase (1.29 mg/ml)	Department of Biochemistry, University of Wuerzburg
RQ1 DNAse (1 U/µl)	Promega
T4 DNA-Ligase (1 Weiss U/µl)	Fermentas
T4 Polynucleotide Kinase (10 U/µl)	Fermentas
RNase H (5 U/µl)	Fermentas
RNase A	Promega
Shrimp alkaline Phosphatase (1 U/µl)	Fermentas
Restriction endonucleases	NEB/Fermentas
Proteinase K	Roth

4.9 Antibodies

Antibody	Antibody type	Antigene/anatomical structures recognized	Dilution/buffer	Distributor
Zpr-1	Mouse monoclonal	Green/red double cones	1:400 PBS + 0.3% Triton X-100 + 5% goat serum	ZIRC
Anti-Rhodopsin (1D4)	Mouse monoclonal	Cow full length Rhodopsin (1D4 epitope)	1:500 PBS + 0.3% Triton X-100 + 5% goat serum	Abcam
Zn-8	Mouse monoclonal	Alcama	1:200 PBDT	ZIRC
Anti-Prpf31	Rabbit polyclonal	Zebrafish full length Prpf31	1:200 TBT	Department of Biochemistry, University of Wuerzburg
Anti-GFP	Mouse monoclonal	Green Fluorescent Protein	1:800 PBS	Roche

Anti-Ctdsp2	Rabbit polyclonal	Zebrafish full length Ctdsp2	1:150 NET-Gelatine	Department of Biochemistry, University of Wuerzburg
Tuj1	Mouse monoclonal	Neuron specific class III β-Tubulin	1:1000 NET-Gelatine	Convance
Anti-brain Tubulin	Mouse monoclonal	Full length native purified porcine brain Tubulin	1:600 TBT	Abnova
Anti-α-Tubulin	Mouse monoclonal	C-terminal end of α-Tubulin	1:1000 NET-Gelatine	Sigma-Aldrich
Anti-β-Actin	Mouse monoclonal	N-terminal peptide of β-Actin	1:1000 NET-Gelatine	Sigma-Aldrich
Texas Red-conjugated anti-mouse	Goat polyclonal	Mouse IgG + IgM	1:150 PBDT	Jackson ImmunoResearch
Anti-mouse IgG-Peroxidase	Goat polyclonal	Mouse Ig	1:5000 TBT	Sigma
Anti-rabbit IgG-Peroxidase	Goat polyclonal	Rabbit Ig	1:5000 TBT	Sigma
AP-conjugated-anti-Digoxigenin (Fab-fragment)	Sheep polyclonal	Digoxigenin	1:2000 PBST	Roche
AP-conjugated-anti-Digoxigenin (Fab-fragment)	Sheep polyclonal	Fluorescein	1:2000 PBST	Roche

4.10 Chemicals

Chemicals were purchased from BD Biosciences, Merck, Serva, Sigma-Aldrich or Roth, radiochemicals from PerkinElmer. If not declared different, all solutions were prepared using deionised autoclaved water.

4.11 Stock solutions

100% Danieau's:
58 mM NaCl
0.7 mM KCl
0.4 mM $MgSO_4x7H_2O$
0.6 mM $Ca(NO_3)_2$
0.5 mM HEPES
0.1 mM Methylene blue

100xPTU
0.02 M 1-phenyl 2-thiourea

10xPBS:
1 M NaCl
19.5 mM KCl
59 mM $Na_2HPO_3x2H_2O$
11 mM KH_2PO_4
→ pH 7.4

20xSSC:
3 M NaCl
0.3 M NaCitrat

5xTBE:	450 mM Tris 440 mM Boracic acid 10 mM EDTA →pH 8.0
10xTBT:	1.5 M NaCl 60 mM Tris 150 mM Tris-HCl 5% Tween 20 → pH 7.5
10xLämmli:	440 mM Tris 2 M Glycine 1.5% SDS → pH 8.3
10xTowbin:	50 mM Tris 192 mM Glycine 3 mM SDS
10xNET:	1.5 M NaCl 0.05 M EDTA 0.5 M Tris 0.5% Triton X-100 → pH 7.5
2xTES:	20 mM Tris-HCl, pH 8.1 2 mM EDTA 0.2 mM NaCl
50xGlycine:	0.1 g/ml Glycine in PBST
10xMOPS buffer:	200 mM MOPS 50 mM NaAc 10 mM EDTA, pH 8.0 → pH 7.0

4.12 Technical equipment

Eppendorf Centrifuge 5415 R

Aviso Primus PCR-Machine

Zeiss Axiovert 200M microscope

Zeiss AxioCam MRm

Zeiss AxioCam MRc 5

Leica CLSM TSC SP2 AOBS

Molecular Dynamics PhosphorImager

Eppendorf BioPhotometer

Miltenyibiotech gentleMACS Dissociator

Peqlab QUANTUM Geldocumentation system

Elma Transsonic T410

Branson Sonifier 250

Sutter Instrument Flaming/Brown type micropipette puller Model P-97

Eppendorf Microinjector FemtoJet

Nikon SMZ 800 stereomicroscope

Bio Rad Gel Dryer Model 583

UVP CL-1000 Ultraviolet Crosslinker

4.13 Software and databases

Databases:

http://www.ensembl.org/index.html

http://www.ncbi.nlm.nih.gov/

http://www.mirbase.org/

Computer software:

Text processing:	Word 2007 (Microsoft)
	Endnote X3 (Thomson ISI ResearchSoft)
Statistical analysis:	Excel 2007 (Microsoft)
	GraphPad Prism 5 (GraphPad software)
Sequence analysis:	Vector NTI advance 10 (Invitrogen)
Image acquisition:	AxioVision (Zeiss)
	Confocal software (Leica)
Image processing:	Photoshop 7.0 (Adobe)
	CorelDraw X4 (Corel)
	Illustrator 10 (Adobe)
	ImageJ (NCBI)

5 METHODS

5.1 Microbiological methods

5.1.1 Heat shock competent bacteria

For production of competent bacteria, 100 ml LB medium were inoculated with 1 ml of an overnight culture (see 5.1.5) derived from a single colony. This culture was incubated under constant shaking at 37°C until optical density (OD_{600}) reached a value between 0.3 and 0.4. After 15 min incubation on ice the solution was centrifuged for 10 min at 4°C and 4500 g. The supernatant was discarded and the pellet was resuspended in 20 ml ice-cold 0.1 M NaCl. After 30 min incubation on ice the bacteria solution was centrifuged for 10 min at 4°C and 4500 g. The supernatant was discarded and the bacteria pellet was resuspended in 10 ml of ice-cold 0.1 M $CaCl_2$/20% glycerol. The competent bacteria were stored in aliquots at -80°C.

Solutions:

LB medium:	10 g/l Bacto-Trypton 5 g/l Yeast extract 0.17 M NaCl → pH 7.4

5.1.2 Transformation of plasmid DNA

2 µl Plasmid were mixed gently with 250 µl of competent bacteria (see 5.1.1) and chilled on ice for 30 min. Transformation was initiated by a heat shock of 1.5 min at 42°C. After heat shock, the bacteria were instantly put on ice again and 1 ml of LB medium was added, followed by 1 h incubation at 37°C.

5.1.3 Bacteria cultivation on agar plates

For agar plates, 1.5% agar in LB was autoclaved and cooled down to 50°C. Ampicillin (50 µg/ml) was added and the liquid was poured into petri dishes. The plates were cooled over night to RT and could be stored at 4°C. To obtain single bacteria clones, bacteria suspensions in LB were streaked out on LB agar plates after transformation.

5.1.4 Selection of positive bacterial clones

Positive colonies were identified by blue/white selection when using the PCRII vector (see 4.3), analytical digest or PCR colony screen. For blue/white selection, LB agar plates were treated with 40 µl of 100 mM IPTG and 40 mg/ml X-gal solution each. Clones containing vectors without insert will express β-Galactosidase and appear blue.

For PCR colony screen, a standard PCR reaction (see 5.2.4) was set up using the bacterial clone as template. A combination of a gene and a vector specific primer gives information about the presence and orientation of the insert. Clones, identified as positive, were sequenced (see 5.2.13) after plasmid isolation (see 5.1.6).

5.1.5 Bacterial cultivation in liquid cultures

Single bacteria colonies were picked and grown over night at 37°C in LB medium containing 50 µg/ml Ampicillin. For plasmid mini preparation 5 ml liquid cultures were used.

5.1.6 Isolation of plasmid DNA from *E. coli*

Plasmid isolation with the Macherey-Nagel NucleoSpin Plasmid QuickPure Kit was performed following the manufacturers protocol.

5.2 Molecular biological methods

5.2.1 Isolation of total RNA

For isolation of RNA from embryos, 50 – 100 embryos were collected and transferred into a sterile, RNase free 1.5 ml Eppendorf tube. Danieau's medium was removed and 500 µl Trizol reagent (Invitrogen) were added before 5 min incubation at RT. Embryos were homogenized by pipetting through canulaes. Another 500 µl Trizol were added before the homogenate was centrifuged with 5000 g at 4°C. The supernatant was transferred to a new tube and placed on ice. The liquid was mixed with 200 µl ice-cold chloroform and centrifuged with 5000 g at 4°C. The aqueous phase was transferred to a new tube, again mixed with 200 µl ice-cold chloroform and centrifuged with 5000 g at 4°C. The aqueous phase was transferred to a new tube and precipitated with 500 µl isopropanol at -20°C over night. RNA was pelletised by centrifugation for 1 h at 16100 g. The resulting pellet was washed with 500 µl ice-cold 70% ethanol for 5 min. After removal of the supernatant, the pellet was air-dried for 10 min at RT and resuspended in water.

For isolation of RNA from adult tissues, zebrafish were dissected with sterile instruments. Tissues were transferred to 1 ml of Trizol reagent in M tubes and homogenized with a gentleMACS dissociator employing gentleMACS program RNA_1. The RNA isolation protocol was identical as for embryos.

Total RNA obtained by this procedure contains small RNAs like snRNAs, pre-mirs and miRs as well as longer mRNAs.

5.2.2 cDNA synthesis

cDNA was synthesized using oligo(dT)-primer and Super Script II reverse transcriptase (Invitrogen) following the manufacturers instructions. After synthesis cDNA was stored at -20°C. If cDNA was used for semiquantitative RT-PCR (see 5.2.4) isolated RNA was treated with RQ1 DNase before reverse transcription to remove genomic DNA and RNase H after reverse transcription to eliminate cDNA-RNA hybrids.

5.2.3 Isolation of genomic DNA

For amplification of genomic regions, genomic DNA was isolated from cultured cells or zebrafish embryos.

Cells were harvested by centrifugation with 5000 g for 10 min. The pellet was washed with PBS and transferred into Proteinase K-solution. Cells were lysed by shaking in proteinase K-solution at 50°C over night. Genomic DNA was phenol/chloroform extracted (see 5.2.14) and precipitated (see 5.2.15).

To obtain zebrafish genomic DNA, 20 embryos were dechorionised and transferred into a microfuge tube. Liquid was removed completely and 50 µl Extraction buffer were added. Samples were boiled at 95°C for 10 min and homogenized with a 200 µl pipette. Homogenates were cold down on ice before completing Extraction buffer with Proteinase K. After incubation for 3 h at 55°C, Proteinase K was inactivated at 95°C for 10 min. Genomic DNA was pelleted by a 1 min centrifugation step at 16100 g.

Genomic DNAs were stored at -20°C until further use for PCR.

Solutions:

Proteinase K-solution:	100 mM NaCl 10 mM Tris-HCl (pH 8.0) 50 mM EDTA (pH 8.0) 0.5% SDS 20 µg/µl RNase A 0.1 mg/ml Proteinase K
Extraction buffer:	10 mM Tris (pH 8.0) 2 mM EDTA 0.2% Triton X-100 200 µg/ml Proteinase K

5.2.4 Polymerase chain reaction (PCR)

DNA fragments were amplified from cDNA or genomic DNA. Amplification of DNA templates for riboprobe synthesis and semiquantitative RT-PCR were done with Taq-polymerase (*Thermus aquaticus*). 3'UTRs and protein coding regions were amplified using Pfu-polymerase (*Pyrococcus fulgidus*). The annealing temperature was adjusted 5°C lower as the calculated melting temperature of the primer pair. To avoid unspecific amplification, the number of PCR cycles should not exceed 30. PCR products were analyzed on agarose gels (see 5.2.7).

The following components were set up on ice in a 0.5 ml PCR tube for a standard PCR using Taq-polymerase:

2xPCR Master Mix	12.5 µl
Primer 1 (10 pmol/µl)	1 µl
primer 2 (10 pmol/µl)	1 µl
cDNA template (300 ng)	/
dH_2O	ad 25 µl

A typical PCR cycle program for Taq-Polymerase:

Step	Temperature	Duration	
Initial denaturation	95°C	3 min	
Denaturation	95°C	30 sec	30x
Primer annealing	Accoding to primer sequence	30 sec	
Elongation	72°C	1 min/1 kb	
Final elongation	72°C	5 min	
Cooling	4°C	Unlimited	

5.2.5 Quantitative PCR.

Total RNA (see 5.2.1) was DNase treated and recovered by chloroform/phenol extraction (see 5.2.14) with subsequent ethanol precipitation (see 5.2.15). cDNA was synthesized from 4µg of total RNA (see 5.2.2). Quantitative PCR was performed using Absolute qPCR SYBR Green Mix (Thermo scientific) in the Stratagene Mx3000P cycler (Agilent Technologies) in triplicates. The average Ct values of triplicates were normalized with *gapdh* or *β-actin* to obtainΔCt values. For expression fold change analysis, $\Delta\Delta$Ct values were calculated. Detection of mature miRNAs was performed using miScript primer assays (Qiagen) according to the manufacturer's instructions. End-point PCR products were ethidium-bromide stained and analyzed by agarose gel electrophoresis (see 5.2.7).

5.2.6 Site-directed mutagenesis PCR

To generate plasmid-DNAs with specific nucleotide exchanges, a PCR-based site-directed mutagenesis approach was carried out. For this special PCR application, KAPAHiFi DNA-Polymerase was used. Mutagenesis primers (see 4.4) were designed with the help of http://www.bioinformatics.org/primerx. To remove wild type template DNA, the mixture was treated with 1 µl DpnI (10 U/µl) after PCR. DpnI digests only methylated DNA and therefore leaves the newly synthesised PCR product unaffected. After that, 20 µl of DpnI treated PCR product was transformed into *E. coli* (see 5.1.2) and bacteria cultivated on agar plates (see 5.1.3). Single clones were sequenced (see 5.2.13) to verify introduction of the mutation.

Components of a mutagenesis PCR:

5xReaction Buffer + Mg	10 µl
dNTPs (10 mM)	2.5 µl
Plasmid DNA template (~25 ng)	/
Primer 1 (10 pmol/µl)	1.25 µl
Primer 2 (10 pmol/µl)	1.25 µl
KAPAHiFi DNA-Polymerase	1 µl
H_2O	ad 50 µl

Cycle program for PCR-based mutagenesis:

Step	Temperature	Duration	
Initial denaturation	96°C	5 min	
Denaturation	96°C	30 sec	18x
Primer annealing	55°C	30 sec	
Elongation	70°C	6 min	
Final elongation	70°C	7 min	
Cooling	4°C	Unlimited	

5.2.7 Agarose gel electrophoresis of DNA/RNA fragments

DNA and RNA fragments were analyzed on agarose gels. For purification of PCR products or analysis of semiquantitative RT-PCR 1% agarose gels were used. DNA or RNA samples were mixed an appropriate volume

of loading buffer and loaded onto the gel. RNA samples were denatured for 10 min at 80°C to avoid secondary structures. After polymerisation, the gels were run in 1xTBE in an electrophoresis chamber. A voltage of 90 – 120 V according to gel size was supplied. To determine the size of DNA fragments the O'GeneRuler 100 bp DNA Ladder Plus (Fermentas) was used as size standard. DNA/RNA was stained for 20 min in ethidium bromide solution (10 mg/ml in 1xTBE). After destaining for 20 min in 1xTBE the gel was analyzed under UV light.

Solutions:

10xRNA loading buffer:	0.25% Bromphenolblue 4 mM EDTA (pH 8.0) 2.5% Formaldehyde 20% Glycerol 30% Formamide 4xMOPS buffer
10xDNA loading buffer:	0.25% Bromphenolblue 0.25% Xylenecyanol 30% Glycerol 100 mM EDTA 1% SDS

5.2.8 Agarose gel extraction

Extraction of DNA fragments from agarose gels was performed with the Macherey-Nagel NucleoSpin Extract II Kit following the producer's manual.

5.2.9 Denaturing polyacrylamide gel electrophoresis of RNA and DNA

Samples were mixed with an appropriate volume of 2xLoading buffer and heated for 4 min at 95°C (in the case of RNA). Tubes were transferred on ice and RNAs/DNAs loaded on denaturing polyacrylamide/8M urea gels after a forerun of 45 min. 8% polyacrylamide/8 M urea gels were run in 0.5xTBE, 15% polyacrylamide/8 M urea gels in 1xTBE. The run was performed with 500 V.

Solutions:

2xLoading buffer:	95% Formamide 18 mM EDTA (pH 8.0) 0.025% SDS 0.25% Bromphenolblue 0.25% Xylenecyanol

5.2.10 Photometric analysis of DNA and RNA

The concentration of purified DNA and RNA was determined photometricaly. For this an Eppendorf Biophotometer was used.

5.2.11 Restriction digest of DNA

Endonucleolytic digest of DNA was used to produce restriction sites for cloning, to analyse amplified and cloned PCR fragments or prepare template DNA for *in vitro* transcription. For this approximately 10 µg DNA were mixed with 10 units of restriction enzyme, recommended reaction buffer and H_2O. Digests were performed at 37°C for 1 h and directly analyzed on an agarose gel (see 5.2.7).

5.2.12 Production of plasmid constructs

PCR products amplified with Taq-polymerase (see 5.2.4) were ligated into the pCRII vector (see 4.3). The ligation reaction was performed following the TA Cloning Kit manual (Invitrogen).
For production of expression constructs, DNA fragments were ligated into the pCS2+ vector (see 4.3). If only one restriction site was used for cloning, the linearized plasmid (see 5.2.11) was dephosphorylated before the ligation reaction.
Components of a dephosphorylation reaction:

Linearized plasmid (100 ng)	/
10xSAP Buffer	0.5 µl
SAP	1 µl
ad 5 µl H_2O	/

The mixture was incubated at 37°C for 1 h. After dephosphorylation SAP was heat inactivated at 65°C for 10 min.
For ligation of DNA fragments a mixture with the following components was set up:

Linearized plasmid (100 ng)	/
Insert (200 ng)	/
10xT4 DNA Ligase buffer	2 µl
T4 DNA Ligase	1 µl
ad 20 µl H_2O	/

The ligation reaction was performed at RT for 1 h and transformed into competent bacteria cells (see 5.1.2). If only one restriction site was used for insert introduction, orientation of the insert was verified by DNA sequencing (see 5.2.13)

5.2.13 DNA sequence analyses

DNA sequences were analyzed by GATC Biotech AG. For this plasmid specific sequencing primers were provided by GATC biotech AG. Obtained DNA sequences were compared to annotated sequences using Vector NTI advance 10.

5.2.14 Phenol/chloroform extraction of DNA

To purify DNA from proteins, a phenol/chloroform extraction was performed. Half a volume of Roti-TE-Phenol (pH 7.5 – 8.0) and chloroform each were added, vortexed for 30 sec and centrifuged for 5 min at 16100 g. The aqueous phase was transferred into a new 1.5 ml Eppendorf tube and half a volume of Chloroform was added,

vortexed and again centrifuged for 5 min at 16100 g. The aqueous, DNA containing phase was removed and DNA was ethanol precipitated (see 5.2.15).

5.2.15 DNA precipitation

To get rid of salts and proteins in DNA solutions or to reach higher concentrations, the DNA was precipitated.
1/10 volume 3 M NaAc (pH 5.2) and two volumes of 100% EtOH were added to the DNA solution and the mixture was cooled down to -80°C for 30 min. The solution was centrifuged at 16100 g and 4°C for 1 h. The pellet was washed with 200 µl 80% EtOH by centrifugation for 10 min, air-dried completely afterwards and redissolved in a suitable volume of sterile water.

5.2.16 *In vitro* transcription of RNA probes (Riboprobes) for *in situ* hybridization

Riboprobes were used for whole mount *in situ* hybridization (see 5.5.3). To produce riboprobes, the template DNA was cloned into the pCRII vector (see 5.2.12). The pCRII vector (see 4.3) contains Sp6 and T7 promoters. By choosing the right RNA polymerase, sense and antisense probes can be synthesised.
The first step of *in vitro* transcription is to linearize the template DNA by cutting with a restriction enzyme (see 5.2.11). The restriction enzyme is chosen in a way that *in vitro* transcription will give rise to either sense or antisense transcripts. The linearized DNA was phenol/chloroform extracted (see 5.2.14) and precipitated (see 5.2.15).
Mixture for *in vitro* transcription of riboprobes:

Linearized DNA template (1 µg)	/
DIG/Flu-RNA labelling Mix (Roche)	2 µl
10xTranscription buffer	2 µl
rRNasin (Promega, 40 U/µl)	0.5 µl
RNA polymerase	1 µl
ad 20 µl H_2O	/

After 2 h of incubation, 1 µl RQ1 DNAse was added and the mixture was incubated for another 30 min at 37°C to remove the DNA template. The labelled RNA was purified with the NucleoSpin RNA Clean-up Kit (Machery-Nagel) following the manufacturers protocol. The RNA was precipitated with 1/10 volume 2 M NaAc (pH 4.2) and three volumes 100% EtOH for 30 min at -80°C. RNA was pelleted for 1 h at 16100 g and 4°C. The pellet was washed with 80% EtOH for 10 min, air-dried and dissolved in 25 µl H_2O. RNA was analyzed on an agarose gel (see 5.2.7). The RNA probes were stored at -80°C in a dilution of 24 µl RNA in 76 µl HybMix.
Solutions:

HybMix:
50% Formamide
150 µg/ml Heparin
5xSSC
5 mg/ml Torula RNA
0.1% Tween 20

5.2.17 *In vitro* transcription of capped mRNA

For overexpression experiments cotranscriptionally capped mRNA was generated from plasmid constructs. For that purpose, insert containing pCS2+ vector was linearized with NotI (see 5.2.11), phenol/chloroform extracted (see 5.2.14) and precipitated (see 5.2.15). *In vitro* transcription reaction was set up and performed with the mMessage Machine SP6 kit (Ambion) as described in the manual. RNA was affinity purified from the reaction mixture with the NucleoSpin RNA Clean-up Kit (Machery-Nagel). To yield mRNA suitable for microinjection experiments (see 5.4.2) RNA was additionally cleaned by precipitation with 1/10 volume 5 M NH_4Ac and three volumes 100% EtOH for 30 min at -80°C. RNA was pelleted for 1 h at 16100 g and 4°C. The pellet was washed with 80% EtOH for 10 min, air-dried and dissolved in 20 µl H_2O. Integrity of RNA was analyzed on an agarose gel (see 5.2.7). Capped mRNAs were stored at -80°C. To ensure satisfying protein translation after microinjection, repeated thawing and freezing of aliquots was avoided.

5.2.18 *In vitro* transcription of microRNA precursor molecules

Pre-mirs for injection experiments were obtained by T7 runoff transcription from a DNA template comprised of the T7-promotor fused to the antisense sequence of the respective pre-mir. To achieve full T7-polymerase activity, the two first nucleotides of pre-mirs were exchanged for "GG". It is noteworthy, that this alters the sequence of the resulting miRNA precursor and therefore could influence its processing. To generate the template for T7-polymerase transcription, 10 pmol T7 runoff template and 10 pmol T7 runoff primer were mixed in a volume of 10 µl of 1xTES. To anneal the two DNA oligos, the mixture was heated to 95°C for 1 min and cooled down to RT. The double stranded template was subsequently used for *in vitro* transcription.
Mixture for *in vitro* transcription of pre-mirs:

DNA template (60 pmol)	6 µl
10xTranscription buffer (Fermentas)	3 µl
ATP (100 mM)	1 µl
GTP (100 mM)	1 µl
CTP (100 mM)	1 µl
UTP (100 mM)	1 µl
rRNasin (Promega, 40 U/µl)	0.5 µl
DTT (100 mM)	1 µl
T7-RNA-Polymerase	1.5 µl
$MgCl_2$ (50 mM)	6 µl
ad 30 µl H_2O	/

After incubation for 2 h at 37°C again 1.5 µl T7-RNA-polymerase were added and transcription was run for another 2 h at 37°C. Transcripts were separated by denaturing 8% polyacrylamide gel electrophoresis (see 5.2.9). RNA bands were excised and frosted for 30 min at -80°C to make the gel porous. Afterwards RNA was eluted by shaking in 300 µl 0.3 M NaCl at 4°C over night. RNA was precipitated from the solution with 900 µl EtOH, 2.5 µl glycogen (Peqlab) and 120 µl 3 M NaAc (pH 5.2) at -80°C. After centrifugation for 2 h at 16100 g and 4°C the pellet was washed with 70% EtOH, air-dried for 10 min and resuspended in H_2O. Transcripts were

dephosphorylated by SAP mainly as described in 5.2.12 with 1 U of SAP/10 pmol of RNA. RNA was recovered by two times extraction with Phenol/chloroform, followed by ethanol precipitation as described above. Transcripts were 5'-[^{32}P]-labeld with γ-[^{32}P]-ATP (6000 Ci/mmol) and T4 Polynucleotide Kinase. The following conditions turned out to be efficient: 10 pmol RNA/10 µl reaction volume, 1.5 µl γ-[^{32}P]-ATP/10 pmol RNA and 5 U PNK/10 µl reaction volume. Phosphorylation was performed for 1 h at 37°C and completed by the addition of 1 µl non-radioactive 100 mM ATP and incubation for another 3 min. 5'-[^{32}P]-labelled pre-mirs were isolated by denaturing 8% acrylamide gel electrophoresis (see 5.2.9 and above).

5.2.19 Western blotting

For western blotting single embryo were transferred to 25 µl Fish protein loading buffer. Embryos were boiled at 95°C for 5 min and frozen in liquid nitrogen. After sonification in an ultrasonic bath embryos were homogenized by pipetting up and down with a 20 µl pipett. Before loading to a gel, samples were again heated at 95°C for 5 min and centrifuged at 16100 g and 4°C for 10 min.

Adult tissues were homogenized in lysis buffer by using M Tubes and a gentleMACS dissociator. Lysates were chilled on ice for one hour and sonified. Protein content was determined by Bradford assay with Bradford solution (Bio-Rad).

20 µg protein in protein loading buffer, or single embryos respectively were loaded on a 12% polyacrylamide gel per lane, run in 1xLämmli with 70 mA and semidry blotted on PVDF or nitrocellulose membrane (PALL) with 1xTowbin buffer or nitrocellulose blot buffer respectively. For transfer amperage of 0.8 mA/cm^2 was applied. Protein transfer was monitored by standard ponceau or amidoblack staining. Before antibody incubation membranes were blocked for 1 h in 5% milk powder in 1xTBT. Primary antibodies were diluted in PBS, TBT or NET-Gelatine and incubation was done over night at 4°C. Unbound primary antibody was removed by three washes with 1xTBT (or PBST) for 5 min each at RT. Secondary antibodies were applied to the membrane for 3 h at RT. Unbound secondary antibody was removed by three washes with 1xTBT (or PBST) for 5min each at RT. Luminol chemoluminescence was detected by exposition to CEA X-Ray Screens (Agfa). Membranes could be stripped in 100 mM Glycine (pH 2.5) at 60°C for two times 30 min and used for further antibody incubations.

Solutions:

Fish protein loading buffer:	2xProtein loading buffer 50 mM NaH_2PO_4 5 mM Tris (pH 8.0) 4 M Urea
4xProtein loading buffer:	10 mM Tris-HCl (pH 6.8) 50% Glycerine 1% SDS 0.25% Xylenecyanol 0.25% Bromphenolblue 5% β-Mercaptoethanol

Lysis buffer:	50 mM Tris-HCl (pH 7.5) 150 mM NaCl 1% Triton X-100
1xTowbin buffer:	20% Methanol 1xTowbin
Nitrocellulose blot buffer:	70% 1xLämmli 30% Methanol
Ponceau staining solution:	0.2% Ponceau 3% Trichloroacetic acid
Amidoblack staining solution:	2.5 mg/ml Amidoblack 45% Methanol 10% Acetic acid
Amidoblack destaining solution:	90% Methanol 2% Acetic acid
Net-Gelatine:	1xNET 0.25% Gelatine
PBST:	1xPBS 0.1% Tween 20
Luminol:	1.25 mM Luminol 100 mM Tris (pH 8.5)
Para-hydroxy coumarin acid solution:	6.8 mM p-Coumarin acid in DMSO
Luminol solution (ready to use):	10 ml Luminol 100 µl Para-hydroxy coumarin acid solution 8 µl 30% Hydrogen peroxide

5.2.20 Northern blotting

Approximately 30 µg total RNA from embryos and 10 µg total RNA from tissues (see 5.2.1) were separated by denaturing 15% polyacrylamide gel electrophoresis (see 5.2.9) and transferred on nylon membrane (GE Healthcare) by electro blotting in 1xTBE for 1 h with 400 mA. RNAs were UV-crosslinked to the membrane with an energy of 200000 µJ/cm^2. Membranes were blocked in Amersham Rapid-hyb Buffer (GE Healthcare) for 45 min at 40°C. Hybridization was carried out at 40°C in Rapid-hyb Buffer for 3 h. After hybridization, membranes were rinsed three times in 1xSSC and signals were detected with Biomax Intensifying Screens (Kodak) and Amersham Hyperfilm MP autoradiography films (GE Healthcare) at -80°C. Intensities of Northern and Western blot signals were quantified using the NIH ImageJ software package. Nylon membranes were stripped by boiling in 0.1XSSC/0.5%SDS for two times 15 min and reprobed. For detection of RNAs, 5'-[^{32}P]-labelled DNA oligos

were used. For efficient phosphorylation DNA oligos should have a 5'-G [162]. If miRNA sequences do not have a 5'-terminal C, a G was added to the probe sequence.
Components of a 5'-[^{32}P]-labelling reaction:

DNA oligo (10 pmol)	1 µl
γ-[^{32}P]-ATP (6000 Ci/mmol)	4 µl
T4 Polynucleotide Kinase buffer A	1 µl
T4 Polynucleotide Kinase	1 µl
H_2O	4 µl

The labelling reaction was performed for 1 h at 37°C. Bands were excised and made permeable at -80°C for 30 min. Probes were eluted by shaking in 300 µl Elution buffer over night at RT and precipitated (see 5.2.15).

Solutions:

Elution buffer: 0.5 M NH_4Ac
0.1 mM EDTA
2 mM $MgCl_2$
0.1% SDS
10 µl Glycogen (Peqlab)

5.2.21 Evaluation of poly(A)-tail lengths by RACE-PAT

To ascertain poly(A) tail lengths of miRNA targets, an application of 3' RACE, rapid amplification of cDNA ends poly(A) test (RACE-PAT) was used. This experimental procedure was mainly performed as described in [163]. Briefly, after GFP-reporter mRNA/miR duplex coinjection (see 5.4.2) RNA was isolated with Trizol (see 5.2.1) and reversely transcribed into cDNA (see 5.2.2) with an oligo(dT) anchor primer (see 4.4). CDNA was subsequently utilised for amplification of poly(A) tails by PCR with Taq DNA-polymerase (see 5.2.4). For this particular PCR, oligo(dT) anchor and pCS2MCSsense primers were used. The pCS2MCSsense primer specifically binds to the multiple cloning site of the pCS2+ vector and is therefore transcript specific for our GFP-reporter mRNAs. PCR products were analysed and visualized in agarose gels (see 5.2.7).

5.3 Bioinformatics

5.3.1 miRNA target site prediction

Zebrafish 3'UTRs were downloaded from the Ensembl genome browser (Zv9) using BioMart. Putative miRNA binding sites were predicted using the RNAhybrid algorithm as described in the respective publication ([164] and [165]). Only perfect 6 or 7mer seed site matches were accepted as putative target interaction sites. G-U wobble base pairs were allowed in the target prediction process.

5.4 Microinjection of zebrafish embryos

5.4.1 Morpholino mediated gene knockdown

Morpholino antisense oligos (see 4.5) were injected in zebrafish embryos for gene knockdown. Morpholino stocks (25 mg/ml) were stored at -80°C and diluted to an appropriate concentration directly before injection. Only one cell stage embryos were injected. For this, a petri dish was filled with 1.5% agarose solution in 30% Danieau's medium. A stencil with rectangular ledges was placed on top of the agarose solution before hardening to form deepenings. Before injection, the agarose was covered with Danieau's Medium and embryos were pushed with forceps into the grooves. Micropipettes for injection were produced from glass capillaries (Harvard Apparatus GC100F-10) by using a micropipette puller. Before injection morpholino solutions were heated to 65°C for 10 min and afterwards kept at RT. A volume of about 0.5 nl solution was injected directly into the yolk. Embryos were cultured as described in 4.1. Knockdown efficiency was controlled by either Western blot (see 5.2.19) or Northern blot (see 5.2.20).

5.4.2 GFP-reporter assay for *in vivo* miRNA target validation

In silico predicted miRNA target sites were validated *in vivo* by employing a GFP-reporter system. For reporter plasmid generation, 3'UTRs were PCR amplified (see 5.2.4) from cDNA (see 5.2.2) using gene specific primers. PCR products were subcloned into the pCRII vector (see 4.3) and cloned downstream of the GFP open reading frame into the pCS2+ vector by using EcoRI sites. Plasmids were linearized by NotI digest and transcribed into capped mRNA (see 5.2.17). Resulting GFP reporter mRNAs were injected at a final concentration of 100 ng/µl. Synthetic control miR (Negative Control #1) and miR-26b duplexes (Ambion) were injected at concentrations of 35 µM. GFP reporter mRNAs and miR duplexes were mixed, heated to 95°C for 3 min to eliminate secondary structures of the mRNA and afterwards kept on ice until transfer to micropipettes. Only 1-cell embryos were used for these experiments and a volume of approximately 0.5 nl of above described solutions were injected per embryo. Efficiency of GFP translation and resulting fluorescence was primarily detected by fluorescence microscopy 24hpf. For this, exposure times were retained between miR-26b and control miR experiments. Furthermore GFP contents of single embryos were analysed by Western blotting (see 5.2.19).

5.4.3 Pre-miRNA processing assay

In vitro transcription, [5'-^{32}P]-labelling, folding of the pre-mir before injection and detection of processing products was basically done as described in [166]. In short, pre-mirs were transcribed and [5'-^{32}P]-labelled (see 5.2.18). Prior to microinjection, pre-mirs were denatured at 95°C for 3 min and folded at RT for 10 min. Pre-mirs were injected at a final concentration of 0.1 µM. From 20 embryos per point in time, RNA was isolated (see 5.2.1) and separated on a 15% polyacrylamid/8 M urea gel (see 5.2.9). After the gel run, gels were incubated in 5% glycerol for 30min and dried at 80°C for 1.5 h. Signals were detected by exposition to a PhosphorImager (Molecular Dynamics).

5.5 Histological examinations

5.5.1 Fixation of zebrafish embryos

The chorion was removed from staged embryos with forceps and the embryos were transferred into a glass vial. Danieau's medium was pipetted off with a sterile transfer pipette and embryos were washed with PBST. Samples were fixed in 4% paraformaldehyde (PFA) over night at 4°C. PFA was washed out by three changes of PBST for 5 min. The embryos were stored in 100% MetOH at -20°C or in PBST at 4°C according to the experimental procedure.

5.5.2 Cryosections of zebrafish embryos

Morphological examinations of the zebrafish larvae were performed on transversal cryosections. For this, larvae were stored in PBST at 4°C after fixation, washed with three changes of PBST for 15 min each and incubated with 30% saccharose over night at 4°C. Up to five larvae were placed into an aluminium receptacle filled with Tissue-Tek (SAKURA) in a vertical orientation. The receptacle was frozen in buthylmethan cooled by liquid nitrogen and stored at -80°C. The temperature in a Jung Frigocut 2800N (Leica) was adjusted to -20°C and sections with a thickness of 8 – 14 µm were cut. Sections were transferred on SuperFrostPlus Microscope Slides (Menzel-Gläser) and stored at -20°C.

5.5.3 RNA whole-mount *in-situ* hybridization

The expression patterns of genes in different developmental stages were analyzed by RNA whole-mount *in-situ* hybridization.

Briefly, after fixation the embryos were stored in 100% MetOH for at least 12 h, rehydrated for 5 min in 75%, 50% and 25% MetOH dilutions in PBST each. After two washes in PBST for 5 min, the embryos were treated for different periods with 500 µl Proteinase K solution (5 µg/ml in PBST) depending on their developmental stage:

Developmental stage	Proteinase K incubation time
1 cell - epiboly	No incubation
1-somite – 6-somite	1 min
18-somite – 24hpf	4 min
31 hpf – 48hpf	20 min

Proteinase K solution was poured off and the reaction stopped by rinsing the embryo two times in 1xGlycine for 1 min. Proteinase K treatment was followed by refixation in 4% PFA in PBST for 20min. PFA was removed by two more washes with PBST. To block unspecific RNA binding sites, the embryos were prehybridized with 500 µl HybMix at 65°C for 1 h before incubating them with DIG- or Flu-labelled RNA probes. For this 1:100 dilutions in HybMix of sense or antisense probes were heated for 10 min at 80°C and chilled on ice for another 2 min. Hybridisation was carried out at 65°C over night. Unbound RNA probes were removed by incubation in two changes of 50% formamid/2xSSCT for 30 min each at 65°C, followed by a washing step in 2xSSCT for 30 min at 65°C and two washes in 0.2xSSCT for 30 min at 65°C either. To detect the specifically bound RNA probes,

embryos were washed once in PBST and incubated in 500 µl 5% sheep serum (heat inactivated) in PBST before adding a 1:2000 dilution of preabsorbed anti-DIG/Flu antibody. Samples were incubated with antibodies for 2 h at RT. Antibody solution was washed out with six washes in PBST, 20 min each, followed by two incubation steps with staining buffer for 5 min. Staining buffer was replaced by 500 µl NBT/BCIP staining solution. A blue colour reaction was obtained by incubation at RT in the dark. The staining reaction was stopped by washing three times with PBST. Stained embryos were stored in PBST at 4°C.

Solutions:

50% Formamid/2xSSCT:	2xSSC 1% Tween 20 50% Formamid
2xSSCT:	2xSSC 1% Tween 20
0.2xSSCT:	0.2xSSC 1% Tween 20
Staining buffer:	0.1 M NaCl 0.05 M $MgCl_2$ 0.1 M Tris-HCl (pH 9,5) 0.1% Tween 20
NBT/BCIP staining solution:	0.2 M NaCl 0.1 M Tris-HCl (pH 9.5) 0.1% Tween 20 2% BCIP/NBT Stock solution (Roche)

5.5.4 LNA whole-mount *in-situ* hybridization

For analysis of microRNA expression patterns, whole-mount *in situ* hybridization with 3'-DIG labelled LNA probes was done. Therefore embryos were fixed in PFA/methanol (see 5.5.1). Embryos were rehydrated by successive incubations in 75%, 50% and 25% methanol in PBS followed by four washes in PBST for 5 min each. Proteinase K (10 µg/ml) digest was performed as described in 5.5.3. After Proteinase K treatment embryos were refixed with 4% PFA in PBS for 20 min at RT and washed five times in PBST for 5 min. Samples were transferred into 500 µl Hybridization mix and prehybridized for 5 h. Hybridization temperature was adjusted 20°C below the calculated melting temperature of the LNA probe. Prehybridization mix was replaced by a 1:200 dilution of LNA probe in Hybridization mix. Hybridization was carried out over night in a water bath. To remove unbound probe, embryos were washed with Hybridization mix for 2 min and a series of 75%, 50% and 25% Hybridization mix in 2xSSC for 15min each. Additionally, embryos were washed for 15 min with 2xSSC and two times 30 min in 0.2xSSC. All steps were performed at hybridization temperature. Washing procedure was completed by incubations in 75%, 50% and 25% 0.2xSSC in PBST and 100% PBST at RT for 10min each. Before antibody incubation embryos were blocked with 2% sheep serum, 2 mg/ml BSA in PBST for several hours at RT. Incubation with AP-

conjugated-anti-digoxigenin antibody (1:5000, 2% sheep serum, 2 mg/ml BSA) was done over night at 4°C. Unbound antibodies were washed out by six changes of PBST for 15 min. Embryos were preincubated with Staining buffer for three times 5 min before staining reaction with NBT/BCIP staining solution. Staining reaction was stopped by several times exchanging Stop solution.

Solutions:

Hybridization mix:	50% Formamide 5xSSC 0.1% Tween-20 50 µg/ml Heparin 500 µg/ml tRNA → pH 6.0 with citric acid
Stop solution:	PBS 1 mM EDTA → pH 5.5

5.5.5 Whole-mount immunofluorescence staining

For whole mount antibody stainings, embryos were fixed with PFA/methanol (see 5.5.1). Specimens were rehydrated in 50% methanol for 5 min and H_2O for 1 h. Embryos were blocked with PBDT for 2 h at RT before primary antibodies (diluted in PBDT) were added. Antibody incubation was performed over night at 4°C. Unbound antibody was removed by four washing steps in PBST + 0.1% Triton X-100 for 30 min each. Incubation with secondary antibodies was also performed over night at 4°C, followed by again washing four times 30 min with PBST + 0.1% Triton X-100.

Solutions:

PBDT:	1% DMSO 1% BSA 0.5% Triton X-100 2.5% Goat serum 1xPBS

5.5.6 Immunofluorescence staining on cryosections

Sections were washed with three changes of PBS in a coplin jar. Unspecific binding sites were blocked with 2% goat serum in PBS for 20 min at RT. Primary antibodies were applied in PBS + 0.3% Triton X-100 + 5% goat serum over night at 4°C in a humidified chamber. The primary antibody was removed by washing three times with PBS for 15 min each. Fluorescent dye conjugated secondary antibody was also diluted in PBS + 0.3% Triton X-100 + 5% goat serum. Secondary antibody incubation was done over night at 4°C. Unbound secondary antibody was removed by three washes with PBS for 15 min each. Stained sections were mounted in Vectashield Mounting Medium with DAPI (Vector Laboratories).

5.5.7 Detection of apoptotic cells in zebrafish embryos

Apoptotic cells in zebrafish embryos were detected with the ApopTag Peroxidase *In Situ* Apoptosis detection Kit (Chemicon International), by TUNEL (TdT-mediated dUTP-biotin Nick End labelling) assay following the manufacturer's protocols.

5.5.8 Cartilage staining in zebrafish

Cartilage formation in the head region of zebrafish larvae was used as a marker for regular development after morpholino mediated gene knockdown. For this, Alcian Green staining was performed beginning with fixation for 10 min in 5% trichloracetic acid. Afterwards, samples were washed for 3min in acid-alcohol and stained for a period of 10 min with 0.1% Alcian Green in acid-alcohol solution. Background staining was removed by incubation with acid-alcohol for 10 min. To achieve a higher transparency, larvae were washed for another 10 min in Glycerol-KOH and stored in Glycerol-KOH at 4°C until microscopic inspection.

Solutions:

Acid-alcohol:	70% Ethanol 0.37% Hydrochloric acid
Glycerol-KOH:	0.25% KOH 43% Glycerol

5.5.9 Microscopic examination

For image acquisition, embryos were transferred from PBST into 3% methylcellulose or an increasing glycerol series with 50%, 70% and 86% glycerol followed by a short incubation each respectively. Samples were positioned in the right orientation for examination and overcastted by a cover slip. To take pictures of the head region with a higher magnification, the yolk was removed with a needle without damaging the remaining tissue.

5.6 Behavioural assays

5.6.1 Analysis of visual capacity of zebrafish larvae

To measure the Optokinetic Nystagmus (OKN), animals were positioned in 3% methylcellulose in a petri dish and placed in a drum with a diameter of 6 cm. The drum has alternating black and white stripes (12°/stripes), which are rotating around the larva. Wild type fish will follow the stripes by moving their eyes, until a distinct angle between the eyes and the anterior-posterior body axis is reached, before moving their eyes back to the start position. Fish with visual defects do not show this reaction. The drum is rotating with 7 rounds per minute. Videos of the eye movement were recorded and analysed with an Excel application.

6 RESULTS

6.1 The miRNA-26 family in zebrafish

6.1.1 Sequence and genomic localization of miRNA-26 family members are conserved in evolution

Four miRNA-26 family members were identified in the zebrafish genome (dre-miR-26a-1: MI0001923, dre-miR-26a-2: MI0001925, dre-miR-26a-3: MI0001926 and dre-miR-26b: MI0001927). To analyze the sequence conservation of this particular miRNA family, sequences of zebrafish, mouse and human orthologues were compared by multiple sequence alignment (Figure 8). The sequence of miR-26a is identical in zebrafish, mouse and human. MiR-26b is identical in mouse and human, whereas zebrafish miR-26b differs in two nucleotides. No miR-26 homologues were identified in invertebrates. The seed region (5'-nucleotides 2 – 8; see 3.1.2) is identical in all miRNA-26 family members from zebrafish, mouse and human (Figure 8). These sequence alignments show that the miRNA-26 family has been highly conserved across species in vertebrate evolution.

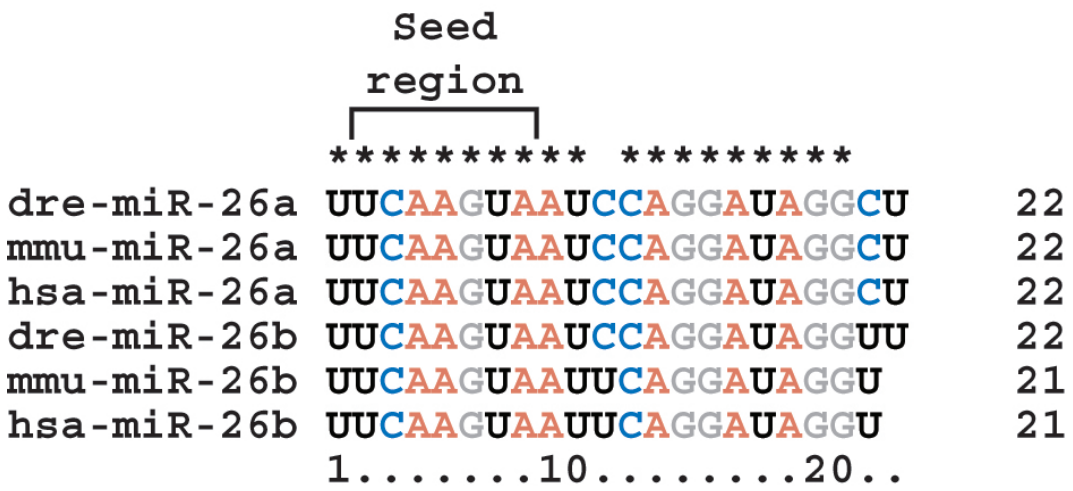

Figure 8: Alignment of miR-26 sequences from zebrafish, mouse and human.
Multiple sequence alignment of miR-26 family members shows evolutionary conservation of miR-26 between zebrafish (dre), mouse (mmu) and human (hsa). MiRNA sequences were exported from miRBase and aligned using Vector NTI alignment tool. Conserved residues are indicated with an asterisk. The seed region is marked with a bracked.

Database enquiry revealed that all four members of the miR-26 family in zebrafish are located in introns of *ctdsp* genes. In detail, in the zebrafish genome pre-mir-26a-1 is located within intron four of *ctdsp1* (ENSDART00000100226), pre-mir-26a-2 in intron four of *ctdsp like b* (*ctdsplb*, ENSDART00000089433), pre-mir-26a-3 in intron four of *ctdspla* (ENSDART00000089428) and pre-mir-26b in intron four of *ctdsp2* (ENSDART00000104035; Figure 9A). This interesting genomic constellation is evolutionary conserved, as all miRNAs-26 in *Xenopus tropicalis*, mouse and human are likewise located in introns of the respective *ctdsp* genes (Figure 9B).

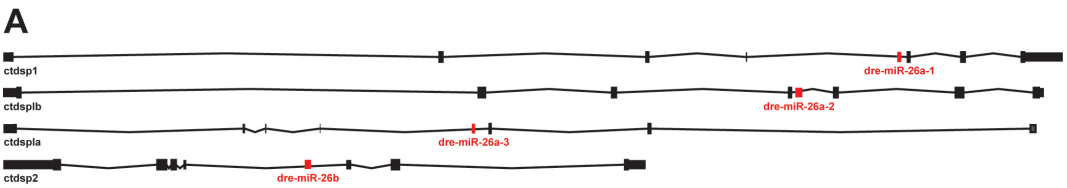

B

Intronic miRNA	Host gene
xtr-miR-26-1	*ctdsp2*
xtr-miR-26-2	*ctdsp1*
mmu-miR-26a-1	*ctdspl*
mmu-miR-26a-2	*ctdsp2*
mmu-miR-26b	*ctdsp1*
hsa-miR-26a-1	*ctdspl*
hsa-miR-26a-2	*ctdsp2*
hsa-miR-26b	*ctdsp1*

Figure 9: Genomic organization of the miRNA-26 family.
Genomic organization of the miRNA-26 family is highly conserved in evolution. **(A)** Schematic drawing of miR-26a and miR-26b host gene primary transcripts in the zebrafish (modified from ENSEMBL). **(B)** MiR-26/host gene combinations in Xenopus tropicalis (xtr), mouse (mmu) and human (hsa). All identified miR-26 family members are located in introns of *ctdsp* genes.

6.2 *In silico* target prediction for the miRNA-26 family

6.2.1 REST complex components are putative target genes of miRNA-26

To analyze the function of the miRNA-26 family in zebrafish development, knowledge of putative targets is indispensable. Therefore, an *in silico* target prediction effort was initially performed for miR-26a and miR-26b. Since both miRNAs share a common seed region (see 6.1) and the seed region is the major determinant for miRNA target recognition (see 3.1.2), most target sites are predicted to be bifunctional for miR-26a and miR-26b. Hence, in context target gene prediction the term miR-26 referes to miR-26a as well as miR-26b. Notably, zebrafish orthologues of REST-complex components and direct interaction partners (see 3.4.1) were identified as good target gene candidates for miR-26 (Table 1). This target prediction serves as basis for further validation experiments (see 6.3).

Table 1: *In silico* target prediction for miRNA-26
3'UTRs of REST-complex components contain putative miR-26 target sites. Numbers of miR-26 target sites correspond to miR-26a and miR-26b together.

3'UTR	Transcript ID	miR-26 target sites
braf35	ENSDART00000061617	3
corest1	ENSDART00000104219	3
corest2	ENSDART00000002961	1
c-ski	ENSDART00000100667	3
ctdsp1	ENSDART00000100226	1
ctdsp2	ENSDART00000104035	5
hdac3	ENSDART00000054626	2
n-cor1	ENSDART00000097574	3

6.3 *In vivo* validation of putative miR-26 targets

6.3.1 MiR-26b inhibits expression of Ctdsp2 in *cis*

Predicted miR-26 target genes in zebrafish are numerous (see 3.5.2 and Table 1). The *ctdsp2*-3'UTR harbours five putative target sites for miR-26, the highest value observed in the target prediction effort (see Table 1). Furthermore, protein products of *ctdsp1* and *ctdsp2* have well known functions in gene expression control and embryonic neurogenesis (see 3.4 - 3.4.2) and *ctdsp1* and *ctdsp2* are host genes of intronic miR-26a and miR-26b, respectively. Altogether, these characteristics make *ctdsp1* and *ctdsp2* very attractive candidates for *in vivo* validation experiments.

To analyze whether miR-26b represses Ctdsp2 protein synthesis *in vivo*, a miR-26b mimic was injected into zebrafish zygotes. Subsequently, expression of endogenous Ctdsp2 was analyzed by Western blotting of whole-embryo extracts using an affinity purified Ctdsp2 antibody. Injection of exogenous miR-26b duplex (35µM) leads to decreased protein levels of endogenous Ctdsp2, when compared to embryos injected with a control miRNA (co-miR; Figure 11A). Remaining amounts of Ctdsp2 were 34% (Figure 11A, lane 2) and 61% (Figure 11A, lane 4) in 31 and 48hpf embryos, respectively. Similar results could be observed for endogenous *ctdsp2* mRNA levels [167].

To test whether this inhibition was due to direct interaction between miR-26b and its predicted target sites within the *ctdsp2*-3'UTR, a set of reporter constructs was generated, containing the cDNA encoding for green fluorescent protein (GFP) and the full length *ctdsp2*-3'UTR in either sense or antisense orientation. These reporter constructs contain all five predicted miR-26b target sites in the *ctdsp2*-3'UTR (Table 1 and Figure 10). As specificity control, a reporter construct carrying mutations in the best candidate target site was generated. Probability of a putative target site to be functional *in vivo* was determined considering three parameters: Overall complementarity between miRNA and target 3'UTR, existence of seed matches (6 or 7mer) and the minimum free energy of the resulting miRNA/target mRNA duplex as thermodynamical feature. In this regard target site 1) (Figure 10) seems to be the best candidate. Sequence of wild type target site 1) (Figure 10) was changed from UACUUGA to UACGCGA by a site directed mutagenesis approach (mutated residues are underlined in Figure 10). Reporter mRNAs were transcribed *in vitro* and co-injected with synthetic miR-26b or a control miRNA.

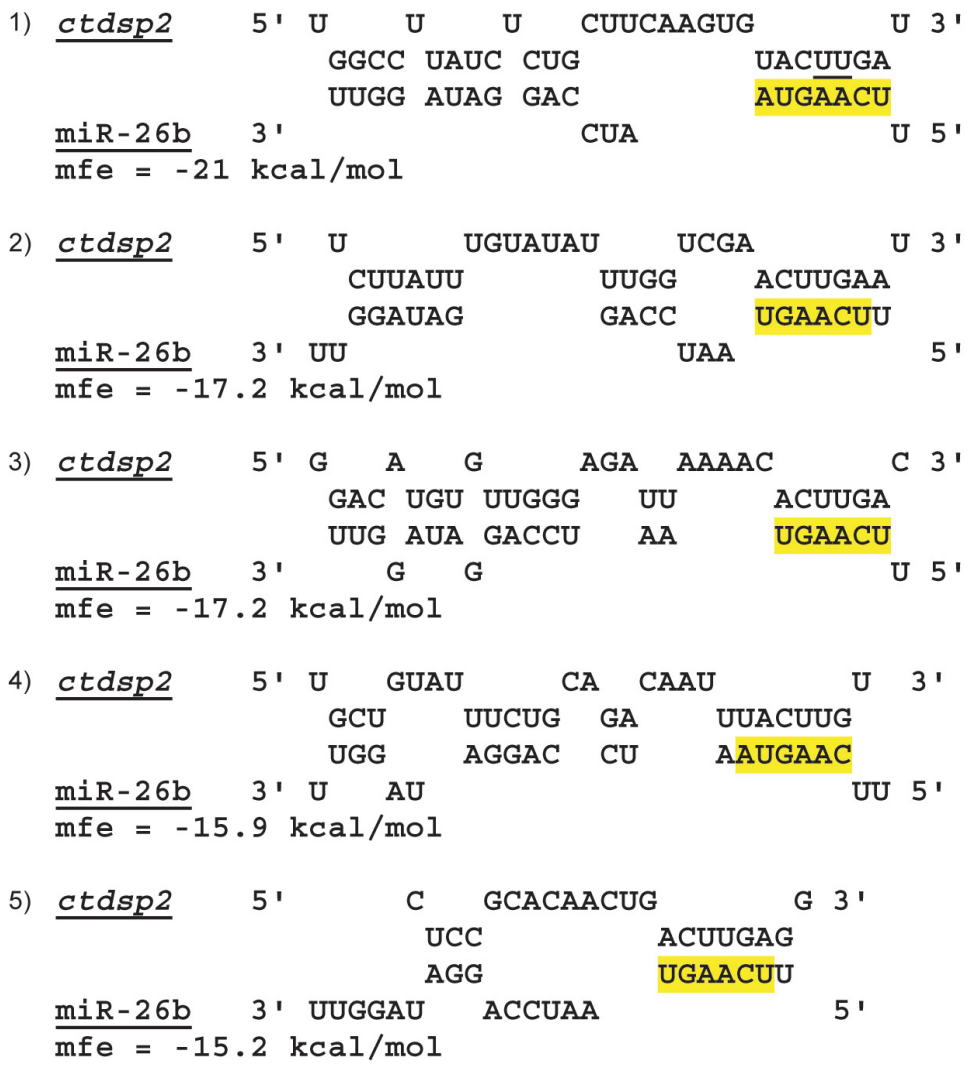

Figure 10: Predicted miR-26b target sites in the *ctdsp2*-3'UTR.
Zebrafish *ctdsp2* contains five putative target sites for its intronic miR-26b. *In silico* target prediction for miR-26b and the *ctdsp2*-3'UTR using the RNAhybrid algorithm. Seed matches are highlighted in yellow. The two nucleotides that were mutated in GFP reporter constructs are underlined in target site number 1. mfe: Minimum free energy.

To perform the GFP-reporter assay, reporter mRNAs and miRNA mimics were injected as described in 5.4.2. When injected alone or together with co-miR, robust GFP expression from all three *ctdsp2* reporters was observed 24hpf by direct fluorescence microscopy and Western blotting (Figure 11B, C). In contrast, coinjection of miR-26b duplex strongly repressed GFP expression from the wild type reporter but not from reporters containing the antisense or point-mutated 3'UTRs (Figure 11B, C, lane 2). These results were reproducible in five independent experiments. The inhibitory effect observed in the GFP-Reporter assay (Figure 11B, C) was highly reproducible and specific for the *ctdsp2* wild type 3'UTR, as the *β-actin*-3'UTR, serving as additional control, was not effected by miR-26b (Figure 12A - H). Together the data indicate that miR-26b silences *ctdsp2* through direct binding to a single active target site in its 3'UTR. The remaining four predicted target sites appear not to contribute to the observed effect. Thus *ctdsp2* is simultaneously host and target gene for intronic miR-26b, and object of an intrinsic inhibitory regulatory loop.

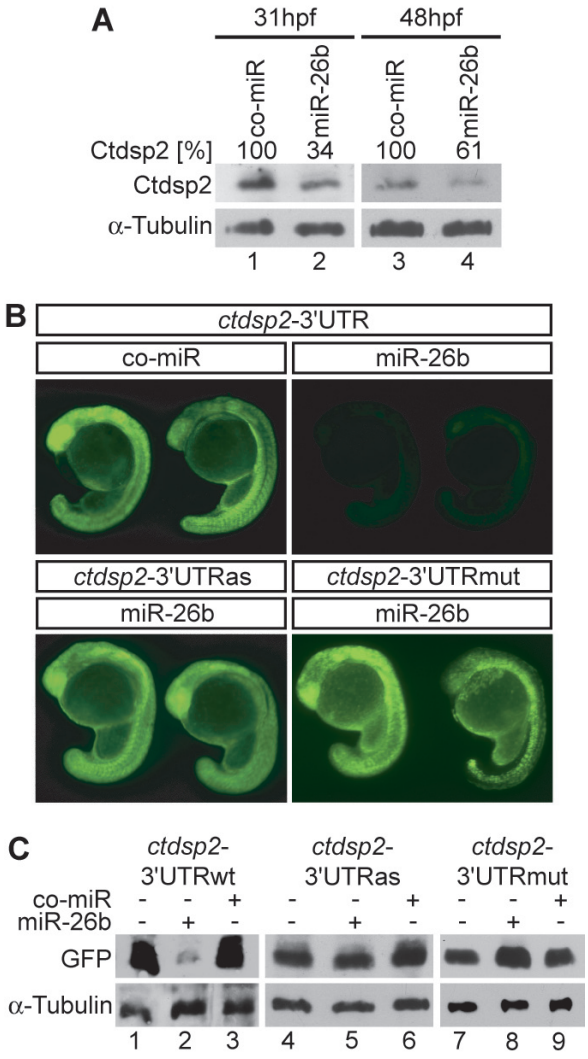

Figure 11: Zebrafish mir-26b inhibits expression of its host gene *ctdsp2*.
MiR-26b represses expression of *ctdsp2* mRNA *in vivo*. **(A)** Immunodetection of endogenous Ctdsp2 protein in extracts of 31 (lanes 1 and 2) and 48hpf (lane 3 and 4) zebrafish embryos injected with co-miR or miR-26b duplex. The percentage of remaining Ctdsp2 in miR-26b injected animals, as determined by densitometry, normalized to α-Tubulin is indicated. **(B)** GFP expression in zebrafish embryos from injected reporter mRNAs containing either the wild type, antisense or mutated (*ctdsp2*-3'UTRmut) 3'UTRs of *ctdsp2*. The expression of GFP in the presence of coinjected co-miR or miR-26b was assessed by fluorescence microscopy. **(C)** Repression of GFP expression from the wild type reporter construct by miR-26b was confirmed by Western blotting (lane 2). MiR-26b inhibits exclusively expression of the reporter containing the wild type sequence.

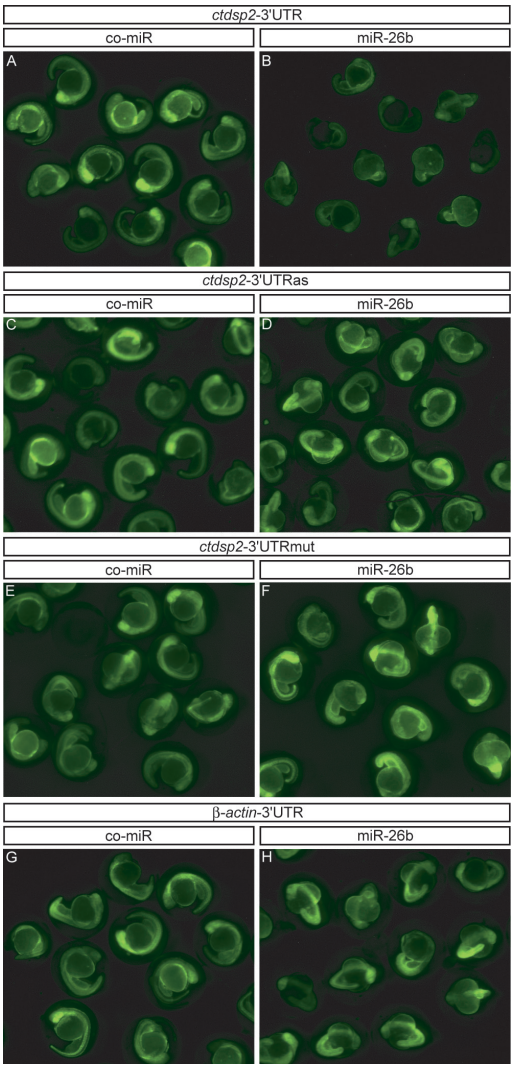

Figure 12: Validation of miR-26b target regulation.
(A - H) Fusion constructs of GFP cDNA and the indicated 3'UTRs were *in vitro* transcribed and coinjected with co-miR or synthetic miR-26b mimic (miR-26b) into zebrafish embryos. GFP expression was analyzed 24hpf by fluorescence microscopy. Inhibition was observed only after coinjection of wild type *gfp-ctdsp2*-3'UTR with miR-26b, whereas the antisense UTR (3'UTRas), the mutated UTR (UTRmut) or the unrelated *ß-actin*-3'UTR was not responsive to miR-26b.

MiRNAs can inhibit target gene expression by two different mechanisms. One mechanism is to cleave the targetmRNA in a siRNA like manner. The second mechanism is to block translation. This is accompanied by deadenylation and results in irreversible destabilization of the target mRNA (see 3.1.2). To analyze how miR-26b exerts its effect on target mRNAs in zebrafish, poly(A)-tail lengths of reporter mRNAs were measured by RACE-PAT. To this end, GFP-reporter mRNAs and indicated miRNAs (Figure 13) were coinjected. Reporter mRNAs contain a poly(A)-signal at their 3'-end and are efficiently poly-adenylated in a wild type background (Figure 13, lane 1 and 3). To measure poly-adenylation states under different conditions and at different points in time, total RNA was isolated 2 and 6h after injection and RACE-PAT was performed. For this particular PCR application a vector specific primer and an oligo(dT) anchor primer were used. With this primer combination 250bp of vector sequence and a variable stretch of the poly(A)-tail are amplified. As shown in Figure 13, reporter mRNAs coinjected with co-miR have estimated poly(A)-tails of 50 – 250 nt at both points in time (Figure 13, lanes 1 and 3). In contrast, reporter mRNAs coinjected with miR-26b duplex exhibit poly(A)-tails of only 50 – 150 nt (Figure

13, lanes 2 and 4). These findings are consistent with the previously reported influence of miRNAs on target poly(A)-tail lengths in zebrafish [7]. Endogenous *gapdh* mRNA levels are not influenced by treatment with miR-26b. These results indicate deadenylation of target mRNAs in presence of miR-26b, probably leading to degradation of these particular mRNAs.

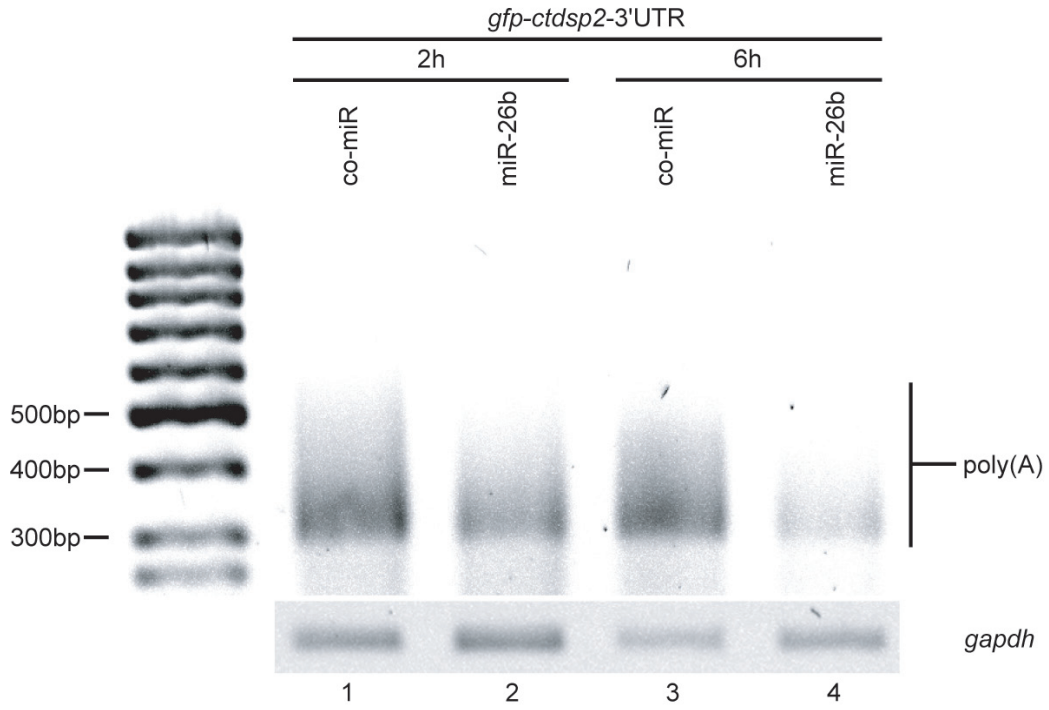

Figure 13: MiR-26b prevents target gene expression by deadenylation in zebrafish.
Poly(A)-tail length of exogenous target mRNAs was detected by rapid amplification of cDNA ends poly(A) test (RACE-PAT). The length of the smear represents the approximate size of all poly(A)-tails in the RNA sample in a transcript specific manner. Time course in the presence of coinjected co-miR or miR-26b duplex. Endogenous *gapdh* serves as loading control for RT-PCR. DNA size standard is shown on the left side. Coinjection of reporter constructs and miR-26b duplex prevents efficient polyadenylation and maintenance of poly(A) tail length of reporter mRNAs.

6.3.2 MiR-26a inhibits expression of Ctdsp2 in *trans*

Intronic miR-26b represses protein synthesis from its host gene *ctdsp2* in *cis* (see 6.3.1). Because miR-26a and miR-26b share identical seed site sequences (see 6.1), it seems likely that the *ctdsp2* transcript is also target of miR-26a. To test this hypothesis, the GFP-reporter system (see 6.3.1) was used in coinjection experiments with a synthetic miR-26a duplex. Mir-26a efficiently prevented GFP synthesis from the wild type 3'UTR construct, whereas co-miR had no effect on translation (Figure 14A). In contrast, no silencing of the mutated *ctdsp2*-3'UTR by miR-26a could be observed (Figure 14A). The effect observed by direct analysis of GFP fluorescence was confirmed by GFP Western blotting (Figure 14B). These results indicate that also miR-26a inhibits expression of Ctdsp2. Interestingly, regulation of Ctdsp2 expression by miR-26a depends on the same target site as by miR-26b (see 6.3.1) because the mutated reporter mRNA is translated in presence of miR-26a. As zebrafish miR-26a is encoded in introns of *ctdsp1* and *ctdspla/b* rather than in *ctdsp2* (see 6.1.1), the observed regulatory event

occurs in *trans*. Thus, not only miR-26b but also its close homologue miR-26a is able to target *ctdsp2* mRNA *in vivo*.

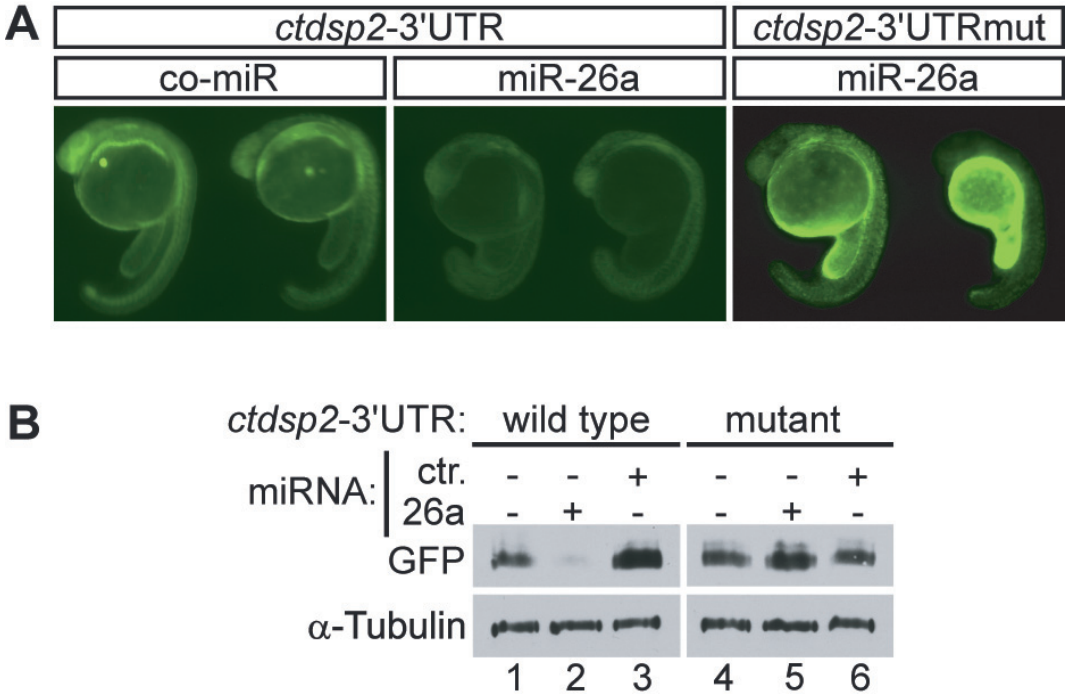

Figure 14: Repression of Ctdsp2 expression by miR-26a in *trans*.
(A) GFP expression in zebrafish embryos injected with *in vitro* transcribed reporter mRNAs containing the GFP coding sequence and wild type or mutated forms of the *ctdsp2*-3'UTR. The expression of GFP after coinjection of control miRNA (co-miR) or miR-26a was assessed by fluorescence microscopy and Western blotting **(B)**. MiR-26a significantly reduces GFP synthesis from the wild type but not the mutated reporter construct.

6.4 Expression patterns of miR-26 and *ctdsp* gene families

6.4.1 Maturation of pre-mir-26 is activated during zebrafish embryonic development

It has been described previously that miR-26b and *ctdsp2* mRNA are coexpressed from the same primary transcript (see 3.5.1). Since intronic miR-26b inhibits translation of the *ctdsp2* mRNA, as demonstrated in 6.3.1., steady coexpression of both RNA species would constitutively prevent Ctdsp2 protein synthesis. Given this, it is reasonable that the expression of miR-26b itself might be controlled posttranscriptionally as reported for other miRNAs [168]. Uncoupling the synthesis of mature miR-26b and *ctdsp2* mRNA by such a mechanism would make independent expression of mature miR-26b and Ctdsp2 protein possible. This would allow a cell-type and developmental stage specific expression of host gene and intronic miRNA. To test, whether miR-26 expression is indeed posttranscriptionally regulated, the expression pattern of miR-26 and its biogenesis intermediates during zebrafish development was analyzed.

A Northern blot analysis was performed to detect miR-26a and miR-26b in the course of early embryonic development. Northern blot probes directed against mature miR-26a and miR-26b also detected their respective pre-miRNAs (Figure 15A, B). The miR-26a probe specifically revealed expression of three RNAs within the size range of pre-mir-26a-1, pre-mir-26a-2 and pre-mir-26a-3 (~70 – 120 nt) in all embryonic stages analyzed (Figure

15A, lanes 1 – 6). Therefore it can be assumed that these three RNAs match the annotated pre-miRNAs of zebrafish miR-26a. Also pre-mir-26b could be detected by a similar Northern blot effort (Figure 15B, lanes 1 – 6). In contrast, mature miR-26a and miR-26b could be detected only at stages later than 24hpf (Figure 15A, B, lanes 4 – 6). Early embryos seem to devoid of mature miR-26a and miR-26b (Figure 15A, B, lanes 1 – 3) as no Northern blot signals were observed.

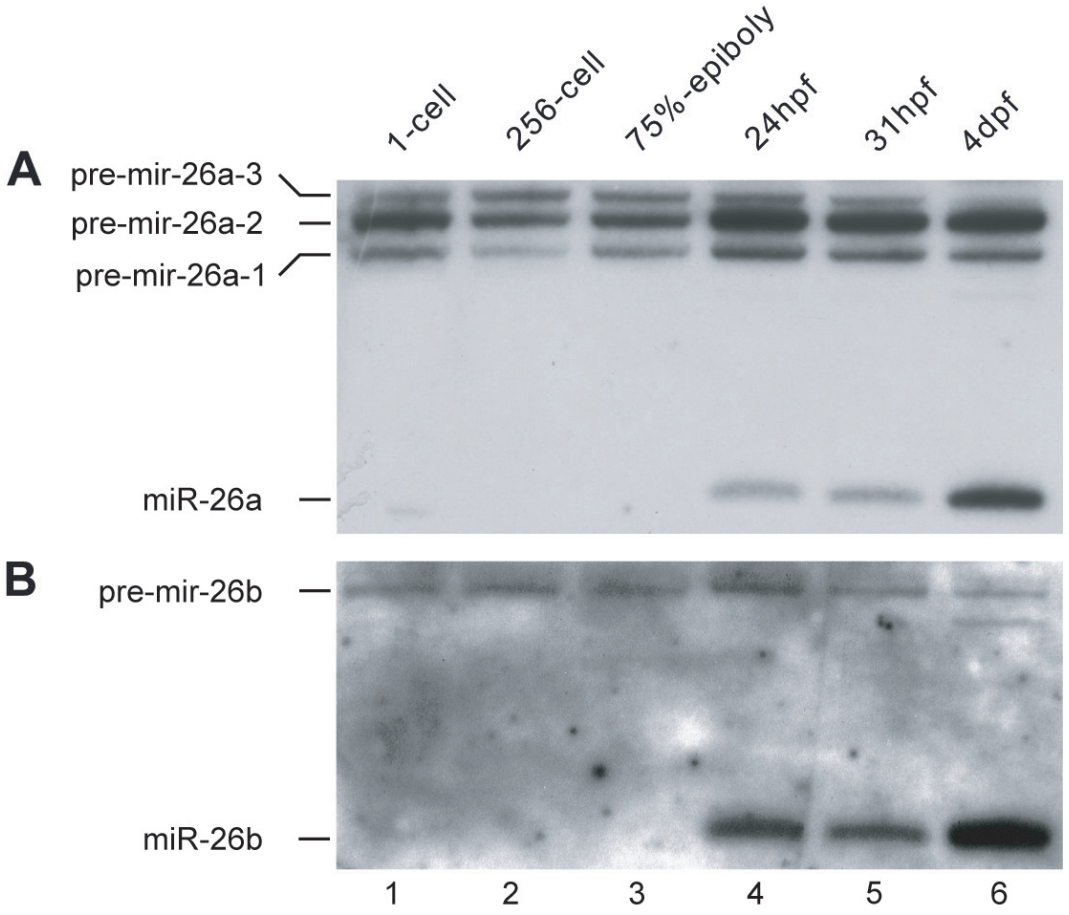

Figure 15: Conservation of posttranscriptionally regulated pre-mir-26 processing.
Simultaneous Northern blot detection of pre-mir-26 and mature miR-26 in zebrafish embryos. **(A)** pre-mir-26a-1, pre-mir-26a-2, pre-mir-26a-3 and mature miR-26a were detected using a 5-[^{32}P]-labelled DNA probe directed against mature miR-26a. **(B)** Detection of miR-26b and its precursor molecule pre-mir-26b as described in (A). Processing of both, pre-mir-26a and pre-mir-26b is inhibited in early zebrafish embryos.

To confirm these findings (Figure 15), expression of miR-26b and *ctdsp2* mRNA was investigated in more detail. The *ctdsp2* mRNA was present only in minute amounts before onset of zygotic transcription at the mid-blastula transition (MBT) as determined by quantitative PCR (qPCR, Figure 16A). Northern blot analysis of whole embryo RNA, using a loop specific probe, revealed that pre-mir-26b was indeed present from the 1-cell stage on and expressed in equal amounts throughout embryonic development (Figure 16A, lanes 1 - 6). In contrast, mature miR-26b was observed only at stages later than 24hpf (Figure 16A, lanes 4-6). Similar expression and processing patterns were found in a further analysis of pre-mir-26a-1 and mature miR-26a [167]. The discrepancy in expression patterns of pre-mir-26b and mature miR-26b seem to be due to regulated processing of pre-mir-26b. First, pre-mir-26b levels were stable before the onset of zygotic transcription (Figure 16A, lanes 1 - 2). This observation argues against constant processing and increased turnover of miR-26b in early embryos. Second, steady levels of pre-mir-26b are not due to generally reduced Dicer activity, as pre-mir-430b-1, a precursor of

embryonic miR-430b [8], was processed efficiently at the 75%-epiboly stage (Figure 16A, lane 3), at which mature miR-26b was still absent. Dicer processing and consequently appearance of mature miR-26b (Figure 16A, lane 4) coincided with expression of miR-124 (Figure 16A, lanes 4-6), which is expressed exclusively in neuronal tissues [139]. Pre-mir-124-1 was hardly detectable in zebrafish embryos (Figure 16A, lanes 1 – 6) indicating efficient processing of this particular miRNA precursor and excluding the possibility that pre-miRNA accumulation is a general effect in zebrafish embryonic development.

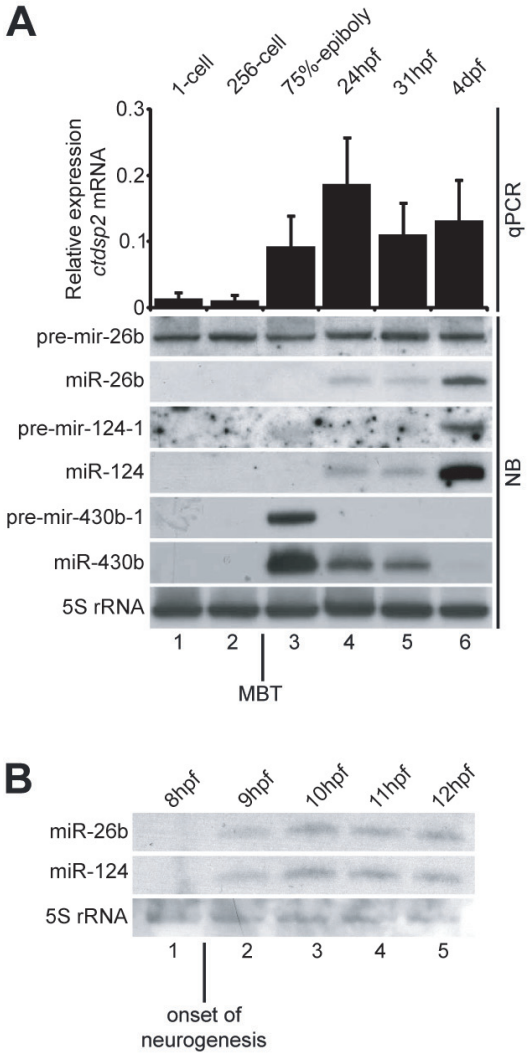

Figure 16: Activation of pre-mir-26b processing during zebrafish embryonic development.
Expression profiling of *ctdsp2* mRNA and miR-26b in zebrafish embryonic development. **(A)** Expression levels of *ctdsp2* mRNA relative to *gapdh* were measured by quantitative real time PCR (qPCR; upper panel). For this, primers spanning exon-intron boundaries were used to avoid amplification of genomic regions. Northern Blot detection (NB; lower panel) of precursor and mature miR-26b, -124 and -430b. Total RNA was blotted and probed with specific 5'-[^{32}P]-labelled DNA oligos. 5S ribosomal RNA serves as loading control. **(B)** Northern blot detection of miR-26b and miR-124 in an early time series of embryonic development as described in (A). The midblastula transition (MBT) and onset of neurogenesis are indicated. Processing of pre-miR-26b is inhibited in embryos before 9hpf.

Northern blot analysis with higher temporal resolution (Figure 16B) revealed expression of miR-26b and miR-124 at stages later than 9hpf (Figure 16B, lanes 2 – 5). Both miRNA species were absent at 8hpf (Figure 16B, lane1; note that 8hpf = 75%-epiboly). These findings are consistent with the results shown in Figure 15 and suggest that fully processed pre-mir-26a and pre-mir-26b are delivered maternally to the embryo, as 1-cell and 256-cell

embryos are still transcriptionally silent [160]. However, pre-mir-26 processing appears to be inhibited in early zebrafish embryos. During later stages inhibition is abrogated, leading to a temporal expression pattern of mature miR-26a and miR-26b very similar to neuronal miR-124.

6.4.2 Pre-mir-26b is processed after onset of neuronal cell differentiation

Appearance of mature miR-26b coincided with the generation of cells of the neuronal lineage in zebrafish. This was evident by the identical expression profile of miR-26b and miR-124 (Figure 16), which is expressed exclusively in neuronal tissue [139].

To specifically analyze the efficiency of pre-mir-26b processing in context of neuronal cell differentiation, miR-26b biogenesis was assessed during induced neuronal differentiation of mouse P19 teratocarcinoma cells ([167], [169] and [170]). P19 cells can be differentiated into neuron like cells and astrocytes by treatment with retinoic acid (RA) and neuronal differentiation is accompanied by loss of stem cell properties [169]. Induced neuronal differentiation of P19 cells is a generally accepted paradigm for cell fate determination and neuronal development ([169] and [170]).

Untreated proliferating cells expressed miR-26b at low levels, as determined by quantitative real-time PCR (qPCR, Figure 17, lane 1, upper panel). Likewise, neuronal markers miR-124 and Tuj1 could not be detected by Northern and Western blotting in these cells (Figure 17, lane 1, middle and lower panel) illustrating the non-neuronal character of these cells. Pre-mir-124-2 precursor was also absent, suggesting that lack of mature miR-124 is due to transcriptional repression (Figure 17, lane 1, middle panel). In contrast, pre-mir-26b was present in similar amounts in undifferentiated cells and throughout RA induced neuronal differentiation (Figure 17, lanes 1 – 6, middle panel). RA induced cell differentiation led to a gradual increase in efficiency of pre-mir-26 processing, as indicated by increasing ratio of mature miR-26b to pre-mir-26b (Figure 17, lanes 1 – 6, middle panel). Interestingly, appearance of miR-26b occurred before expression of neuronal markers miR-124 and Tuj1 (Figure 17, lanes 1 – 6, middle and lower panel) and hence before terminal cell differentiation. The observed increase of pre-mir-26b processing efficiency during neuronal cell differentiation very well reflects the situation observed during zebrafish embryonic development (Figure 15 and Figure 16). These data indicate that biogenesis of mature miR-26b is posttranscriptionally regulated during neuronal cell differentiation at the level of precursor processing and is an early marker for differentiating cells of the neuronal lineage.

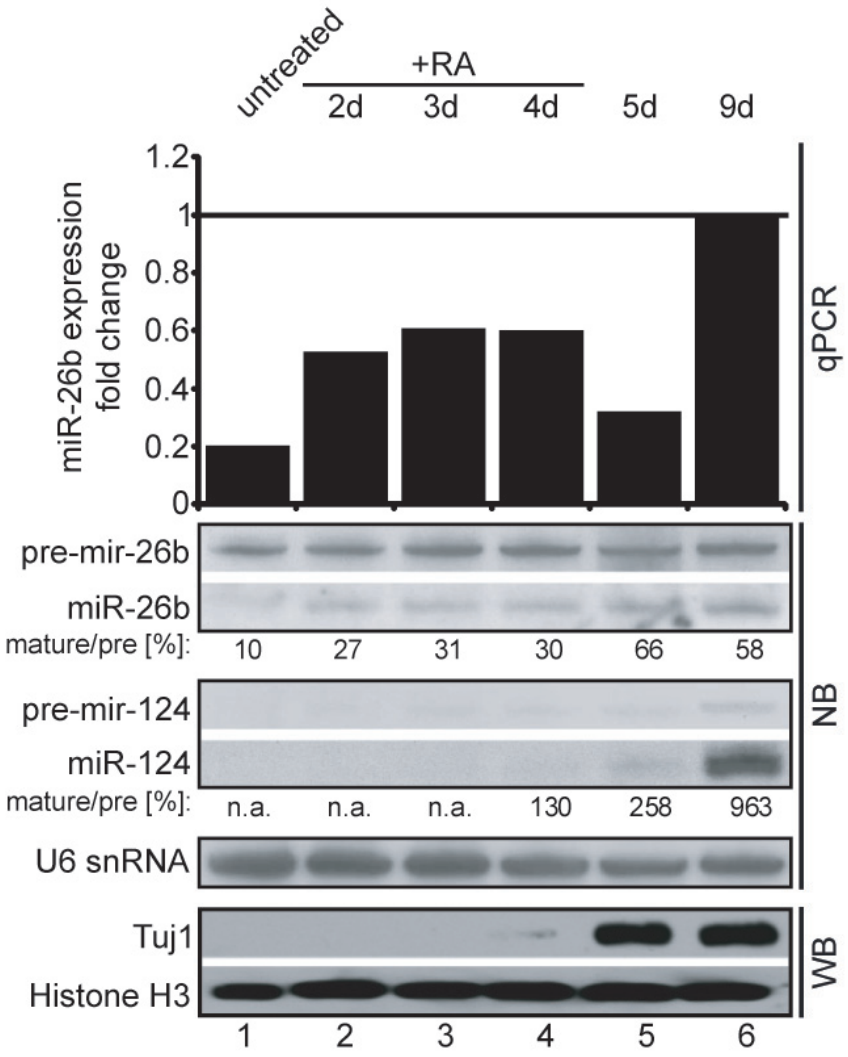

Figure 17: Activation of miR-26b maturation in differentiating neurons.
Pre-mir-26b expression and processing during retinoic acid (RA) induced neuronal differentiation of mouse P19 cells. Total RNA was extracted at indicated points in time and expression of the indicated miRNAs analyzed by quantitative real-time PCR (qPCR, upper panel) or Northern blot (NB, middle panel) detection with 5'-[^{32}P]-labelled DNA probes. Fold change expression of miR-26b was calculated from qPCR data. NB signals were quantified by densitometry and ratios between mature and precursor miRNAs calculated. U6 snRNA served as loading control. As a marker for terminally differentiated neurons, expression of the Tuj1 antigen was analyzed by Western blotting (WB, lower panel). Histone H3 served as loading control. Pre-mir-26b is stably expressed in undifferentiated cells. Induction of neuronal cell differentiation stimulates processing of pre-mir-26b and consequently accumulation of miR-26b during differentiation. d: days. n.a.: not applicable due to expression below detection limit. Note that these data were partially obtained in collaboration with other employees of the Department of Biochemistry.

6.4.3 Differential processing leads to neuronal enrichment of miR-26b

To test whether pre-mir-26b processing is also regulated in adult tissues containing mainly differentiated cell types, a Northern blot analysis was performed with RNA from isolated adult zebrafish tissues. Pre-mir-26b was detected in equal amounts in all tissues tested, indicating that it was produced with similar efficiency in all analyzed tissues (Figure 18, lanes 1 – 5). The *ctdsp2* transcript could likewise be detected in all analyzed tissues by quantitative real time PCR (qPCR, Figure 18, lanes 1 – 5). However, *ctdsp2* expression level was highest in brain and similar in skin, fin, eye and muscle (Figure 18, lanes 1 – 5). To exclude the possibility of PCR amplification from genomic DNA, these findings were further supported by semi-quantitative PCR with a different primer pair. No PCR product from genomic DNA contaminations was amplified by qPCR using exon-intron

boundary spanning primers or from the –RT control in semi-quantitative PCR (Figure 18, lanes 1 – 5). Together, these results show that *ctdsp2* mRNA is expressed ubiquitously in adult zebrafish. Likewise, mature miR-26b was also ubiquitously expressed, however, this miRNA was significantly enriched in eye and brain, as evident by highest ratios of mature miR-26b to pre-mir-26b in these neuronal tissues (Figure 18, lanes 3 – 4). These findings could be reproduced in three independent Northern blot experiments (also for miR-26a; [167]). MiR-124 was only detected in eye and brain, demonstrating strictly neuronal expression of this particular miRNA and that non-neuronal tissues were not contaminated with neurons during preparation (Figure 18, lanes 3 – 4). Importantly, the expression pattern of mature miR-26b and miR-124 was reciprocal to that of Ctdsp2 protein in neuronal tissues. By Western blotting, Ctdsp2 could only be detected in skin and fin and muscle (Figure 18, lanes 1 – 5). However, Ctdsp2 was completely absent from eye and brain (Figure 18, lanes 2 – 3). This is consistent with its previously described function as negative regulator of neurogenesis (see 3.4.2).

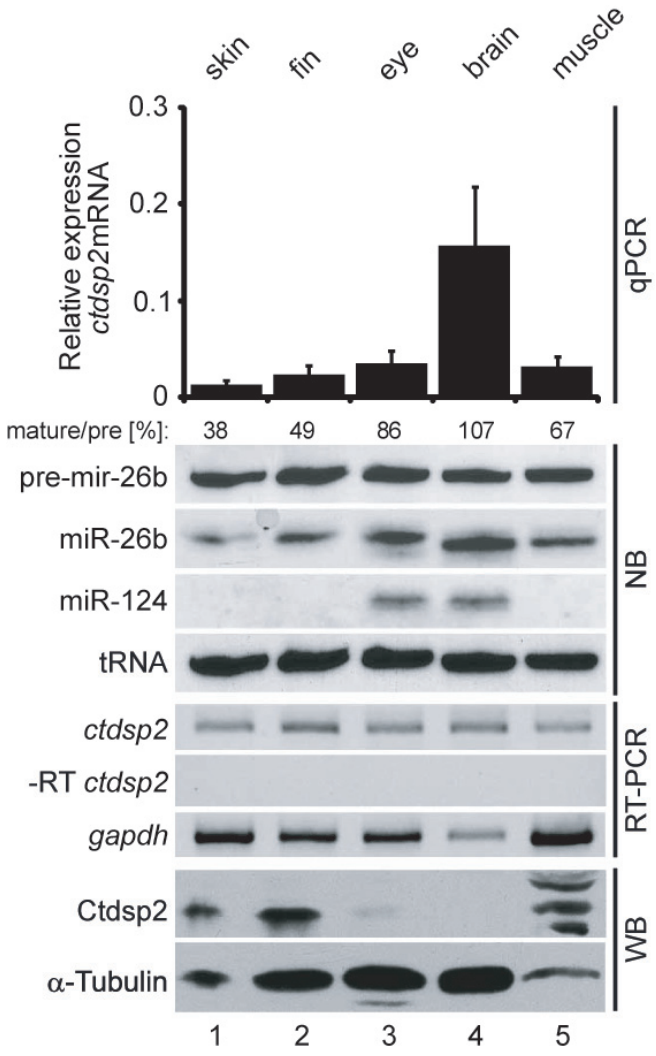

Figure 18: MiR-26b is enriched in neuronal tissues.
Expression profiling of the indicated factors in dissected adult zebrafish tissues. Expression level of *ctdsp2* mRNA was analyzed by quantitative real-time PCR (qPCR) and semiquantitative RT-PCR (RT-PCR). Expression relative to *β-actin* (in case of qPCR) and *gapdh* (in case of RT-PCR) was calculated, consistently showing ubiquitous expression. Pre-mir- and miR-26b were analyzed by Northern blotting (NB). Northern blotting shows neuronal enrichment of mature miR-26b. Northern blot signals were quantified by densitometry. The ratios of mature miR-26b to its pre-mir-26b are indicated on the top. TRNA served as loading control. Ctdsp2 protein was detected by Western blotting (WB) with affinity purified antibody. α-Tubulin antibody was used to prove equal loading. Expression patterns of mature miR-26b and Ctdsp2 protein are complementary.

Taken together, this analysis suggests that on the organismic level, pre-mir-26b is ubiquitously expressed. It is co-expressed with its *ctdsp2* host transcript and uniformly Drosha processed. Further processing to mature miR-26b, however is inefficient in non-neuronal tissues, thus leading to low expression levels of mature miR-26b in these tissues. This mechanism uncouples expression of *ctdsp2* mRNA and mature miR-26b, leading to repression of Ctdsp2 protein production in zebrafish neuronal tissues, while allowing its expression in non-neuronal tissues. Inhibition of Ctdsp2 protein synthesis is caused by posttranscriptional mechanisms, most likely the combined action of mir-26a, miR-26b and miR-124 (see also 6.3.1., 6.3.2 and 6.6).

6.4.4 Spatiotemporal expression pattern of miR-26 in zebrafish embryos

In previous sections, experiments were described that show differential processing of miR-26 precursors during zebrafish embryonic development and in dissected adult zebrafish tissues (see 6.4.1 and 6.4.3). However, Northern blot analysis fails to provide spatial information about the dynamics of gene expression. To investigate embryonic expression patterns of miR-26 and *ctdsp* gene family members *in situ* hybridization (ISH) was performed. Locked nucleic acid ISH to specifically detect miRNAs, revealed very similar expression patterns for mature miR-26a and miR-26b. Both are expressed ubiquitously 12hpf (Figure 19A, D). In later developmental stages (24 and 31hpf) expression of miR-26a and miR-26b is still ubiquitous, except the notochord (Figure 19B, C, E, F; arrows in C and E). By using a GFP-reporter containing an artificial miR-26b target site, very similar data were obtained [167]. Nevertheless stronger ISH signal could be observed in the head region, including the eyes (Asterisks in Figure 19B, C, E, and F). These findings confirm the previously described adult expression pattern of miR-26b (see 6.4.3). Expression pattern of pri-mir-26b was analyzed 24hpf by RNA ISH using a specific probe for intron four of the *ctdsp2* primary transcript. Nearly ubiquitous expression was observed with highest levels in the head (Figure 19H) and no expression in the notochord (arrow in Figure 19H). This is consistent with the expression pattern found for *ctdsp2* mRNA in adult zebrafish (see 6.4.3). Taken together ISH experiments show that mature miR-26 and its precursors are ubiquitously expressed throughout zebrafish embryonic development, but expression is stronger in neuronal tissues (brain and eye) in later stages. In this context, it has to be considered that the LNA probes used in this assay are directed against mature sequences of miR-26a or miR-26b. These probes will also detect the respective pre-miRNA which is ubiquitously expressed at high levels (see 6.4.1 and 6.4.3) and therefore eventually masking a more tissue specific expression pattern of mature miR-26.

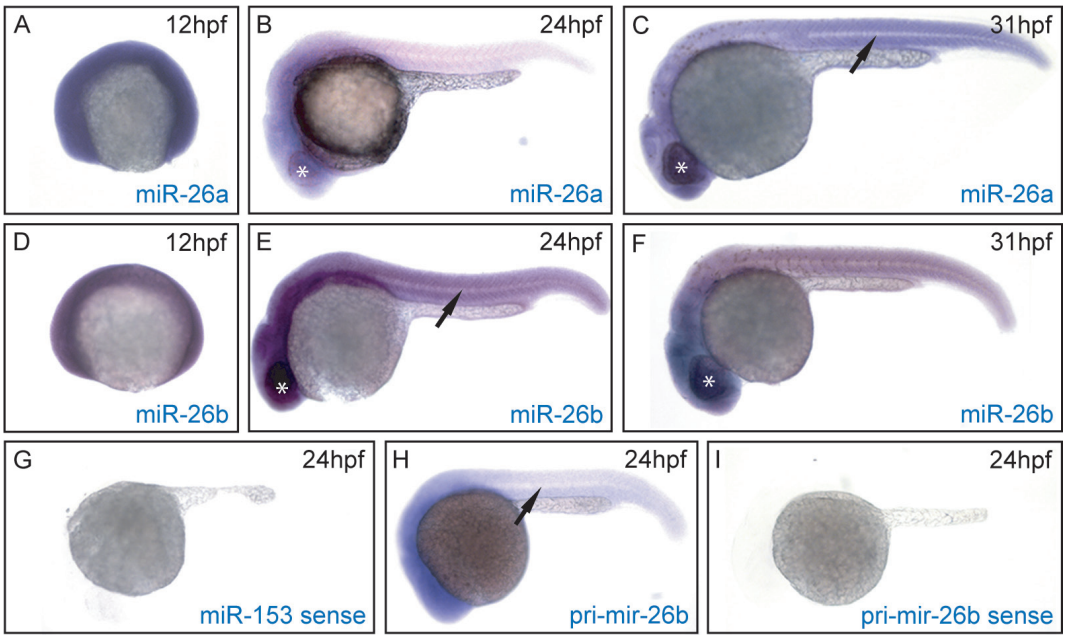

Figure 19: Embryonic expression pattern of the miR-26 family.
Analysis of pri-mir-26, pre-mir-26 and mature miR-26 spatiotemporal expression patterns in developing zebrafish embryos. **(A - C)** MiR-26a is expressed ubiquitously in the developing zebrafish embryo. Whole mount locked nucleic acid (LNA) *in situ* hybridization of dre-miR-26a. (A) 12hpf; (B) 24hpf; (C) 31hpf. **(D - F)** MiR-26b is expressed ubiquitously in the developing zebrafish embryo. Whole mount locked nucleic acid (LNA) in situ hybridization of dre-miR-26b. (D) 12hpf; (E) 24hpf; (F) 31hpf. Expression of either miR-26a or miR-26b is detectable in all cell types except the notochord (arrows in (C) and (E)). **(G)** To eliminate the possibility of unspecific background staining a LNA probe with miR-153 sense sequence was used as a negative control. **(H - I)** Pri-mir-26b is broadly expressed in zebrafish embryos. Whole mount RNA *in situ* hybridization of *ctdsp2* intron 4. A 500 nt RNA probe covering a part of *ctdsp2* intron 4 containing pre-mir-26b was used to stain regions with expression of *ctdsp2* pre-mRNA/pri-mir-26b. **(I)** Negative control using a pri-mir-26b sense probe.

6.4.5 Embryonic expression patterns of *ctdsps* in zebrafish

Ctdsp2 mRNA is expressed after activation of embryonic transcription at MBT (Figure 16A). In adult individuals *ctdsp2* mRNA is expressed ubiquitously with strongest expression in brain (Figure 18). To gain more insight into the embryonic expression patterns of *ctdsp* gene family members, whole mount RNA ISH was performed. Although all *ctdsp* gene family members are closely related and redundant in their function ([110] and [114]), they differ enough in their nucleotide sequence to be distinguished from each other by ISH. Furthermore, to avoid cross reaction of probes with other *ctdsp* transcripts, probes were designed to detect more unique 3'UTR sequences when necessary. *Ctdspla*, *ctdsp1* and *ctdsp2* show very similar expression patterns. 12hpf all three are expressed ubiquitously (Figure 20A, G and J). 24 and 31hpf expression is more restricted to head and brain regions (Figure 20B, C, H, I, K and L). For all three genes, a domain of strong expression could be observed overlaying the yolk sac. So far the cell type or tissue which forms the basis for this observation could not be identified. *Ctdsplb* differs in its expression pattern from the other *ctdsp* gene family members. In the 24 and 31hpf stage, *ctdsplb* mRNA is strongly expressed in somites (arrows in Figure 20E – F). Together the described ISH experiments show that *ctdsp* genes are ubiquitously expressed in the developing zebrafish embryo between 12 and 31hpf. Only *ctdsplb*, as exception is strongly expressed in somites, a non-neuronal tissue.

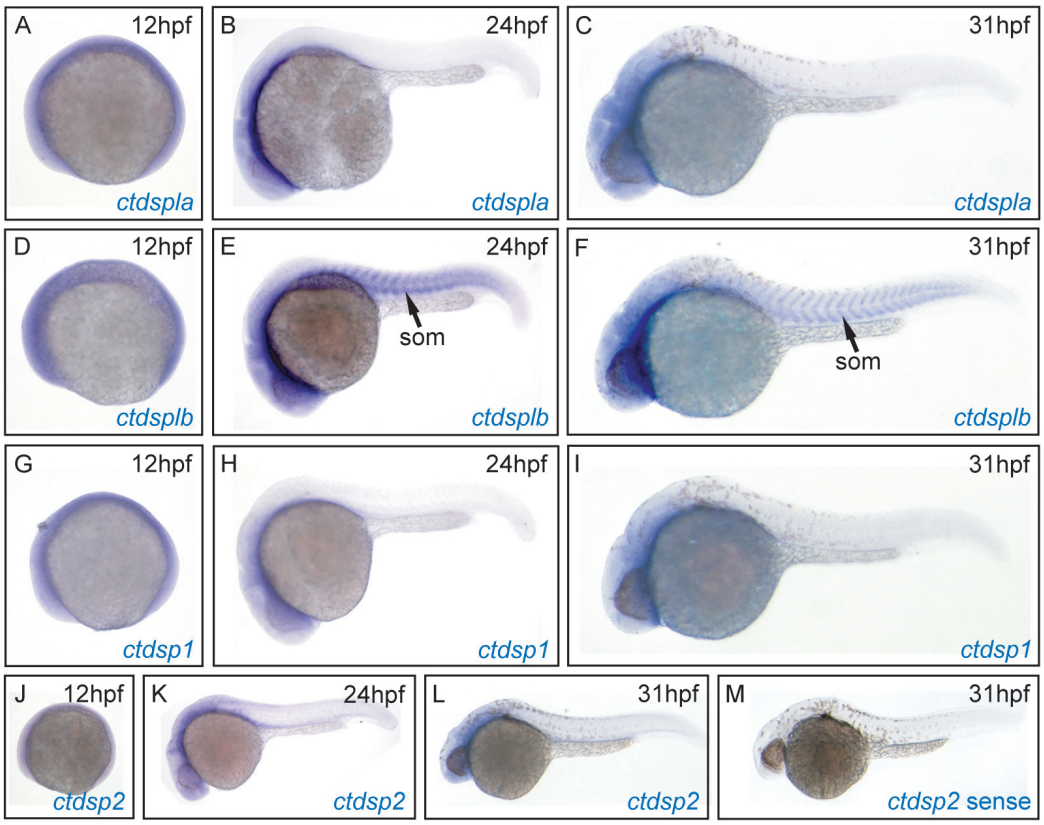

Figure 20: Embryonic expression pattern of the *ctdsp* gene family.
The *ctdsp* gene family shows ubiquitous expression patterns on mRNA level. Pictures represent lateral views of whole mount RNA ISH of **(A-C)** ctdspla, **(D-F)** ctdsplb, **(G-I)** ctdsp1 and **(J-L)** ctdsp2. **(M)** Sense control for *ctdsp2*. Som: somite.

6.5 Phenotypic characterization of miR-26 depleted zebrafish embryos

6.5.1 Inactivation of miR-26b leads to impaired neuronal cell differentiation

In context of the REST-complex, Ctdsps function in repression of neuronal genes during embryogenesis. In neurons, expression of Ctdsps is inhibited by neuronal miR-124. As transcription of miR-124 is itself under negative control of the REST-complex, additional factors are required to initially abrogate this inhibition and allow expression of miR-124 and other RE1 containing neuronal genes (see 3.4.2). Experiments described in this study show that during neuronal cell differentiation miR-26b is upregulated and expressed prior to miR-124 already in pre-mature neurons (see 6.4.2). As miR-26b represses expression of Ctdsp2 protein (see 6.3.1), it might contribute to early events during transition from neuronal progenitor cell to neuron and consequently development of the CNS.

To test this, miR-26b expression was reduced by injection of an antisense morpholino (miR-26bMo) in zebrafish embryos. As reported for other miRNAs [171], injection of a morpholino (0.7mM) designed against the sequence of mature miR-26b efficiently reduced both, pre-mir-26b and miR-26b levels in 31hpf embryos (Figure 21A) by 98% and 61%, respectively. A Northern blot analysis also revealed that the highly homologues miR-26a was likewise targeted by this morpholino (Figure 21A). MiR-26bMo injected embryos undergo regular development. No malformations were observed and the survival rate after 14 days of development was 26% compared to 33%

of control morpholino (cMo) injected siblings. Hence, miR-26bMo at this concentration is neither toxic nor causes unspecific defects during embryogenesis.

To investigate whether inactivation of miR-26 has an effect on expression of RE1 controlled neuronal genes, key markers of neuronal lineage specification were analyzed. Neuronal class III β-Tubulins and miR-124 are good candidates for this approach. Class III β-Tubulins are among the earliest markers for postmitotic, differentiating neuroblasts ([172] and [173]) and miR-124 is expressed strictly neuronal in zebrafish embryos and larvae [139]. In addition, both have RE1s in their promotor regions and are therefore controlled by the REST/Ctdsp-complex ([100] and [117]). Two days after injection of either cMo or miR-26bMo expression level of miR-124 was determined by Northern blotting (Figure 21B) and strong reduction of mature miR-124 was observed (compare Figure 21B, lanes 1 and 2). No significant changes in expression of muscle specific miR-206 [174] were observed (Figure 21B), indicating selective impact of miR-26 knockdown on neuronal miRNAs. Abundance of class III β-Tubulins was tested by Western blotting (2dpf) with two different antibodies (Tuj1 and purified native brain class III Tubulin antibody M154; Figure 21C) and *tubb5* [175] *in situ* hybridization (31hpf; Figure 21D). These experiments revealed a strong reduction of neuronal β-Tubulin expression on protein and mRNA level. Of note, class III β-Tubulins are expressed pan-neuronally, pointing towards a general defect in terminal differentiation of neuronal precursor cells.

Together these data indicate that depletion of miR-26 family members from developing zebrafish embryos leads to decreased expression of RE1 controlled neuronal genes. Because markers for early neuronal cell lineage commitment (class III β-Tubulins) as well as for differentiated neurons (miR-124) are affected, miR-26 might have important functions at the transition from NSC to neuron and maintenance of the neuronal cell identity.

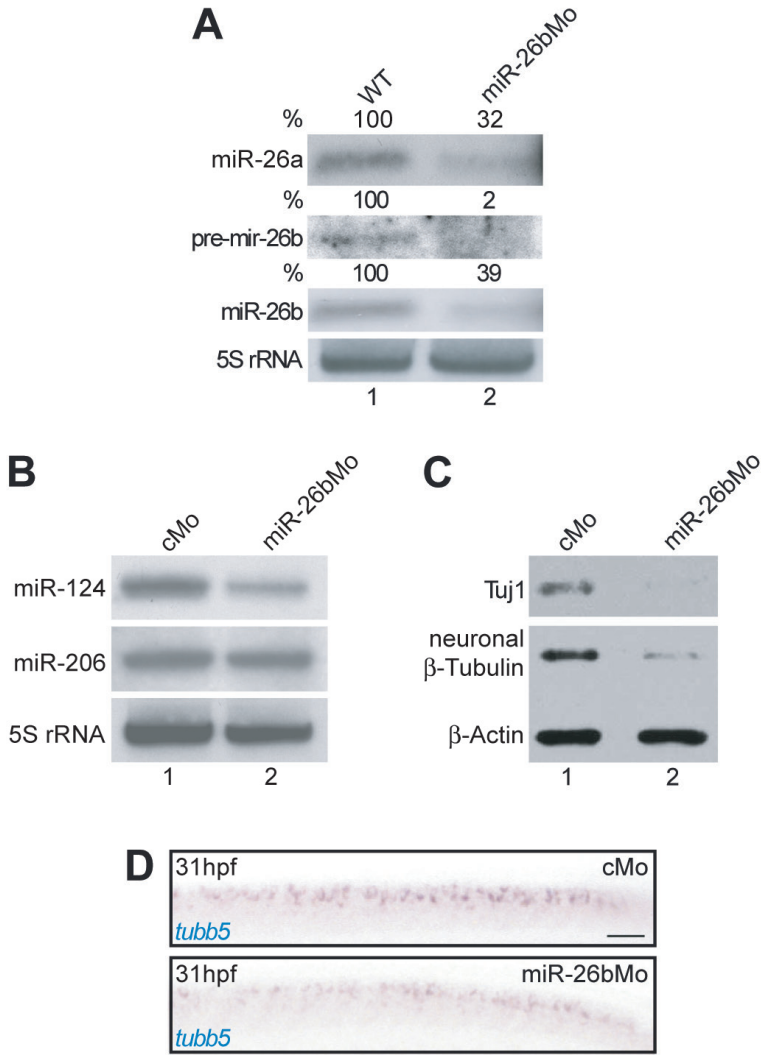

Figure 21: MiR-26 inactivation impairs expression of RE1 controlled genes.
(A) Expression of mature miR-26a and precursor/mature miR-26b was reduced by injection of a morpholino complementary to miR-26b (miR-26bMo) in 31hpf embryos. Northern blot detection with specific 5-[^{32}P]-labelled DNA probes. 5S rRNA served as loading control. **(B)** Injection of miR-26bMo specifically decreased miR-124 levels in whole embryo preparations (as determined by Northern blotting 2dpf) while expression of an unrelated control miRNA (miR-206) was only marginally affected. 5S rRNA served as a loading control. **(C)** Immunodetection of neuronal β-Tubulin on Western blots of extracts from embryos injected with cMo (lane 1) or miR-26bMo (lane 2). Two different antibodies were used (Tuj1 and native brain Tubulin antibody M154). β-Actin served as a loading control. **(D)** MRNA levels of neuronal *β-tubulin 5* (*tubb5*) are decreased after miR-26b inactivation. Whole mount RNA *in situ* hybridization of embryos injected with a control morpholino (cMo) or miR-26bMo using a specific *tubb5* probe. Trunk regions of 31hpf embryos are shown. Scale bar represents 100µm.

6.5.2 Formation of neuronal stem cell domains is not affected by miR-26 knockdown

The data shown in the previous section revealed that neuronal cell differentiation is disturbed in miR-26 deficient embryos (see 6.5.1). To examine the impact of miR-26 on embryonic neurogenesis in a more detailed manner, the development of spinal motor neurons as a cellular sub-population of the CNS was analyzed next. Motor neurons and oligodendrocytes develop from a well defined common neural progenitor cell (NPC) population (see 3.3). For this reason, motor neurons and oligodendrocytes are especially suitable to investigate basic principles of neuronal and glial cell fate determination and to compare underlying molecular mechanisms.

To detect effects on the pool of neurogliablasts that give rise to motor neurons and oligodendrocytes, expression of the *olig2* marker was analyzed after cMo or miR-26bMo injection. RNA ISH (Figure 22A – D) revealed that

formation and maintenance of the NPC population was unaffected by miR-26bMo injection, as delineated from robust *olig2* detection (16 and 31hpf) and a staining pattern in the ventral spinal cord that was indistinguishable from controls. At both developmental stages analyzed (i.e. 16 and 31hpf), *olig2* expression was not diminished or increased in morphant compared to control embryos (Figure 22A – D). This indicates that the NPC pool forms normal from ESCs and no accumulation of NPCs occurred in miR-26b morphants (Figure 22A – D). In addition, qRT-PCR (Figure 22E) and Western blotting (Figure 22F) failed to detect a severe significant alteration of *olig2* expression in miR-26b morphants.

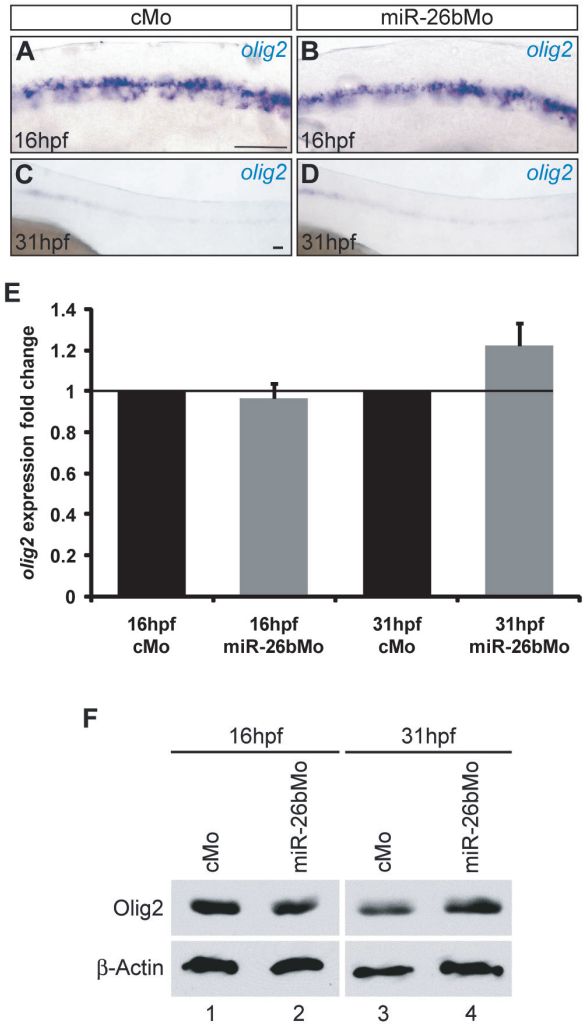

Figure 22: MiR-26 knockdown does not affect motor neuron precursor cells.
Analysis of *olig2*+ neurogliablasts in miR-26b morphant zebrafish embryos. (**A – D**) *In situ* hybridization of *olig2* positive motor neuron precursor cells in cMo (A, C) and miR-26bMo (B, D) injected embryos at 16hpf (A, B; n=35 for cMo and n=43 for miR-26bMo) and 31hpf (C, D; n=38 for cMo and n=40 for miR-26bMo). Scale bars represent 100 µm. (**E**) *Olig2* mRNA levels were determined by quantitative real time PCR and normalized to *gapdh*. Values obtained for control Morpholino (cMo) were set 1 and expression fold change in miR-26bMo injected embryos was calculated using the ΔΔCt method. (**F**) Western blot analysis of Olig2 levels in control and miR-26bMo injected embryos at the indicated points in time. β-Actin served as a loading control. Expression of NPC marker *olig2* is not affected by miR-26b knockdown.

6.5.3 Differentiation of oligodendrocytes is not disturbed in miR-26 morphant embryos

All motor neurons and oligodendrocytes in the spinal cord originate from the *olig2*+ precursor cell population in the ventral neural tube (see 3.3). To test whether miR-26 expression is necessary for oligodendrocyte lineage commitment, intermediate stages during oligodendrocyte differentiation were monitored by ISH of relevant marker genes. *Olig2*+ NSCs develop normal in a miR-26 deficient background (see 6.5.2). These cells divide asymmetrically to generate primary motor neurons and oligodendrocyte progenitor cells (see 3.3).

As evident by *in situ* staining of *sox10* mRNA 48hpf (Figure 23A, B), first premyelinating oligodendroblasts develop normally in the brain of miR-26b morphant embryos (asterisks in Figure 23A, B). All analyzed miR-26b morphant embryos had wild type expression levels of *sox10*. These cells are still cycling and will produce postmitotic, myelinating oligodendrocytes at a later stage (see 3.3). *In situ* hybridization of *mbp* at day five revealed that also formation of mature, myelinating oligodendrocytes appears in a wild type manner after miR-26 knockdown (Figure 23C – H). No differences in morphology of oligodendrocyte populations could be observed in the hindbrain and anterior neural tube (brackets in Figure 23C – F) or lateral line organ (arrows in Figure 23C – F and Figure 23G, H) of the majority (88%) oft analyzed larvae, compared to control morpholino injected individuals.

Together, these results show that the miR-26 family does not play a major role in oligodendrocyte or glia cell fate determination and cell differentiation in zebrafish.

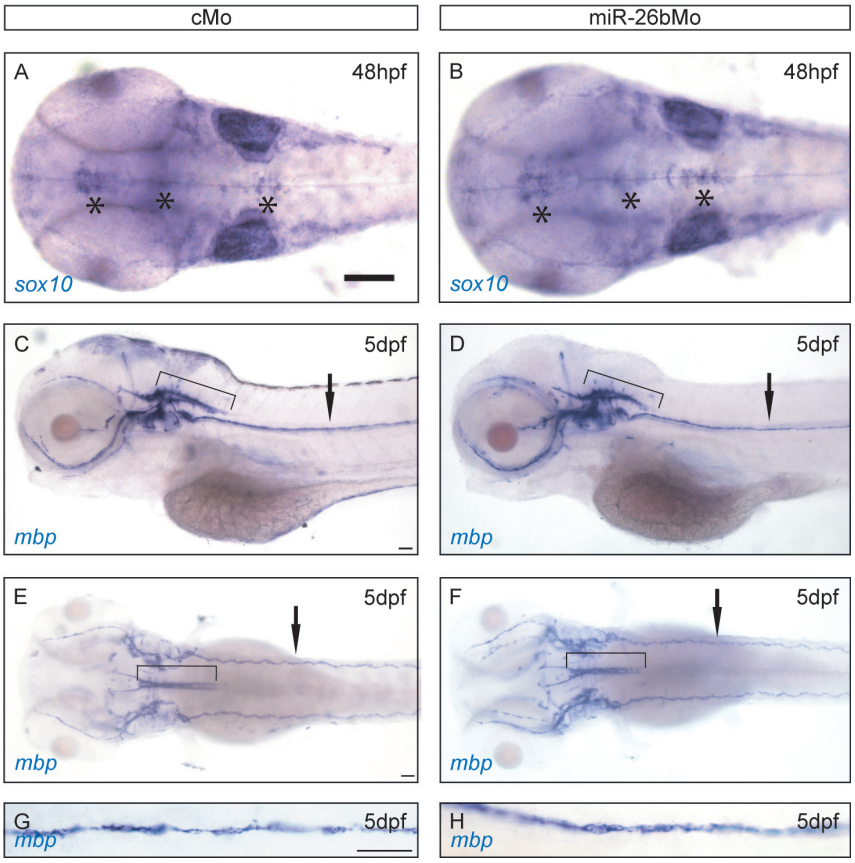

Figure 23: Knockdown of miR-26 does not effect oligodendrocyte formation.
Histological analysis of oligodendrocyte formation in miR-26b morphant zebrafish larvae. **(A, B)** *In situ* hybridization of *sox10* mRNA in 48hpf embryos. Dorsal views are shown. Asterisks mark brain regions with specific *sox10* staining. n=53 for cMo and n=63 for miR-26bMo. **(C – F)** Detection of mature oligodendrocytes by ISH of *mbp* in 5dpf larvae. Lateral views (C, D) and dorsal views (E, F) are shown. Brackets mark hind brain and anterior neural tube, arrows mark the lateral line organ. n=3 for cMo and n=8 for miR-26bMo. **(G, H)** Higher magnification oft he lateral line organ shown in (C – F). Oligodendrocyte progenitor cells as well as mature oligodendrocytes develop normal in miR-26 depleted zebrafish larvae. Scale bars represent 100µm.

6.5.4 MiR-26 knockdown interferes with correct formation of the motor neuron domain

To analyse if the differentiation if *olig2*$^{+}$ NSCs into motor neurons is affected by reduced levels of miR-26, formation of the motor neuron domain was analyzed in zebrafish larvae. *Gata2*:GFP transgenic zebrafish, expressing GFP in ventrally projecting secondary motor neurons [159] are especially suitable for microscopic observation of motor neuron formation. Motor neuron formation was assessed by the analysis of GFP expression 60hpf. Morpholino mediated downregulation of miR-26 interfered with the formation of secondary motor neurons, as evident by reduced numbers of GFP-positive cell bodies compared to control injected larvae (Figure 24A, E). Numbers of GFP-positive secondary motor neurons in the ventral neural tube were dramatically reduced in 80% of miR-26b morphant *gata2*:GFP larvae. Immunostaining with zn-8 antibody, which recognizes neurolin on the surface of all three secondary motor axons present at this larval stage [176], revealed that outgrowth and path finding of dorsal, ventral and rostral motor axons was normal, except slight but statistical significant shortening of ventral and rostral projecting axons (arrows in Figure 24B, F and [167]). Together with observation of some remaining GFP-positive motor neuron cells, this shows that motor units were intact, but reduced in quantity. These motor neurons were functional and able to innervate their target regions in myotomes, as miR-26b morphants were not paralyzed and fulfilled normal touch response [177].

From these data it can be concluded that differentiation of motor neurons is impaired in miR-26 morphant larvae. The few remaining motor neurons that are still formed under these conditions develop normal motor neuron morphology and are fully functional. Also the development of distinct brain regions (forebrain and mid-hind-brain boundary [167]) is disturbed and expression of general neuronal markers like Tuj1 is effected (see 6.5.1) by miR-26 knockdown. Thus, it seems likely that the miR-26 family has important functions in neuronal cell differentiation, not only for motor neurons.

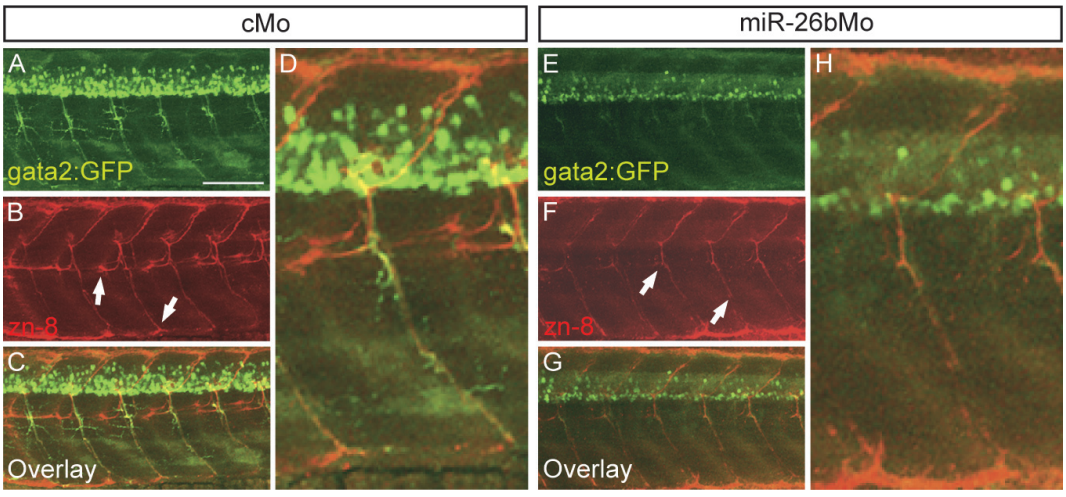

Figure 24: Mir-26 knockdown leads to reduced numbers of secondary motor neurons.
(A – H) Confocal analysis of immunofluorescence staining using zn-8 antibody (red) in 60hpf *gata2*:GFP (green) larvae. *Gata2*:GFP positive cells were reduced in miR-26b morphants compared to control injected larvae (A and E; n=5 for cMo and n=5 for miR-26bMo). Ventral and rostral motor axons were shortened after miR-26bMo injection (arrows in B and F). Trunk regions are shown. An overlay is shown in panels (C) and (G). (D) and (H) show higher magnification of larvae presented in (C) and (G). Scale bar: 100µm.

6.5.5 Depletion of miR-26 family members causes enhanced apoptosis in the CNS

Regular formation of motor neuron precursor cells on the one side and loss of differentiated motor neurons on the other side point to a block of neuronal cell differentiation in miR-26b morphant embryos. Precursor cells which do not differentiate due to low levels of miR-26 could hypothetically accumulate during embryonic development. However, experiments shown in Figure 22 indicate that this is not the case (see also 6.5.2). It was therefore analyzed if excess precursor cells are removed from the neural tube by apoptosis.

To detect apoptotic cells in miR-26 morphant embryos, TUNEL (TdT-mediated dUTP-biotin Nick End labelling) assay was performed. Although miR-26b morphant embryos are morphologically indistinguishable from their wild type siblings (Figure 25A, B), increased TUNEL-staining in the CNS was observed after knockdown of miR-26 (Figure 25C – H). 73% of miR-26b morphants exhibit increased apoptotic cell numbers in neuronal tissues compared to cMo injected embryos. Cell death was not restricted to motor neurons or their precursor cells, as increased TUNEL signal was also observed in hind brain (Figure 25C, D), eye (Figure 25E, F) and dorsal neural tube (Figure 25G, H). These findings hinted towards apoptotic clearance of cells which are prevented from differentiation.

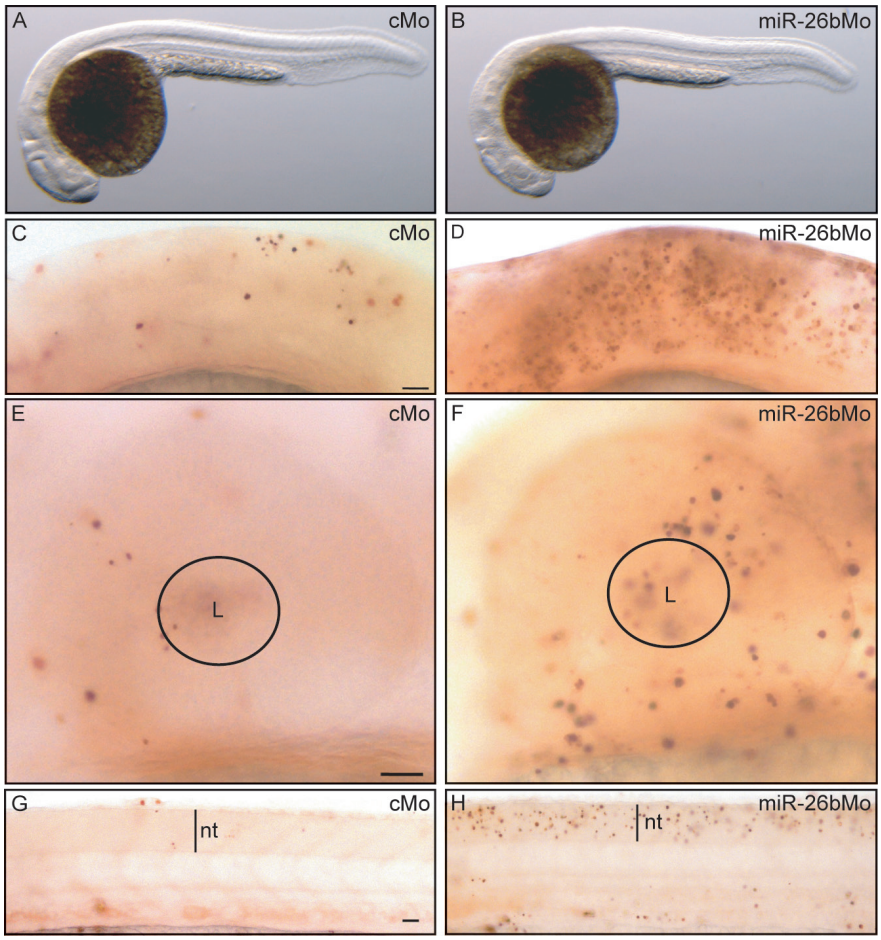

Figure 25: Inactivation of miR-26b causes apoptosis in embryonic neuronal tissues.
TUNEL-assay with miR-26b morphant zebrafish embryos. (**A** – **B**) Bright field images of cMo (A) and miR-26bMo (B) injected 31hpf embryos. No significant morphological abnormalities were observed. (**C** – **H**) TUNEL-assay revealed increased numbers of apoptotic cells (brown) in the hindbrain (D) and eye (F) and neural tube (H) compared to control morphants (C, E and G). n=50 for cMo and n=56 for miR-26bMo. The circles in E and F indicate the position of the lens. Scale bars represent 100µm. nt: neural tube; L: lens.

6.6 MiR-26b mediated repression of Ctdsp2 expression contributes to neurogenesis

As described in previous sections, knockdown of the miR-26 family results in decreased expression of neuronal markers (see 6.5.1) and impaired neurogenesis (see 6.5.2 and 6.5.4). A question arising from this observation is whether miR-26b directly triggers neuronal cell differentiation by targeting *ctdsp2*. As the vast majority of miRNAs also miR-26b has hundreds of potential target transcripts [5]. Therefore, derepression of any unknown target by miR-26b knockdown could possibly cause the observed neuronal phenotype. To test whether it is indeed the reduced silencing of *ctdsp2* that is primarily responsible for the block in neuronal differentiation in miR-26bMo injected embryos, effect of *ctdsp2* knockdown on expression of neuronal markers was analyzed.

Injection of a *ctdsp2* antisense morpholino (*ctdsp2*Mo), blocking translation of the *ctdsp2* mRNA (0.35mM), decreased expression of endogenous Ctdsp2 to 61% of the wild type level (WB in Figure 26A). Strikingly, this inhibition resulted in a slight but significant increase in expression of miR-124 (NB in Figure 26A), suggesting a relief of REST/Ctdsp-complex mediated transcriptional repression [117]. Biosynthesis of miR-26b was not affected by translational inhibition of its host gene (Figure 26A). Furthermore, employing the GFP-reporter assay described in 6.3, it could be demonstrate that *ctdsp2* is a target of miR-124 also in zebrafish (Figure 26B, C), as reported previously for other vertebrates (see 3.4.2). Together these data suggest existence of a gene regulatory network, involving miR-26b, miR-124 and *ctdsp2* in zebrafish (Figure 26D).

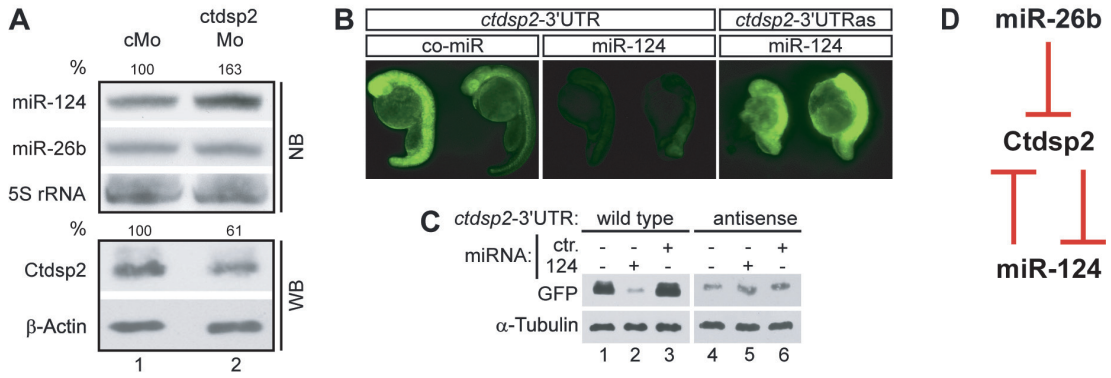

Figure 26: Reciprocal functions of Ctdsp2 and miR-124 in zebrafish embryos.
(A) Injection of *ctdsp2*Mo resulted in downregulation of Ctdsp2 protein levels (lower panel) and miR-124 derepression (upper panel). Expression of mature miR-26b from the *ctdsp2* transcript was not affected by *ctdsp2*Mo. ß-Actin and 5S rRNA levels were taken as loading controls for the Western blot and Northern blot, respectively. The percentage of Ctdsp2 and miR-124 levels in *ctdsp2*Mo injected animals, as determined by densitometry and normalized to controls is indicated above. WB: Western blot; NB: Northern blot. **(B, C)** MiR-124 represses expression of Ctdsp2 in zebrafish. GFP expression in zebrafish embryos from injected reporter mRNAs containing either the wild type or antisense *ctdsp2*-3'UTR. The expression of GFP in the presence of coinjected control miRNA or miR-124 was assessed by fluorescence microscopy (B) and Western blotting (C). MiR-124 represses GFP synthesis from the reporter fused to the wild type but not antisense sequence. **(D)** Regulatory network controlling neuronal gene expression in zebrafish.

Based on the model described in Figure 26D reduced Ctdsp2 expression (mediated by injection of *ctdsp2*Mo) would be predicted to compete with miR-26bMo activity and restore neurogenesis. Considering this constellation, it was next analyzed if the motor neuron phenotype observed in Figure 24 could be rescued by miR-26b/*ctdsp2* double knockdown. For this, miR-26bMo was coinjected with *ctdsp2*Mo into *gata2*:GFP transgenic embryos. CMo injected embryos (n=35) showed strong GFP expression in the neural tube 31hpf (Figure 27B), indicating normal neurogenesis. GFP expression was considerably reduced in 89% (n=18) of miR-26bMo injected embryos (Figure

27C). However, coinjection of *ctdsp2*Mo together with miR-26bMo recovered wild type like GFP expression in 55% of analyzed embryos (n=22). This represents a 44% rescue of the miR-26b morphant phenotype. To substantiate these findings with more sophisticated statistical data, the number of GFP-positive secondary motor neurons in the trunk area indicated in Figure 27A was quantified by confocal microscopy. For this GFP-positive cells were counted in five body segments per embryo. The reduction of differentiated motor neurons by miR-26bMo injection alone, that was already observed for 60hpf larvae (Figure 24) was confirmed 31hpf by this way (Figure 27B, C, E). Coinjection of *ctdsp2*Mo partially restored the number of secondary motor neurons (Figure 27D and E). Therefore, the observed neuronal phenotype seems to be mainly induced by misregulated Ctdsp2 expression after miR-26b knockdown. In addition, these data suggest that miR-26b mediated repression of *ctdsp2* directly contributes to neuronal cell differentiation.

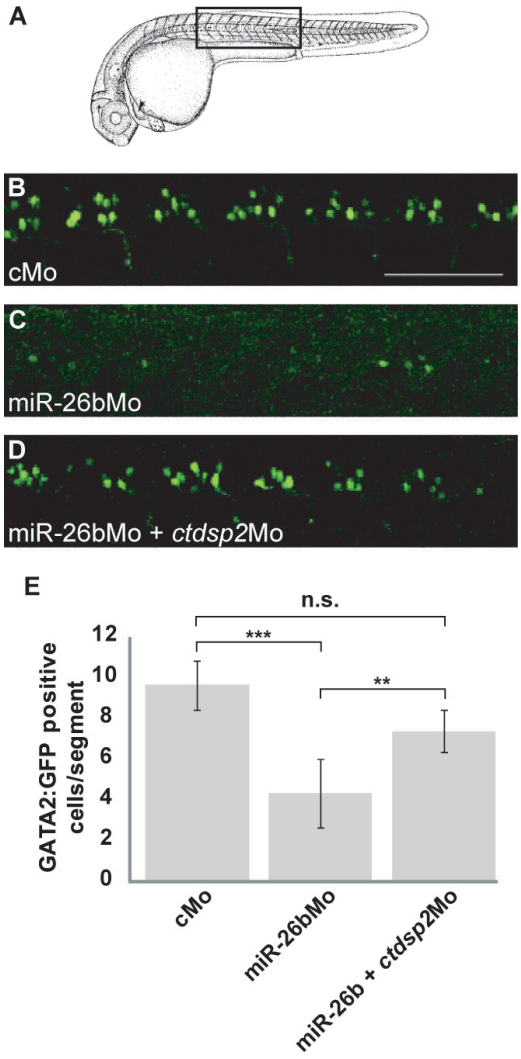

Figure 27: MiR-26b promotes neuronal differentiation via silencing of *ctdsp2*.
Coinjection of miR-26bMo and *ctdsp2*Mo rescues the phenotype generated by miR-26bMo alone. **(A)** Schematic representation of a 31hpf zebrafish embryo (modified from [160]). **(B – D)** Confocal microscopy of *gata2*:GFP transgenic embryos at 31hpf injected with either cMo (B), miR-26bMo (C) or a mixture of a *ctdsp2* translation-blocking morpholino (*ctdsp2*Mo) and miR-26bMo (D). Scale bar represents 100 μm. **(E)** Quantitative analysis of the number of motor neuron cells per body segment shows that the *ctdsp2*Mo mediated rescue is statistically significant (mean±S.D., paired t-test, ***=highly significant (p<0,0001), **=significant (p<0.05), n.s.=not significant, cMo n=50, miR-26bMo n=65, miR-26bMo + *ctdsp2*Mo n=25).

7 DISCUSSION

Transition from ESC to neural progenitor cell and generation of terminally differentiated neurons is controlled by a complex gene regulatory network. In non-neuronal tissues, the neuronal gene expression program is suppressed by the repressor element 1 (RE1) silencing transcription factor (REST) complex. REST binds to RE1 containing genes and causes their silencing via chromatin-remodelling and formation of inactive heterochromatin or modulation of Pol II activity. Pol II inactivation is achieved by the activity of three closely related phosphatases, termed Ctdsp1, Ctdsp2 and Ctdspl. As part of the REST complex, these enzymes dephosphorylate the C-terminal domain of Pol II and thereby inhibit the expression of RE1 containing genes. During neural fate commitment and terminal differentiation, expression of REST/Ctdsp-complex components is gradually inhibited to allow the expression of RE1 containing genes. Inactivation of the REST/Ctdsp pathway and consequently neuronal gene expression is known to depend on the action of miRNAs (for example miR-124), which prevent expression of REST-complex components, including Ctdsps. However, the neuron-specific miR-124 is itself repressed by the REST/Ctdsp pathway, and therefore can not be solely responsible for derepression of neuronal genes. As mRNAs often are under the control of a collection of miRNAs, it is feasible that additional miRNAs might be involved in the regulation of Ctdsp activity.

A main goal of this study was to identify additional miRNAs, which target REST-complex components and therefore contribute to activation of neuronal gene expression. MiR-26b was shown to specifically silence translation of *ctdsp2* mRNA. Strikingly, miR-26b is located in an intron of the *ctdsp2* primary transcript itself and coexpressed with its host gene. A so far unknown posttranscriptional mechanism uncouples synthesis of mature miR-26b and *ctdsp2* mRNA, leading to upregulation of this particular miRNA during neurogenesis and inhibition of Ctdsp2 protein synthesis in neuronal tissues. Knockdown experiments in zebrafish embryos showed that depletion of miR-26b indeed results in decreased expression of RE1 containing genes and disturbed neuronal cell differentiation, most likely as a consequence of deregulated expression of Ctdsp2. The obtained data indicate that miR-26b activity contributes to neurogenesis by abrogating REST/Ctdsp2 mediated translational repression in differentiating neurons, allowing expression of neuronal genes during vertebrate CNS development.

7.1 MiR-26b silences protein expression from its host gene *ctdsp2*

MiRNAs inhibit expression of their target genes by base pairing to complementary sequences frequently located within 3'UTRs of mRNAs and target silencing by miRNAs regulates the neuronal gene expression program during CNS development [115]. The miRNA-26 family was previously reported to be predominantly expressed in neuronal cell types and to be upregulated during neuronal cell differentiation ([135] and [137]) To get more information about a possible role of mR-26 in neurogenesis, a bioinformatical target prediction was performed. This analysis revealed presence of miR-26 target sites within 3'UTRs of known REST-complex components, indicating a function of the miRNA-26 family in modulation of REST-complex activity.

Five putative miR-26b target sites were found in the 3'UTR of the *ctdsp2* transcript (Figure 10). These target sites exhibit 6 – 7 nt seed site matches and extensive base pairing of nucleotides 13 – 16 of the miRNA with the

ctdsp2-3'UTR. Therefore these target sites show important characteristics of functional miRNA target sites ([36] and [178]). The capability of miR-26b to posttranscriptionally silence Ctdsp2 expression via the predicted target sites was tested in zebrafish embryos and two lines of evidence suggest that miR-26b indeed reduces Ctdsp2 protein synthesis. First, microinjection of miR-26b duplex decreases the amount of endogenous Ctdsp2 (Figure 11A). Second, coinjection of miR-26b and GFP-reporter mRNAs containing the *ctdsp2*-3'UTR specifically inhibits translation of GFP (Figure 11B, C and Figure 12). Further experiments revealed that mutation of only one of the five target sites (Figure 10) restores translation of the reporter mRNA (Figure 11B, C and Figure 12), whereas the remaining four target sites seem not to contribute to the observed effect.

MiRNAs downregulate target gene expression by two posttranscriptional effector mechanisms: mRNA cleavage and translational inhibition ([26]). Repression of productive translation is often accompanied by deadenylation of target mRNAs ([7] and [25]). Deadenylation enhances target mRNA decay and helps to avoid inappropriate target gene expression for instance at the transition from one developmental state to the other [7]. Also miR-26b mediated suppression of *ctdsp2* translation is accompanied by deadenylation of the *ctdsp2* mRNA (Figure 13). Hence, miR-26b shares this common mechanism with other miRNAs during vertebrate embryogenesis [179].

The obtained data strongly suggest that intronic miR-26b is able to inhibit protein production from its host gene *ctdsp2* in a negative autoregulatory loop (Figure 28). This particular miRNA/target regulation was already predicted in different vertebrate species [180] and a large scale analysis revealed a miR-26 target site in the *ctdsp2*-3'UTR, that physically interacts with a miRNA silencing complex in mouse brain [124]. Although no experimental evidence exists, the expression of other *ctdsp* genes might also be regulated by their intronic miRNA. In line with this idea, all genes that encode Ctdsp homologues contain a miRNA of the miR-26 family in one of their introns (Figure 9) and at least some of them have miR-26 target sites in their respective 3'UTRs. Hence, the *ctdsp2*/miR-26b autoregulatory loop might be conserved for other *ctdsp* genes and vertebrate species.

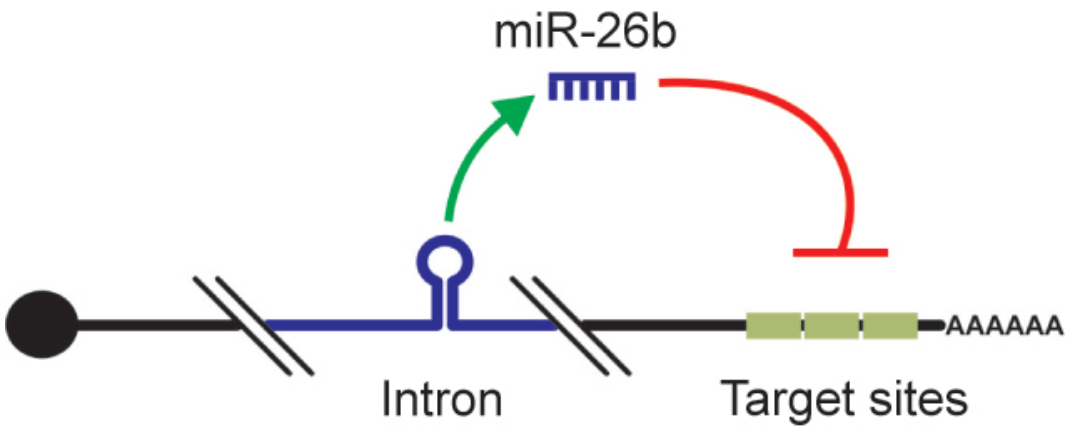

Figure 28: The *ctdps2*/miR-26b autoregulatory loop
The hairpin structured precursor of miR-26b is located in an intron of the *ctdsp2* primary transcript. By Drosha and Dicer processing, mature miR-26b is generated from this host intron. The mature form of miR-26b is able to silence Ctdsp2 protein synthesis from the fully spliced *ctdsp2* mRNA via target sites in the *ctdsp2*-3'UTR, building up an autoregulatory loop to control Ctdsp2 expression.

7.2 Expression of the miR-26 family is regulated at the posttranscriptional level

Inhibition of Ctdsp2 expression by miR-26b observed in this study and resulting possible inactivation of one operating mode of the REST-complex, might be important for derepression of neuronal genes. Continuous coprocessing of *ctdsp2* mRNA and intronic miR-26b [126] would however lead to global silencing of Ctdsp2 protein expression. Such a scenario would interfere with functions of this well characterized phosphatase in maintaining stem cell properties. Hence, it can be speculated that biogenesis of mature miR-26b and *ctdsp2* mRNA are posttranscriptionally uncoupled by some unknown mechanism. Such a mechanism would make cell type or developmental stage specific expression of miR-26b possible, independently of protein expression from its host gene *ctdsp2*. Shedding light on this putative mechanism was another central point of this study. To analyze a possible posttranscriptional regulation of miR-26b biogenesis, expression of its processing intermediates was monitored in different cellular systems.

Several lines of evidence suggest posttranscriptional regulation of miR-26 maturation in a cell context dependent manner. MiR-26 precursors are expressed throughout zebrafish embryonic development, including fertilized eggs. In contrast, mature miR-26 seems to be completely absent from early embryos (Figure 15 and Figure 16). In line with data obtained in this study, miR-26 was previously reported not to be expressed at the first day of zebrafish development ([140] and [141]) and in undifferentiated ESCs ([132], [133], [134] and [135]). 1-cell and 256-cell embryos are still transcriptionally silent and expression of the miR-26b host gene *ctdsp2* is absent before midblastula transition (Figure 16). Hence, pre-mir-26 is likely to be delivered maternally to the oocyte, but kept as inactive precursor. In later stages, such as neurula, this inhibition is relieved and mature miR-26 is produced. The conclusion that pre-mir-26 processing is inactive under certain conditions is further supported by the observation that in undifferentiated neuronal progenitor cells pre-mir-26b is expressed but only inefficiently processed into its mature form. However, processing efficiency of pre-mir-26b increases upon induction of neuronal cell differentiation leading to upregulation of mature miR-26b as reported previously [135]. Production of mature miR-26b coincides with appearance of neuronal markers miR-124 and Tuj1 (Figure 17), indicating neuronal character of these cells. In line with this, a similar observation can be made in zebrafish. In early stages of development, mature miR-26b and miR-124 can be detected from 9hpf on, a stage where first neurons differentiate ([76] and [85]). The described posttranscriptional regulation of miR-26 processing during cell differentiation events might also transform in a cell type specific enrichment of miR-26. In fact, pre-mir-26b is expressed at similar levels in isolated adult zebrafish tissues (Figure 18). Likewise, mature miR-26b is also expressed ubiquitously but enriched in neuronal tissues (Figure 18). This indicates posttranscriptional regulation of miR-26 expression occurring also in fully differentiated cells. Complementary to mature miR-26b, Ctdsp2 protein is expressed in non-neuronal tissues but absent from neurons (Figure 18). Because the *ctdsp2* mRNA is ubiquitously expressed, Ctdsp2 protein production seems to be repressed by posttranscriptional means in neurons, most likely by combined action of miR-124 and miR-26b. These findings connect posttranscriptional regulation of miR-26 expression to its physiological function, the silencing of *ctdsp2* and probably other key regulators of neuronal gene expression during neurogenesis.

Posttranscriptional regulation of miRNA processing, as observed for miR-26, was already observed during embryonic development of other vertebrate species. In *Xenopus laevis* embryos, miR-15 and miR-16 are very abundant at the ventral side of the embryo, whereas their primary miRNAs are equally distributed in the embryo. So, miR-15 and miR-16 are spatially enriched by differential Drosha processing events [181]. Furthermore, Obernosterer and colleagues [182] described posttranscriptional inhibition of pre-mir-138 processing. In mouse embryos pre-mir-138 is expressed in a wide range of tissues, whereas mature miR-138 could only be detected in the CNS and liver [182]. Hence, tissue specific inhibition of miRNA maturation seems to be a widespread effect in vertebrate embryonic development. Nevertheless, underlying molecular mechanisms remain elusive.

The observation that pre-mir-26 is not processed in early embryos and undifferentiated neural stem cells, could possibly be explained by nuclear retention of pre-mir-26, a block of Dicer processing in the cytoplasm or rapid turnover of mature miR-26. Some miRNAs were reported to localize to the nucleus rather than the cytoplasm depending on the cell cycle phase [183]. Therefore, it could be hypothesised that pre-mir-26 is not exported from the nucleus in proliferating cells to prevent cytoplasmic processing. This possibility could not be figured out in this study, as preparation of nuclear RNA, in amounts sufficient for Northern blotting failed. Furthermore, absent processing of pre-mir-26 is not due to generally reduced Dicer activity as maternal Dicer is active in early zebrafish embryos ([8] and [141]) and pre-mir-430b-1, a precursor of embryonic miR-430b [8], is processed efficiently in embryos lacking pre-mir-26 processing (Figure 16). The Dicer regulatory factors of the let-7 miRNA family, TUT4 and KSRP, have already been implicated in the regulation of miR-26 family members *in vitro* ([69] and [70]). However, *ksrp* and *tut4* knockdown in zebrafish embryos did not influence steady state levels of mature miR-26b in preliminary experiments (data nor shown). Nevertheless, these factors might be involved in selective processing of the miR-26 family.

This study uncovers a role for posttranscriptionally regulated biogenesis of miR-26b in control of the REST/Ctdsp-pathway during neuronal differentiation. In this regulatory mechanism, the primary transcript of the *ctdsp2*/miR-26b locus serves as both pre-mRNA and pri-miRNA (Figure 29A). While splicing towards *ctdsp2* mRNA proceeds normally in all cell types, the biogenesis of miR-26b is arrested at the precursor level in NSCs and non-neuronal tissues allowing Ctdsp2 protein synthesis (Figure 29A). The underlying inhibitory mechanism is currently unknown, but it is reasonable to hypothesise that terminal uridyl polymerases like TUT4 might be involved. During neuronal differentiation and in differentiated neurons the processing block is relieved and as a consequence levels of mature miR-26b rise, leading to repression of *ctdsp2* mRNA (Figure 29A). The *ctdsp2*/miR-26b autoregulatory loop (Figure 28) contains the *ctdsp2* primary transcript as source for *ctdsp2* mRNA and miR-26b. As the biogenesis of *ctdsp2* mRNA and mature miR-26b are uncoupled and miR-26b directly targets the *ctdsp2*-3'UTR the *ctdsp2*/miR-26b autoregulatory loop represents a novel variant of an incoherent Feedforward loop ([184]; Figure 29B). This form of regulation allows strong expression of Ctdsp2 as long as miR-26b biogenesis is blocked. As soon as neuronal differentiation is triggered, the block is relieved and pre-mir-26b is available for

Dicer processing. This mechanism accomplishes rapid accumulation of mature miR-26b and downregulation of Ctdsp2 to allow transcription of neuronal genes.

Interestingly, mature miR-26b is expressed prior to miR-124 during neuronal cell differentiation (Figure 17). As miR-26b targets *ctdsp2*, it might serve as a kind of trigger factor to eliminate repression of neuronal genes by the REST-complex. As a consequence of this, neuronal gene products like miR-124 would be expressed to further stabilize neural cell identity and completely remove REST-complex components from the cell. Hence, a possible function of miR-26b in initial events of neuronal cell differentiation is plausible.

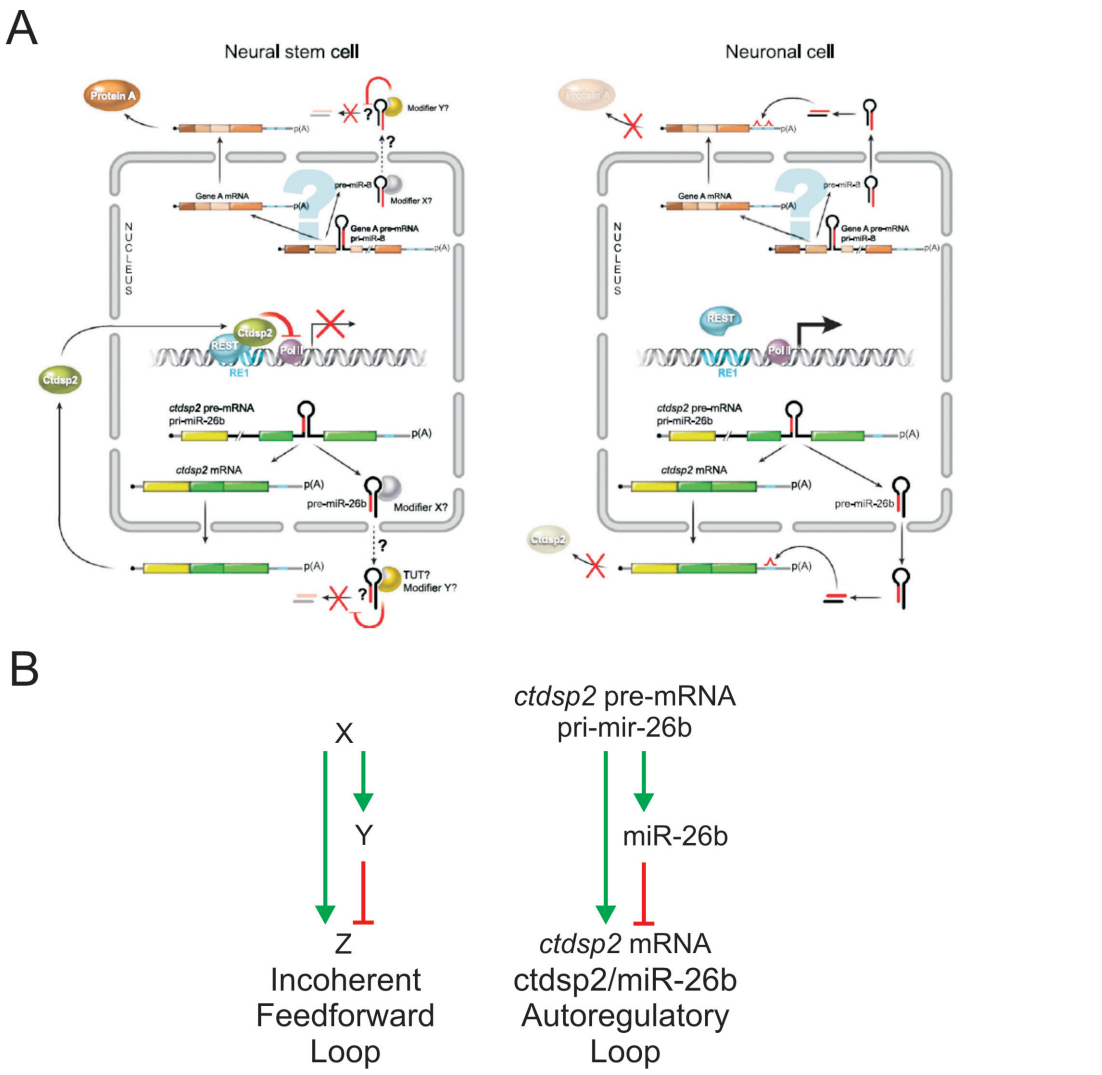

Figure 29: The role of regulated miR-26b processing in neuronal cell differentiation [185]
(A) MiR-26b (red), which targets ***ctdsp2*** mRNA (green), is located in an intronic region of ***ctdsp2*** and is cotranscribed with its host gene (black lines denote introns). The shared RNA transcript ***ctdsp2*** pre-mRNA/pri-miR-26b generates ***ctdsp2*** mRNA and pre-miR-26b concurrently in the nucleus. In neural stem cells (left panel), ***ctdsp2*** mRNA is translated into the Ctdsp2 protein, which contributes to the inhibition of neuronal gene expression by REST via suppression of Pol II activity on RE1 sites (denoted as a blue stretch of double helix). Translation of ***ctdsp2*** is possible because pre-miR-26b is not processed into functional miR-26b. Stem cell-specific RNA-binding proteins and/or -modifying enzymes (denoted as modifier X in the nucleus or Y in the cytoplasm) may block pre-miR-26b processing. In differentiated neuronal cells (right panel), miR-26b is processed from pre-miR-26b and prevents ***ctdsp2*** translation. Top portions (brown) represent a general model for host gene inhibition by intronic miRNAs. **(B)** Mir-26b and *ctdsp2* are parts of an incoherent Feedforward loop to control Ctdsp2 protein expression. In this regulatory cascade the upstream element X influences expression levels of factors Y and Z directly and activity of factor Z indirectly via Y. Figure adapted from [185].

7.3 MiR-26 function in embryonic neurogenesis

7.3.1 Target silencing by miR-26 contributes to neuronal cell differentiation

As discussed in previous sections, miR-26b is upregulated during neuronal cell differentiation and specifically targets *ctdsp2* mRNA in this process. Since Ctdsp2 is a well known negative regulator of neuronal gene expression [110], this correlation of miRNA expression pattern and target gene function suggests a role for miR-26b in neurogenesis.

To analyze the function of miR-26b in CNS development, overexpression and knockdown experiments in zebrafish embryos were performed. If miR-26b was able to trigger neurogenesis from NSCs, overexpression of miR-26b should lead to increased expression of neuronal markers or even numbers of postmitotic neurons as observed for miR-124 in chicken embryos [115]. Previously, it was described that injection of exogenous miRNA duplices into zebrafish embryos has tremendous unspecific effects on development ([186], [187] and [188]). This is also true for miR-26b, as injection of a miR-26b mimic leads to strong malformations and embryonic lethality. For this reason, a specific miR-26b overexpression phenotype was not observed in this study.

Nonetheless, to analyze physiological functions of miR-26b, this miRNA was depleted from zebrafish embryos. Transient knockdown of miR-26 family members (Figure 21) leads to decreased expression of RE1 controlled neuronal genes like miR-124 or neuronal β-Tubulins (Figure 21). This observation can be cogently explained by deregulation of Ctdsp2 expression by loss of miR-26 activity and resulting aberrant repression of neuronal genes by the REST-complex. Furthermore, miR-26 knockdown has negative impact on regular formation of the CNS, as evident by reduced numbers of differentiated secondary motor neurons (Figure 24 and Figure 27). These findings point to a role of the miR-26 family in neuronal cell differentiation in zebrafish embryos.

Individual miRNAs can repress hundreds of target genes [5]. Thus, interrupted silencing of *ctdsp2* by the miR-26 knockdown needs not to be primarily responsible for the observed neuronal phenotype. To test whether the observed negative effect of miR-26 knockdown on neurogenesis indeed is a consequence of *ctdsp2* misregulation, influence of depletion of Ctdsp2 itself on expression of neuronal genes was analyzed first. Indeed, injection of a *ctdsp2*Mo leads to derepression of the RE1 containing miR-124 gene (Figure 26A), which exerts additional negative feedback to Ctdsp2 expression (Figure 26B, C). Thus, silencing of *ctdsp2* by miR-26 and miR-124 cooperate to allow the neuronal gene expression program. Consequently, double knockdown of miR-26b and its target *ctdsp2* significantly rescues the observed motor neuron phenotype (Figure 27). These experiments validate *ctdsp2* as a major miR-26b target in context of neuronal cell differentiation, and highlight the specificity of the phenotype caused by the miR-26 knockdown. Nevertheless, the rescue is only partially and motor neuron numbers are still reduced in *ctdsp2*/miR-26b double morphants compared to control embryos. Other REST-complex components are predicted to be miR-26 targets, and deregulation of these transcripts may also contribute to the observed phenotype.

Loss of neuronal cells in miR-26b morphants is accompanied by strong apoptotic cell death in the developing CNS (Figure 25). Neuronal cell death is frequently observed as a consequence of morpholino off-target effects and is triggered by the activation of the p53 dependent cell death pathway [189]. Two results argue against

unspecific neuronal apoptosis as reason for reduced numbers of neurons in miR-26b morphant embryos. First, the observed miR-26 loss-of-function phenotype can efficiently be rescued by coinjection of *ctdsp2*Mo. Although it was not investigated whether also increased apoptosis can be reduced to a wild type level by coinjection of miR-26bMo and *ctdsp2*Mo, the rescue approach argues against morpholino off-target effects as explanation for reduced neuronal cell numbers. Second, morpholino independent knockdown of miR-26a also causes apoptosis in a model system for aortic smooth muscle cell differentiation [156]. Hence, increased apoptosis of miR-26 depleted cells is rather due to blocked differentiation events than morpholino off-target effects and part of a highly specific neuronal phenotype. Phenotypic consequences of depletion of single miRNAs are often marginal and hard to detect in the lab [36]. Strikingly, knockdown of the miR-26 family in zebrafish produces a marked neuronal phenotype. Probably this is due to the fact that miR-26 is part of an intricate gene regulatory cascade (Figure 30). Downstream factors within this cascade, like miR-124, execute additional negative feedback on the REST/Ctdsp pathway. Thus, to unbalance this system might have a relatively strong effect on gene expression and consequently cellular processes.

Motor neurons and oligodendrocytes develop from a common precursor cell population in the embryonic neural tube. Differentiation of mature oligodendrocytes from these progenitor cells depends amongst other determinants on activity of miRNAs [190]. To test whether miR-26 activity is also necessary for oligodendrocyte lineage commitment, as it is for differentiation of motor neurons, oligodendrocyte formation was monitored in the developing CNS of miR-26b morphant embryos and larvae (Figure 23). *In situ* hybridization of appropriate marker genes revealed step-wise formation of the oligodendrocyte domain, comparable to control siblings. Premyelinating oligodendroblasts and postmitotic myelinating oligodendrocytes develop in miR-26b morphant embryos as expected for the respective developmental stages (Figure 23). These results allow the conclusion that the miR-26 family controls neural cell differentiation, but is dispensable for oligodendrocyte or even glia cell fate determination in general. These findings are conform to recently published data showing that miR-26a and miR-26b are downregulated during oligodendrocyte differentiation ([191] and [192]). Hence, knockdown of miR-26 should not affect oligodendrocyte differentiation, in contrast to neurons. Thus, miRNA mediated regulatory mechanisms, underlying neuronal and glia cell lineage differentiation, including regulation of REST-complex activity, seem to differ in central aspects.

7.3.2 The function of miR-26 in cell cycle control and its implication in tumorigenesis

MiRNAs control cell proliferation by silencing negative and positive regulators of the cell cycle machinery. Therefore erroneous expression of miRNAs can lead to both, cell cycle re-entry and consequently tumorigenesis, or unscheduled cell cycle exit [193]. As mentioned in previous sections, there is increasing evidence for an implication of the miR-26 family in cell differentiation and cell cycle exit. Consistent with that, miR-26 was found to be downregulated in T- and B-cell lymphoma ([127] and [146]), head and neck/oral cancer [194], carcinoma of nasopharyngeal epithelia ([145] and [148]), squamous cell carcinoma [195], hepatocellular carcinoma [147], breast cancer tumors [152] and clear renal cell carcinoma [196]. According to its underrepresentation in various

cancer types, miR-26 exhibits anti-tumorigenic function in a broad range of cancer model systems ([145], [146] [147] and [197]). Noteworthy, overexpression of miR-26 causes tumor specific inhibition of cell proliferation and tumor regression also in an *in vivo* mouse model for hepatocellular carcinoma [147]. Thus miR-26 is a negative regulator of cell proliferation and a potent cancer therapeutic agent. In this respect it is worth mentioning that miR-26a is part of an amplicon frequently occurring in gliomas and miR-26a promotes gliomagenesis by targeting the tumor suppressor PTEN. This situation is in clear contrast to the anti-proliferative effect observed in other cancer types and possibly reflects cell type specific differences in miR-26 function ([154] and [198]).
Deregulation of most miRNAs, underrepresented in cancer cells, may be due to transcriptional repression, for instance by the c-MYC oncogene ([127], [146] and [199]). Alternatively expression of these miRNAs could be inhibited at the posttranscriptional level. For example C-MYC was shown to induce transcription of *lin-28* which blocks maturation of certain miRNAs like let-7 [193]. As expression of the miR-26 family was shown to be posttranscriptionally regulated and uncoupled from host gene expression it is possible that posttranscriptional mechanisms also contribute to the downregulation of miR-26 family members in cancer cells.

In this study it was demonstrated that *olig2*$^{+}$ NSCs develop normal in miR-26 deficient zebrafish embryos (Figure 22) indicating that high levels of miR-26 are not necessary to maintain stem cell properties but differentiation in motor neurons is prevented by miR-26 knockdown. However, this study did not focus on the role of the miR-26 family in cell cycle control. If motor neuron precursors do not differentiate in miR-26b morphants because they can not leave cell cycle remains unclear. Anyway, *olig2*$^{+}$ NSCs are able to stop proliferation and differentiate into oligodendrocytes (Figure 23). These observations could be explained by cell type specific differences, as oligodendrocytes develop considerably later than motor neurons. Alternatively, miR-26 knockdown does not interfere with cell cycle exit but subsequent steps of neuronal differentiation. However, overexpression of Ctdsp1 in chicken neuroepithelial cells interferes with cell cycle exit and induces ectopic cell proliferation, indicating a role in cell cycle regulation for Ctdsps [115] and consequently also miR-26.
The matter of fact that miR-26 target genes are described as negative and positive regulators of cell differentiation seems to be contradictory. So far it is controversial, if miR-26 plays a role in cell differentiation, but most data suggest that miR-26 directs cell cycle exit and differentiation into diverse cell types. Further studies are necessary to shed light on that, especially in the context of developing organ systems.

7.4 Functional relationships between intronic miRNAs and host genes

Since many intronic miRNAs are coexpressed with their host genes, both spatially and temporally, cellular functions of host gene products and miRNAs are connected. Intronic miRNAs and host genes could therefore cooperate or antagonize each other. Indeed, there are some examples for cooperation of intronic miRNAs and host gene proteins in regulation of cell function. Apoptosis-associated tyrosine kinase (AATK), essential for neuronal cell differentiation, encodes miR-338. MiR-338 is coexpressed with AATK and silences negative regulators of neurogenesis. Hence, miR-338 represses genes which are functional antagonistic to its host gene [200]. MiR-218 is located in introns of the *slit* gene family and targets the Slit-receptor Roundabout (Robo) during

vascular patterning. This way, miR-218 fine-tunes the Slit-Robo signalling pathway [201]. The muscle gene expression program is controlled by miR-208a, which is encoded in an intron of α-Myosin heavy chain. MiR-208a influences expression of other Myosins by silencing transcriptional repressors of these genes. So, *myosins* not only encode for major contractile components of muscle cells but also for gene regulatory molecules affecting expression of other muscle specific genes [202]. As described in these studies, intronic miRNAs and host gene proteins frequently cooperate to accomplish their functions. Furthermore, the relation between intronic miRNAs and host genes apparently is often conserved for whole families of miRNAs and host genes.

In contrast, functions of miR-26b and *ctdsp2* counteract each other in neuronal cell differentiation. As demonstrated in this study, miR-26b silences expression of its host gene, the anti-neuronal factor Ctdsp2, in neurons (Figure 30). This regulation is rendered possible by posttranscriptional uncoupling of *ctdsp2* mRNA and miR-26b expression (Figure 30). By targeting *ctdsp2*, miR-26b controls the neuronal gene expression program and contributes to neuronal cell differentiation (Figure 30). Such ultra-short feedback loops have been predicted by the analysis of gene regulatory networks containing intronic miRNAs ([180] and [203]), but experimental evidence remained elusive. It is tempting to speculate that the *ctdsp2*/miR-26b autoregulatory loop has evolved to reduce the susceptibility of the REST/Ctdsp pathway to transcriptional noise [204], which might otherwise interfere with the fine-tuned low level expression required for neurogenesis [118]. Also cooperative function of the miR-26 family and its *ctdsp* host genes was reported [128]. Authors report that in primary fibroblasts miR-26a and miR-26b are coexpressed with their respective *ctdsp* host genes and cooperate to inhibit cell cycle progression. However, expression was only analyzed at the level of mature miR-26 and *ctdsp* mRNA, but not pre-mir-26 and Ctdsp2 protein. Hence, in the light of results presented in this study the readout of the study presented by Zhu *et al.* [128] is limited.

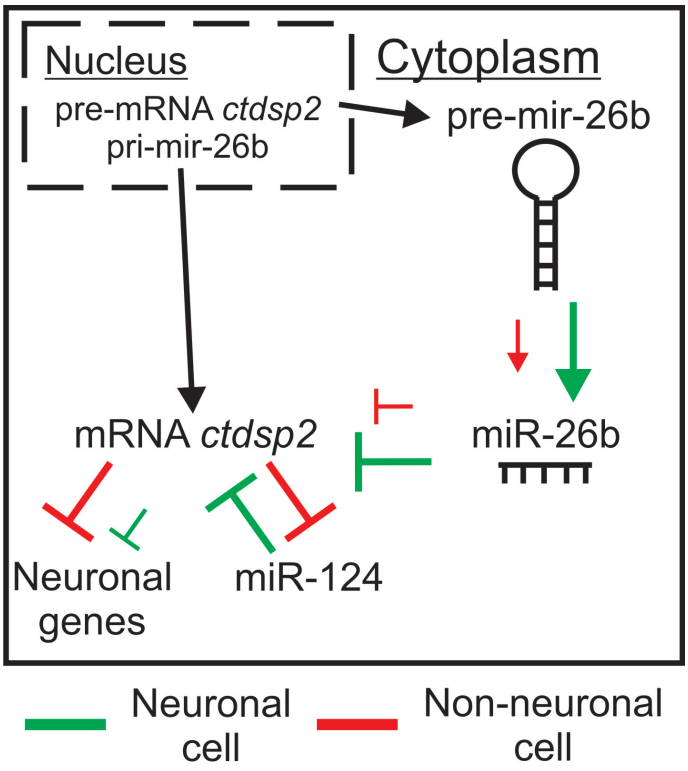

Figure 30: Regulation of neuronal gene expression by the *ctdsp2*/miR-26 autoregulatory loop
MiR-26b and its host gene *ctdsp2* have antagonistic functions. In context of the REST-complex, Ctdsp2 inhibits expression of neuronal genes like miR-124. Mature miR-26b is enriched in neurons by posttranscriptional regulation of pre-mir-26b processing and silences Ctdsp2 expression at the transition from neuronal stem cell to neuron. This *cis*-regulatory event allows derepression of neuronal genes and consequently neuronal gene expression.

7.5 Non-neuronal functions of the REST/Ctdsp-complex and miR-26

The REST-complex was described as a negative transcriptional regulator of neuronal genes in non-neuronal tissues and there is hard evidence that this is its main function. Nevertheless, RE1 consensus sequences are frequent in vertebrate genomes ([121] and [205]) and functional RE1s were discovered also in a small group of non-neuronal genes ([102], [105] and [206]). Thus, the REST/Ctdsp-complex might act in cell type specific way and also influence transcription of non-neuronal genes. Furthermore, REST was identified as a tumor suppressor [207] and can be converted to an activator of neuronal gene expression by binding of a small non-coding double stranded RNA [208]. Also the arthropod homologue of REST, *charlatan*, acts as a repressor or activator of neuronal genes dependent on cell context [209]. Increasing evidence suggest that also the composition of the REST complex itself varies between different cell types or even promotors ([105], [120] and [125]) and some REST-complex components were shown to have additional functions independent of the REST-complex ([210] and [211]). Together with the embryonic lethality of REST knockout mice [100], this indicates a somewhat broader functional spectrum for the REST-complex. During early embryonic inductive events, Ctdsps influence transcription of down-stream targets by fine tuning of Smad signalling. First, Ctdsps stimulate the Transforming Growth Factor-β (TGFβ) pathway by dephosphorylating the linker regions of Smad1/2/3. This is the first scenario including Ctdsps as positive regulators of transcription ([212] and [213]). Second, Ctdsps inhibit BMP activity by

dephosphorylating the C-terminal SXS motif of Smad1 ([214], [212] and [215]). This mechanism is biochemically clearly distinct from inhibiting transcription of neuronal genes in CNS development.

Control of the gene expression program by miR-26a and miR-26b might be important not only in neurons, but for differentiation events in general, as both family members have been implicated in differentiation of other cell types, stemness and cancer ([144], [147], [154] and [216]). These events are mediated by other targets than *ctdsp2* and seem to be independent from the *ctdsp2*/miR-26b autoregulatory loop.

As shown in this study, Ctdsp2 is expressed in non-neuronal tissues in presence of low levels of miR-26b. So, one has to speculate that the *ctdsp2* mRNA somehow escapes translational silencing by miR-26b in these tissues. This could happen by interaction with RNA binding proteins covering the miR-26b target site, as demonstrated for other miRNA targets ([217] and [218]). Probably miR-26 acts as a global regulatory factor, which induces differentiation of neurons and other cell types in a concentration dependent manner and supports maintenance of tissue identity. However, non-neuronal tissues developed normal in miR-26b morphant embryos and no block of differentiation of non-neuronal cell types was observed. More experimental work is necessary to elucidate the mechanisms of fine-tuning Ctdsp2 expression in non-neuronal tissues and its function in differentiation towards non-neuronal cell types.

7.6 Final considerations and perspective

This study provides the first experimental evidence for host gene regulation by its intronic miRNA. Such interactions have been computationally predicted before and similar regulatory networks exist involving intron-derived siRNAs in plants, controlling host gene transcription [219]. However, no direct interaction between an intronic miRNA and its host transcript was demonstrated before. As the host gene silencing by miR-26b is connected to posttranscriptional regulation of its own biosynthesis, findings presented in this study are innovative and open up new ideas about gene regulatory networks.

Nevertheless, the question remains open why such a complicated system evolved. The anti-neuronal function of Ctdsps is beyond question and sufficiently documented. *Ctdsp2* mRNA is produced in zebrafish neuronal tissues, but instantly silenced by miR-26b. In fact, expression levels of *ctdsp2* are highest in zebrafish brain. This seems to be contradictory. One could assume that in neurons the *ctdsp2*/miR-26b locus does not mainly serve as blueprint for Ctdsp2 protein, but mature miR-26b. In such a case the *ctdsp2* mRNA would only be a waste-product and needs to be eliminated. Furthermore, miR-26 has other predicted anti-neuronal targets. High levels of miR-26 originating from the ctdsp loci, might be necessary to inhibit expression of these targets.

Posttranscriptional regulation of miRNA maturation is a widespread phenomenon under physiological and pathological conditions ([59] and [220]). There may be other intronic candidate miRNAs, which might be expressed in stem cells and downregulated during differentiation by posttranscriptional mechanism. In future studies it would be interesting to analyze whether other intronic miRNAs are subject to regulatory events, similar to miR-26, during differentiation of stem cells and elucidate these mechanisms on the molecular level [185].

8 APPENDIX

8.1 Functional analysis of PRPF31 in a zebrafish model for Retinitis Pigmentosa

Malfunctions in mRNA metabolism are thought to be responsible for many hereditary neurodegenerative diseases. These dysfunctions can concern RNA editing, polyadenylation, nuclear export, mRNA stability or pre-mRNA splicing [221]. Splicing-associated diseases can be grouped into three major classes depending on the mutated component. The first group encompasses diseases where mutations affect *cis*-regulatory sequences in distinct mRNAs and hence interfere with their accurate maturation. In contrast to this group stand the second and third class of diseases, which are characterized by mutations in the spliceosome assembly machinery or general *trans*-acting factors involved in pre-mRNA splicing. Because in the latter cases, a more widespread defect in mRNA metabolism can be anticipated, the pathomechanism of these diseases is expected to be rather complex and difficult to analyze. One prominent example for a hereditary disease caused by mutations in general pre-mRNA processing factors is late-onset Retinitis Pigmentosa (RP). This neurodegenerative disease with an incidence of 1 in 3000 people [222], is characterized by severe photoreceptor degeneration and resulting loss of vision [223]. RP is commonly caused by mutations in genes with specific functions in visual perception [224]. However, approximately 11% of autosomal dominant RP cases result from mutations in one of the three splice factor genes *prpf3* [225], *prpf*8 [226] and *prpf*31 [227]. Their gene products are part of the U4/U6.U5 tri-snRNP (small nuclear Ribonucleoprotein particle), a spliceosomal sub-unit that is formed by an intricate network of interactions between more than 30 proteins and three snRNAs (small nuclear RNAs) [228]. This snRNP contributes substantially to the active centre of the spliceosome and contains essential components for the dynamic rearrangements that occur during its assembly and activation [229].

The question arises, how mutations in ubiquitously expressed splice factors can transform into a highly tissue specific phenotype as observed in RP patients. To answer this question, a valuable disease model is required. In previous studies it could be shown that knockdown of *prpf31* in *Drosophila* leads to significant reduction of eye size [230] and decreased levels of functional PRPF3, PRPF8 or PRPF31 cause a degenerative phenotype of the mouse retinal pigmented epithelium [231]. Furthermore, mutations in these factors cause aberrant pre-mRNA splicing *in vitro* [232]. However, all these studies could not contribute new insights about the etiology of splice factor-associated RP.

The zebrafish *Danio rerio* offers several advantages for this type of investigation over other common model organisms. First, using a morpholino-based knockdown approach allows fine-tuned gene-silencing [233], an important condition when analyzing essential proteins such as splice factors. Second, effects on photoreceptor cell morphology and function can be directly studied in a functionally cone-dominated retina that is similar to its human counterpart [234]. Finally, it allows for the expression profiling of eye-specific transcripts and is thus advantageous over cell culture systems [235]. Graziotto *et al.* described heterozygous *prpf3* zebrafish mutants as devoid of any phenotype [236]. We have previously established the zebrafish as a vertebrate model for Spinal Muscular Atrophy (SMA; [237]) and provide a zebrafish model for RP caused by *prpf31*-mutations in this study

([238]; reprinted in the following section with permission from Oxford University Press). This model resembles important aspects of RP, like retinal apoptosis, decreased expression of retina-specific transcripts, loss of photoreceptor cells and consequently vision ([238], see also [239]). In a related study, Christoph Winkler and coworkers used this model to further elucidate the molecular mechanism underlying splice factor associated RP [240].

Appendix

Human Molecular Genetics, 2011, Vol. 20, No. 2 368–377 doi:10.1093/hmg/ddq473 Advance Access published on November 3, 2010

Systemic splicing factor deficiency causes tissue-specific defects: a zebrafish model for retinitis pigmentosa

Bastian Linder[1], Holger Dill[1], Anja Hirmer[1], Jan Brocher[2], Gek Ping Lee[3], Sinnakaruppan Mathavan[3], Hanno Jörn Bolz[4], Christoph Winkler[2], Bernhard Laggerbauer[1] and Utz Fischer[1]

[1]Department of Biochemistry, University of Würzburg, 97074 Würzburg, Germany, [2]Department of Biological Sciences, National University of Singapore, 117543 Singapore, Singapore, [3]Genome Institute of Singapore, 138672 Singapore, Singapore and [4]Institute of Human Genetics, University Hospital of Cologne, 50931 Cologne, Germany

Received May 27, 2010; Revised and Accepted October 29, 2010

To whom correspondence should be addressed at: Department of Biochemistry, Biocenter, University of Würzburg, Am Hubland, 97074 Würzburg, Germany. Tel: +49 9318884029; Fax: +49 9318884028; Email: utz.fischer@biozentrum.uni-wuerzburg.de

Microarray data have been submitted to Gene Expression Omnibus with the accession number GSE20424.

Retinitis pigmentosa (RP) is a common hereditary eye disease that causes blindness due to a progressive loss of photoreceptors in the retina. RP can be elicited by mutations that affect the tri-snRNP subunit of the pre-mRNA splicing machinery, but how defects in this essential macromolecular complex transform into a photoreceptor-specific phenotype is unknown. We have modelled the disease in zebrafish by silencing the RP-associated splicing factor Prpf31 and observed detrimental effects on visual function and photoreceptor morphology. Despite reducing the level of a constitutive splicing factor, no general defects in gene expression were found. Instead, retinal genes were selectively affected, providing thefirst *in vivo* link between mutations in splicing factors and the RP phenotype. Silencing of Prpf4, a splicing factor hitherto unrelated to RP, evoked the same defects in vision, photoreceptor morphology and retinal gene expression. Hence, various routes affecting the tri-snRNP can elicit tissue-specific gene expression defects and lead to the RP phenotype.

INTRODUCTION

Retinitis pigmentosa (RP) is a hereditary eye disease that leads to night blindness, a severely constricted visual field and in many cases to legal blindness (1). These symptoms are the result of a progressive degeneration of photoreceptor cells in the retina. Consistent with this tissue-specific phenotype, RP is caused mainly by mutations in genes that are preferentially or exclusively expressed in the retina and play important roles in photoreceptor development, their maintenance or phototransduction (2). However, 12% of autosomal dominant RP cases result from mutations in genes that are ubiquitously, rather than eye-specifically expressed. These include the genes PRPF3, PRPF31, PRPF8 and SNRNP200, which encode components of the pre-mRNA splicing machinery (3–6). During splicing, intronic sequences are removed from pre-mRNAs and the coding exons are joined to give rise to mature mRNAs. This reaction is catalyzed by the spliceosome, a macromolecular complex composed offive small nuclear ribonucleoprotein particles (snRNPs) and a large number of non-snRNP factors. Each snRNP contains a name giving uridine-rich small nuclear RNA (U1, U2, U4, U5 and U6 snRNA, respectively), a set of proteins common to all snRNPs (Sm proteins) and numerous snRNP-specific factors (reviewed in 7). The spliceosome is a highly dynamic entity which assembles anew in a step-wise fashion on each intron of a given pre-mRNA. In a first step, binding of the U1 and U2 snRNPs to the 5 ' -splice site and branchpoint, respectively, gives rise to the pre-spliceosome. The pre-catalytic spliceosome is completed by the joining of a pre-assembled U4/U6.U5 tri-snRNP. Finally, structural rearrangements accompanied by the release of the U1 and U4 snRNPs lead to catalytic activation so that splicing can occur. All RP-associated splicing factors are part of the U4/U6.U5 tri-snRNP, which is formed by an intricate network of interactions between 30 proteins and three snRNAs [see (8) and references therein]. This large snRNP contributes substantially to the active center of the spliceosome and contains essential components for the dynamic rearrangements that occur during its assembly and activation. In addition, recent data suggest that the joining of the tri-snRNP to the assembling spliceosome plays an important role in splice site definition and therefore may contribute to the regulation of alternative splicing events (9–11).

How RP mutations in constitutive splicing factors transform into a cell-type-specific phenotype is currently under debate. It is hypothesized that such mutations impair the tri-snRNP in a way that decreases splicing activity and, as a result, alters the steady-state levels of transcripts with weakly spliced introns. Consequently, cells that require gene products encoded by these transcripts would degenerate. Twofindings support the hypothesis of such a scenario in RP. First, all known RP-linked splicing factors are part of one and the same spliceosomal subunit, i.e. the tri-snRNP, and no other function has been described for them thus far. Secondly, it has been shown that haploinsufficiency of these factors can lead to disease, suggesting that their reduced activity in the context of the spliceosome rather than a toxic gain of function is causative (12). However, a direct link between RP and mRNA metabolism is still lacking.

To identify such a potential link, we have modelled the disease in zebrafish by interfering with the expression of the RP-linked splicing factor Prpf31. These fish presented an eye-specific phenotype remarkably similar to that of RP. Gene expression analysis revealed that the majority of transcripts were unaffected by reduced levels of Prpf31. However, a small group of mRNAs was strongly down-regulated. Strikingly, retina-specific transcripts were highly enriched in this group, providing a list of candidate genes for mediating the tissue-specific phenotype.

Extending our study to another tri-snRNP factor, Prpf4, we observed that its knockdown elicited the same RP-like phenotype and defects in gene expression. Our data suggest that reduced levels of tri-snRNP proteins cause RP by affecting the expression of genes in a selective, rather than a general manner and give a plausible explanation for the tissue specificity of the disease.

RESULTS

Prpf31 haploinsufficiency in zebrafish causes defects in visual function

We chose Prpf31 for a detailed investigation in zebrafish as it is most commonly affected and its pivotal role in splicing is established (2, 13). Injection of 3.5 ng of antisense morpholino directed against the translation start site of *prpf31* mRNA resulted in an almost complete suppression of Prpf31 protein expression (Fig. 1A). Embryonic lethality and extensive deformations were the consequence (Fig. 1C). This phenotype was specific, as coinjection of a morpholino-insensitive *prpf31* mRNA largely reduced deformations and lethality (Fig. 1D). Interestingly, mRNA carrying the RP-causing missense mutation p.A216P (3) failed to rescue Prpf31-deficient fish, although expression levels were comparable with the endogenous protein of wild-type fish (Fig. 1A and E). These data confirm *prpf31* as an essential gene in zebrafish and suggest that p.A216P mutant protein is non-functional *in vivo*.

Next, we wished to define conditions under which potential tissue specific effects may occur. Lowering the amount of injected *prpf31* morpholino correlated with a decline in both, deformations and lethality of the fish (Supplementary Material, Fig. S1). When 2.5 ng of morpholino was injected, a knockdown efficiency of ~70% was achieved at 4 days post-fertilization (dpf) (Fig. 2A and B) but no gross morphological defects were observed (Fig. 2C and Supplementary Material, Fig. S1). To test these animals for visual deficits as the key symptom of RP, we analyzed the optokinetic nystagmus (OKN), a reflex elicited by presenting a moving striped pattern to immobilized larvae (14). At 4 dpf, eye movements were recorded from control and morphant fish (see Supplementary Material, Movies, and Fig. 2D for experimental setup). When the angle of the eye was plotted over time, uninjected controls produced a sawtooth-shaped curve, representing alternating slow pursuit movements and fast saccades (Fig. 2E, left panel) that closely resembled previously published patterns (14). In contrast, *prpf31* morphants showed a markedly reduced OKN, and in severe cases no saccadic movements were present at all (Fig. 2E, right panel). In order to quantify this phenotype, the average number of saccades during 20 s of stimulation was evaluated from five independent injection experiments. It was reduced >2-fold upon *prpf31* morpholino injection (Fig. 2F). As an additional control, we tested larvae that had been injected with a morpholino directed against the survival motor neuron (*smn*) mRNA. The knockdown of this U snRNP biogenesis factor elicits defects in motoneurons of zebrafish *(15, 16)*. However, the *smn* morpholino had no significant effect on the OKN of the injected zebrafish (Fig. 2F), indicating the specificity of the *prpf31*-morphant phenotype.

In order to assess the ability of p.A216P mutant Prpf31 protein to rescue eye-specific defects, in vitro transcribed *prpf31* mRNA and 2.5 ng of *prpf31* morpholino were co-injected into zebrafish larvae. However, expression of the exogenous Prpf31 protein did not last beyond 24 hours post-fertilization (hpf), thus leading to a period of splicing factor deficiency that preceded eye development (data not shown). This prevented the analysis of visual defects

in these animals. Nevertheless, the data presented here show that reduced levels of Prpf31 specifically affect the visual system, either directly or indirectly by interfering with other neuromuscular activities required for OKN function.

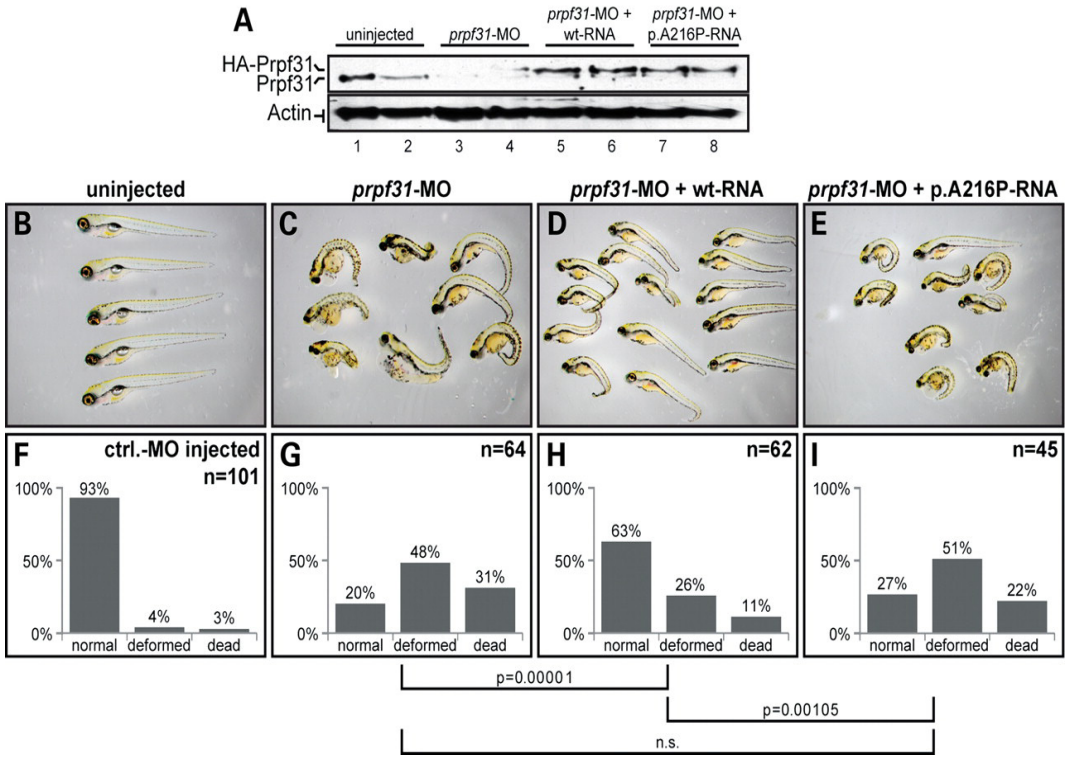

Figure 1. Knockdown of Prpf31 in zebrafish leads to embryonic lethality that can be rescued by co-injection of wild-type but not RP-mutant *prpf31* mRNA. (A) Prpf31 expression levels were monitored in single larvae by western blotting (upper panel). Injection of 3.5 ng of *prpf31* morpholino (31MO) led to a severe reduction in the expression of endogenous Prpf31 (lanes 1–4). Co-injection of *prpf31* mRNA resulted in the expression of exogenous wild-type (lanes 5 and 6) and p.A216P mutant (lanes 7 and 8) HA-tagged Prpf31. Actin served as a loading control (lower panel). (B–E) Phenotype of control and injected larvae at 4 dpf. (B) Normal morphology of uninjected controls. (C) Knockdown of Prpf31 caused lethality and severe deformations. (D) In morphants that expressed exogenous HA-tagged wild-type Prpf31, an improvement in the phenotype was observed. (E) Expression of p.A216P mutant Prpf31 failed to improve the phenotype. (F–I) Quantification of four independent experiments; percentage of normal, deformed and dead animals in control-injected (F), *prpf31* morphant (G), wild-type rescue (H) and p.A216P rescue (I) animals. The rescue effect (G versus H) and the loss-of-function effect of the p.A216P mutation (H versus I) were highly significant (Pearson χ^2-test; n is the total number of injected animals).

Photoreceptor morphology is disturbed in *prpf31* morphants

We next analyzed whether reduced expression of Prpf31 leads to defects in photoreceptors, the cell type primarily affected in RP patients. To assess photoreceptor integrity, embryos were injected either with control morpholino or the *prpf31* morpholino at a concentration that evokes the OKN phenotype (Fig. 3A). At 4 dpf, transversal cryosections of these animals were analyzed by immunohistochemistry using the monoclonal anti-rhodopsin antibody 1D4 to visualize photoreceptor outer segments and 4', 6-diamidino-2-phenylindole (DAPI) for nuclear staining. All six retinal layers were apparent in control animals and *prpf31* morphants (Fig. 3B and C), although layering was less pronounced in some animals of the latter group. In contrast, 1D4 staining in the photoreceptor cell layer (PCL) was severely reduced in 81% (21/26) of the *prpf31*-morphant eyes analyzed (Fig. 3B–E).

Next, the morphology of photoreceptor cell bodies was assessed using the zpr1/Fret43 antibody (17). No significant differences between control and morphant eyes were observed, suggesting that eye development in

general was unaltered and Prpf31 deficiency primarily affected photoreceptor outer segments (Fig. 3F and G). Importantly, a series of histological experiments further showed that the phenotype was not caused by a non-specific defect or delay in development. First, *in situ* hybridization (ISH) using probes specific for myoD, pax2a and *myf5* confirmed normal development of the trunk, early brain structures and eye musculature, respectively (Fig. 3H–M). Secondly, no crucial delay in development was detected at 4 dpf, neither by evaluating the concomitance of the five branchial arches (Fig. 3N and O) nor by analyzing mitotic cells in the eye by ISH with a proliferating cell nuclear antigen (*pcna*)-specific probe (Fig. 3P–S). Together, these data uncover a photoreceptor-specific phenotype that is unlikely to be caused by a general developmental defect or delay in Prpf31-deficient fish.

Sublethal knockdown of Prpf31 predominantly affects retinal transcripts

Interfering with an essential splicing factor such as Prpf31 in principle could impair the transcriptome on a genome-wide level, as nearly all protein-coding genes in vertebrates contain introns. Their inefficient or aberrant removal is predicted to decrease the steady-state levels of affected mRNAs, as nonsense-mediated decay is active in zebrafish and very efficiently degrades mis-spliced transcripts (18, 19). We therefore analyzed the transcriptome of dissected eyes from control and Prpf31-deficient larvae using a genome-wide comparative microarray.

Interestingly, only 2.6% of the 19.917 transcripts present on the microarray were down-regulated with a fold change (FC) higher than 1.5x, arguing against a widespread splicing defect (Fig. 4A; for a complete list, see Supplementary Material, Table S1). Retinal mRNAs in particular were affected as they accounted for 8.6% of the down-regulated transcripts (Fig. 4B). To exclude a bias from using 'retina-enriched' tissue for the microarray, the portion of retinal transcripts in the most severely affected group was determined (FC>3x). It was significantly higher than in the total down-regulated set (65 versus 8.6%), indicating that Prpf31 deficiency indeed selectively affected retinal transcripts (Fig. 4B). Our discovery that only a small set of transcripts is affected strengthens the hypothesis that splicing in general is unaffected in RP patients (20, 21).

Strikingly, more than half of the down-regulated retinal transcripts are encoded by genes implicated in the pathogenesis of RP or an allied disease (marked in red in Fig. 4A). These mRNAs were confirmed as targets of Prpf31 deficiency by semiquantitative RT–PCR and ISHs (Fig. 4D and E). Furthermore, some of them (marked with a dot in Fig. 4A) were likewise affected in a previously reported zebrafish mutant that carries a lesion in the U4/U6 snRNP recycling factor p110, suggesting that they do not represent morpholino-induced artefacts (22). These data reveal a set of candidate transcripts whose impaired expression could mediate the retina-specific phenotype.

Despite the fact that the observed defects in gene expression were restricted to a small set of transcripts, our microarray also provides evidence that Prpf31 knockdown indeed affected the splicing machinery. Analogous to what has been described as a compensatory pathway for impaired snRNP recycling (22), our microarray analysis showed that a number of splicing factor transcripts were significantly up-regulated in *prpf31* morphants (Fig. 4A and C). Hence, we conclude that Prpf31 deficiency disturbs the function of the tri-snRNP in a way that selectively affects photoreceptor cells.

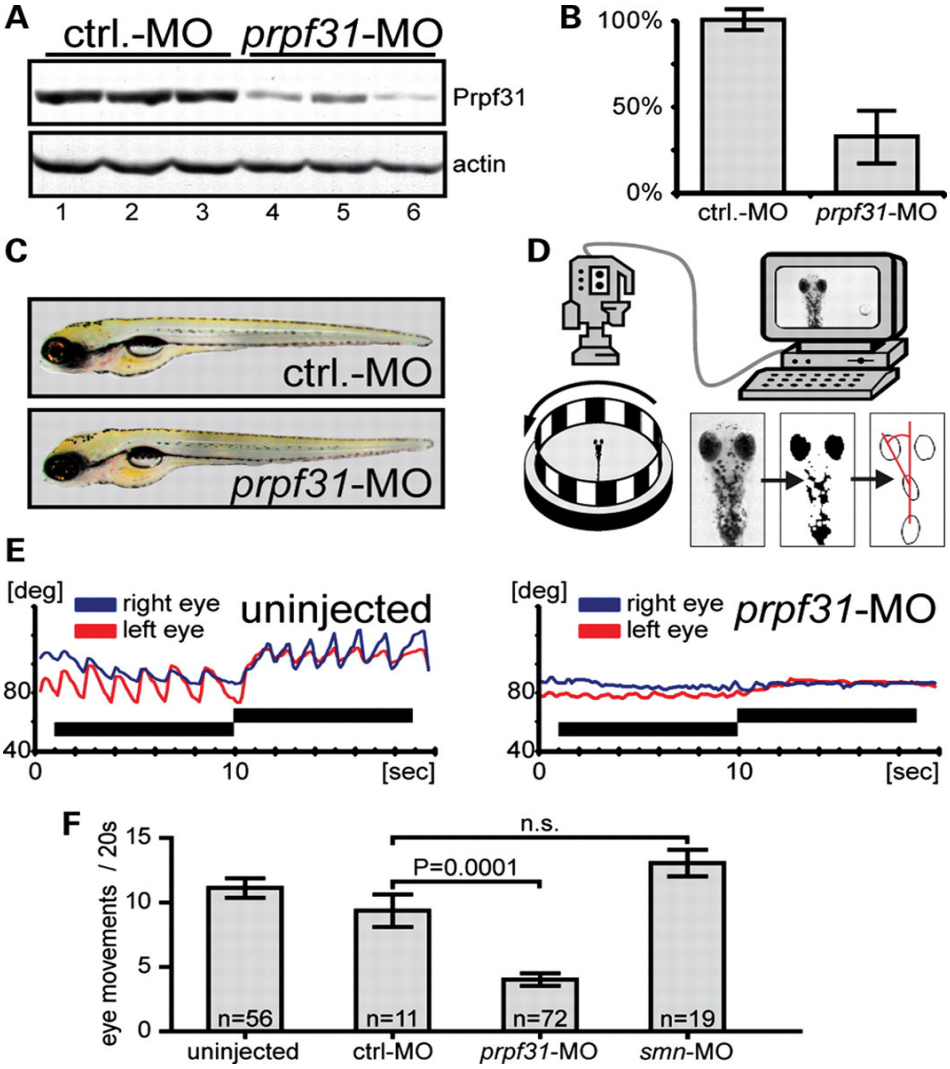

Figure 2. Zebrafish larvae with a sublethal reduction of Prpf31 expression show defects in visual processing. (A) Western blot analysis of 4 dpf larvae injected with control morpholino (lanes 1–3) or a sublethal dose of *prpf31* morpholino (2.5 ng; lanes 4–6). (B) Densitometric quantification of Prpf31 expression levels (error bars: SEM). (C) Normal phenotype of control morpholino-injected fish and the sublethal *prpf31* morphants at 2 dpf. (D) Experimental setup for OKN tests. (E) Representative eye movements of uninjected controls (left panel) or *prpf31* morphants (right panel). Graphs represent the angle of the eye relative to the image plotted over time. (F) Quantification of OKN results from five independent experiments. Mean number of saccades presented during 20 s of stimulation for uninjected fish and fish injected with control morpholino, *prpf31* morpholino or smn morpholino. Error bars represent the SEM; n is the total number of animals analyzed; significance was determined by an unpaired t-test.

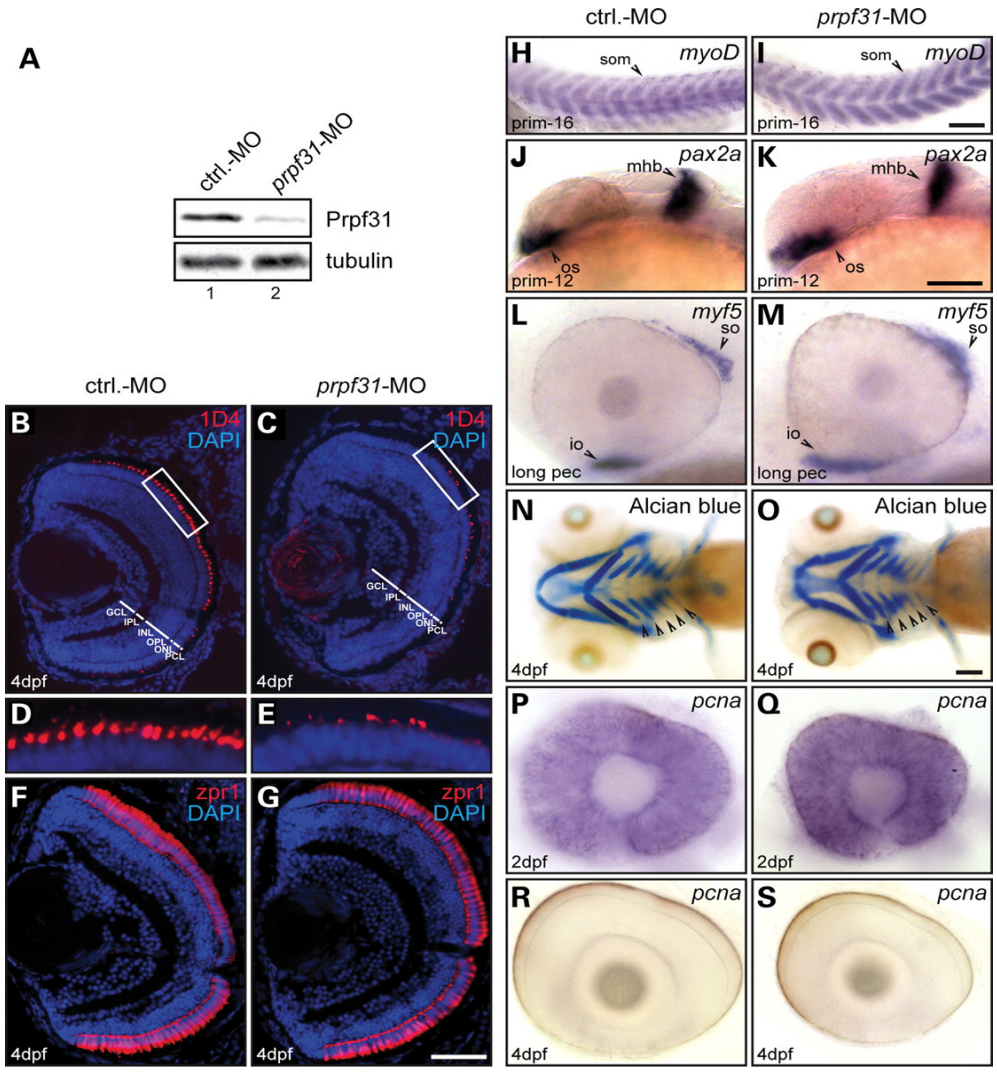

Figure 3. Reduced Prpf31 expression leads to defective photoreceptor cells. (A) Prpf31 expression levels at 4 dpf. (B–E) Immunohistochemistry on retinal sections of 4 dpf larvae using the 1D4 antibody. DAPI staining (blue) detects the six retinal layers in control (B) and Prpf31-deficient (C) animals (GCL, ganglion cell layer; IPL, inner plexiform layer; INL, inner nuclear layer; OPL, outer plexiform layer; ONL, outer nuclear layer; PCL, photoreceptor cell layer). Photoreceptor outer segments (red) were strongly reduced in Prpf31-deficient animals. (D and E) Higher magnification identified individual outer segments. (F and G) Double-cone pair photoreceptor cell bodies were stained using the zpr1/FRet43 antibody. Scale bar in (G) is 50 μm and accounts for (B), (C), (F) and (G). (H–M) To control for the specificity of the phenotype, the expression patterns of the markers *myoD* (H and I), *pax2a* (J and K) and *myf5* (L and M) were analyzed by *in situ* hybridization of control morpholino (H, J and L) and *prpf31* morpholino (I, K and M) injected animals. Somites (som), mid–hindbrain boundary (mhb), optic stalk (os) and the eye muscles superior oblique (so) and inferior oblique (io) were normal in stage-matched larvae. (N–S) At 4 dpf, no developmental delay was detectable in control-injected (N) and *prpf31*-morpholino-injected (O) larvae using Alcian-blue staining, as all five branchial arches were detected (arrowheads). (P–S) *In situ* hybridizations revealed *pcna* expression in control (P and R) and morphant (Q and S) eyes at 2 dpf (P and Q), which was lost at 4 dpf (R and S), indicating that most cells at this time point were post-mitotic and eye development in general was not delayed.

Prpf4 deficiency causes a photoreceptor-specific defect in zebrafish

The previous identification of four core components of the tri-snRNP as RP disease genes suggested that photoreceptors are particularly vulnerable to defects in the general function of this snRNP. We tested this hypothesis experimentally by silencing the expression of Prpf4, a tri-snRNP component essential for splicing and cell viability that interacts with the protein product of the RP disease gene *prpf3* (23–26).

Injection of a morpholino directed against *prpf4* resulted in embryonic lethality that was dose dependent and could be rescued by the co-injection of in vitro transcribed *prpf4* mRNA (Supplementary Material, Fig. S2). Using a sublethal morpholino dose, the overall morphology of the larvae was unaffected, while a strong reduction of

Prpf4 protein was still achieved (Fig. 5A). The OKN of these animals was assessed at 4 dpf as described for *prpf31* morphants. The average number of saccades was significantly reduced (Fig. 5B) and, in severe cases, saccades were almost absent (Fig. 5C and D and Supplementary Material, Movies).

This pointed to a visual defect in the *prpf4* morphants, and their retinal morphology was analyzed by immunohistochemistry.

While retinal layering was mostly normal, 1D4 staining was found to be substantially decreased in 16 out of 20 eyes analyzed (Fig. 5E–H). As in the Prpf31-deficient larvae, photoreceptor outer segments were primarily affected and the cell bodies were morphologically unaffected (Fig. 5I and J). This phenotype was not a consequence of a defect in general development since ISHs using probes specific for *myoD*, *pax2a* or *myf5* failed to show significant differences from controls (Fig. 5K–P). Furthermore, no developmental delay could be observed at 4 dpf by Alcian-blue staining of the branchial arches and *pcna* ISH of the eye (Fig. 5Q–V).

As the Prpf4-deficient fish were phenotypically indistinguishable from our Prpf31 RP model, we next tested whether in both fish the same transcripts were affected. For this, semi-quantitative RT–PCR analysis of the RP-relevant transcripts *opn1lw1*, *opn1mw1*, *gnat2*, *irx6a*, *rx3*, *crx* and *rhodopsin* as well as the controls *gapdh* and *lsm7* was performed. A very similar pattern of down-regulation was observed for these transcripts (Fig. 5W). We conclude that the molecular events which link mutations in RP-associated splicing factors to photoreceptor degeneration can likewise be triggered by defects in *prpf4*.

DISCUSSION

To reconstruct the mechanisms by which defects in general splicing factors cause tissue-specific effects, we have established a zebrafish model for Prpf31 and Prpf4 deficiency. The phenotype of these fish was remarkably similar to RP. First, photoreceptor morphology was defective, as 1D4 staining was almost completely abolished in their outer segments. Secondly, because the optokinetic response in zebrafish larvae is mediated mainly by cones (27), the observed OKN defect indicates that the function of these photoreceptors was also impaired. Thirdly, the photoreceptor defects were specific, since a detailed morphological and developmental analysis failed to show systemic defects of the morphants. Together, these data imply that our model reflects a late-stage RP phenotype with a severe rod–cone dystrophy. It will now be interesting to analyze whether the retinal phenotype is the consequence of a degenerative event (as in humans) or due to a defect in photoreceptor development.

In our model, splicing factor deficiencies were >50%. This suggests that the tri-snRNP has to be compromised in a way that exceeds haploinsufficiency to cause RP, a scenario supported by the finding that mice and zebrafish that are heterozygous null for either *prpf3* or *prpf31* fail to develop RP-like symptoms (28, 29). In line with this, even though many people carry RP mutations in one PRPF31 allele, they do not develop RP throughout their lifespan. It has been proposed that this reduced penetrance is associated with a low expressing wild-type allele, and our data confirm such a hypothesis (30, 20).

How the shortfall of essential splicing factors transforms into a tissue-specific phenotype is one of the puzzling aspects of splicing-factor-linked RP. Our microarray study for the first time provides an unbiased molecular clue to this tissue-specificity paradox, as among the most strongly affected transcripts, those encoded by retinal genes

and — even more importantly — retinal disease genes were enriched. However, although our microarray analysis preceded the major phenotype and thus was designed to enrich for primary targets, extreme care has to be taken when dissecting the direct targets of an impaired tri-snRNP from secondary effects that will almost certainly arise due to photoreceptor cell damage. One such example is the rhodopsin transcript that was affected in *prpf31* and *prpf4* morphants, but is devoid of introns in zebrafish (31). Of note, several components of the photoreceptor -specific transcription factor network controlling *rhodopsin* expression were downregulated in *prpf31* morphants (*crx*, *nrl*, *rx3* and *pax6a*; see Supplementary Material, Table S1), providing an alternative explanation for impaired *rhodopsin* mRNA levels. These data show that our zebrafish model is a valuable tool for analyzing the transcriptome of splicing-factor-deficient photoreceptors.

Although the spliceosome consists of a large number of proteins and snRNAs, all splicing factors that have been linked to RP so far are components of the tri-snRNP. There is accumulating evidence that RP mutations in splicing factors indeed affect the integrity of this spliceosomal subparticle. For example, biochemical studies in yeast have revealed a U5 snRNP maturation defect caused by PRPF8 RP mutations, suggesting that an inactive form of the U5 snRNP accumulated (32). Furthermore, for PRPF31, it has been reported that the pathogenic mutation p.A216P impairs its integration into snRNPs, while reduced levels of functional PRPF31 inhibit tri-snRNP formation (33, 34). These data imply that not the individual splicing factor defect but its impact on the general function of the tri-snRNP causes RP. In line with this assumption, we failed to detect specific eye defects in zebrafish with reduced levels of the U1-specific splicing factor protein C (Supplementary Material, Fig. S3). Our finding that the silencing of Prpf4, a tri-snRNP component hitherto unrelated to RP, can evoke a retina-specific phenotype confirms such a model. Moreover, similar molecular mechanisms might underlie this pathology, as transcripts that were down-regulated in *prpf31* morphants were likewise affected in Prpf4-deficient animals. Further support for this comes from the p110 mutant zebrafish, which displays reduced levels of U4/U6 di-snRNPs rather than defects in individual factors of this particle. Although it is unclear at the moment whether these fish have a retinal phenotype, it has been shown that photoreceptor mRNA levels were decreased (22).

In summary, our data strongly support the hypothesis that tri-snRNP dysfunction in a broader sense can affect gene expression in a way that elicits retinal defects, an idea that is of special importance in the context of the large fraction of unknown RP disease genes (1,2). The microarray study not only gives a molecular clue for the tissue specificity paradox of RP, but also sets the stage for a further in-depth analysis of the affected transcripts. One question we can now address is why these mRNAs might be more susceptible to alterations in the splicing apparatus. We may speculate that some of them contain introns that are intrinsically weakly spliced and hence are more sensitive to alterations in the general splicing machinery than others. Such studies will allow a detailed insight into the pathway from mutations in general splicing factors to tissue-specific diseases.

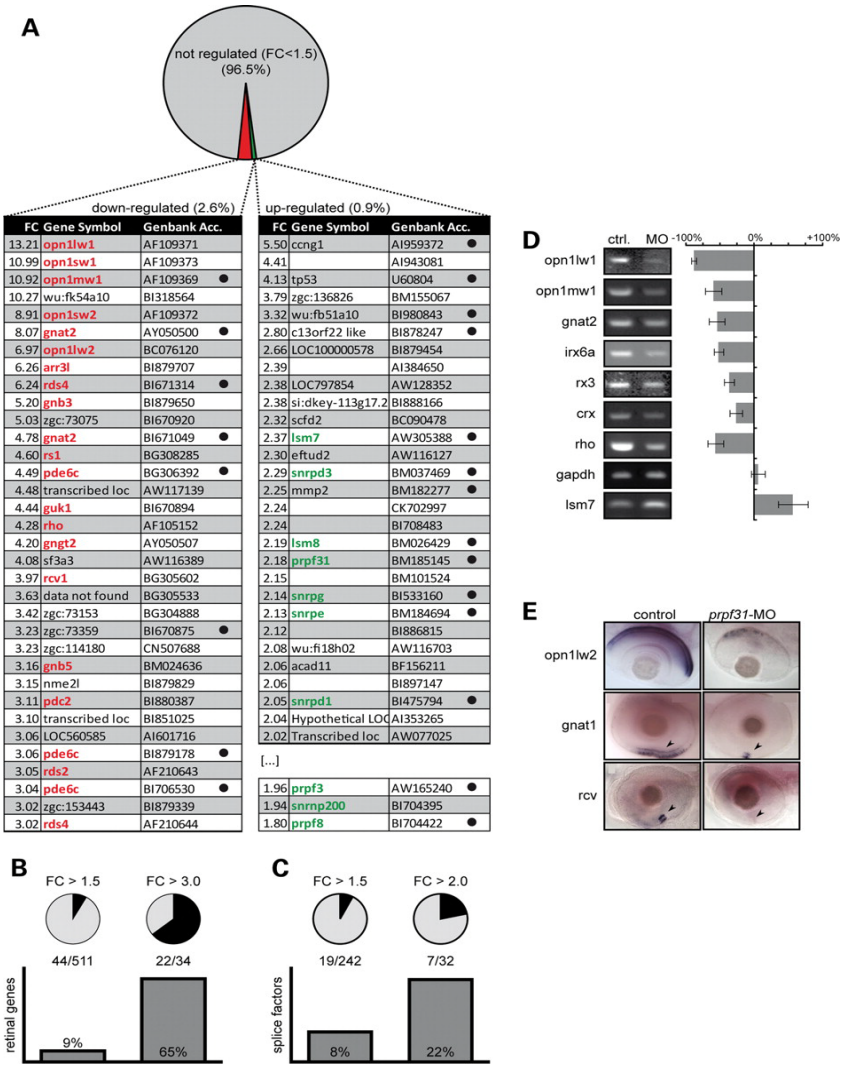

Figure 4. Photoreceptor transcripts are specifically affected in the eyes of *prpf31* morphants. (A) Genome-wide microarray analysis revealed that only a small fraction of transcripts was affected with an FC higher than 1.5x. The top fractions of down-and up-regulated transcripts are shown (left and right panel, respectively; for a complete list, see the Supplementary Material); retinal genes and splicing factors are marked in red and green, respectively. Transcripts that have been shown to be similarly affected by a deficiency of the tri-snRNP recycling factor p110 (22) are marked with a dot. (B) Retinal genes were enriched among the most highly down-regulated transcripts. (C) Splicing factors were enriched among the most highly up-regulated transcripts. (D) Validation of Prpf31-sensitive mRNAs by semi-quantitative RT–PCR. Transcripts from the most strongly affected set (>3x; *opn1lw1*, *opn1mw1*, *gnat2*, *rho*) and from those that showed a milder down-regulation (>1.5x; *irx6a*, *rx3*, *crx*) were tested. Transcripts of an unaffected housekeeping gene (*gapdh*) and an up-regulated splicing factor (*lsm7*) served as controls. The mean FC (as a percentage relative to controls) was determined from three independent injection experiments; error bars represent SEM. (E) Validation of the down-regulation of selected mRNAs in the eyes of *prpf31* morphants. ISH was performed using probes specific for *opn1lw2* (dorsal view), *gnat1* (lateral view) and *recoverin* (*rcv*, lateral view).

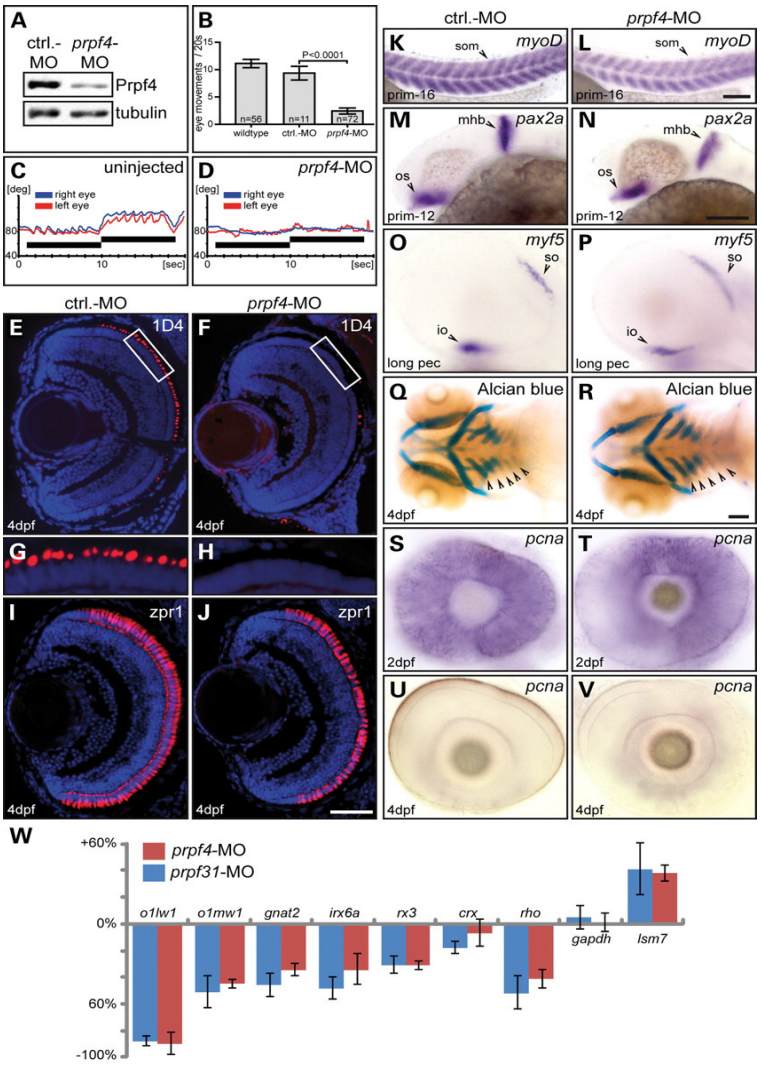

Figure 5. Reduced levels of Prpf4 cause defects in vision, photoreceptor morphology and retinal gene expression. (A) Injection of a sublethal dose of *prpf4* morpholino (0.5 ng) reduced Prpf4 expression. (B) Quantification of OKN of *prpf4* morphants and uninjected control fish. (C and D) Representative saccades of controls (C) and Prpf4-deficient fish (D). (E–J) Immunostaining on retinal cryosections revealed a loss of photoreceptor outer segments in *prpf4* morphants (red in E–H) while cone cell bodies remained unaffected as determined by zpr1 staining (red in I and J). Scale bar in (J) is 50 μm and accounts for (E), (F), (I) and (J). (K–P) The specificity of the phenotype was confirmed by analyzing the development of somites (som in K and L), the mid–hindbrain boundary (mhb in M and N), the optic stalk (os in M and N) and the eye muscles superior oblique (so in O and P) and inferior oblique (io in O and P) by ISH as described in Figure 3.(Q–V) A severe general developmental delay at 4 dpf was excluded using Alcian-blue staining of the five branchial arches (Q and R) and *pcna* ISH as described in Figure 3 (S–V). (W) Semi-quantitative RT–PCR revealed a similar down-regulation of retinal transcripts in *prpf4* (blue) and *prpf31* morphants (red). In both morphants, *gapdh* was unaffected and the level of *lsm7* mRNA was increased. Bar graphs represent the mean FC compared with controls; error bars show the SEM.

MATERIALS AND METHODS

Plasmids and antibodies

Zebrafish *prpf31* and *prpf4* were amplified from 14 hpf embryonic oligo-dT cDNA using gene-specific primers (see Supplementary Material, Table S3 for sequences). cDNAs were inserted into a modified version of the pcDNA3 vector that adds an N-terminal hemagglutinin (HA) tag for the transfection of HeLa cells into the pET21a, pET28a and the pGEX-6P1 vector for the production of recombinant proteins and into an HA-tagged version of the pCS2+ vector (35) for in vitro transcription.

For the generation of antibodies, His-tagged versions of full-length human *hPrp4*, *hPrp3* or zebrafish Prpf4 and Prpf31 were expressed in Escherichia coli BL21 (DE3) cells and purified on fast-flow Ni-NTA (Qiagen, Germany).

Rabbits were immunized with the purified proteins (Immuno-Globe, Germany) and antisera affinity-purified on immobilized antigen columns.

Microinjection of zebrafish and western blotting

Morpholino oligos (MOs) (Gene Tools, LLC) were designed against the ATG regions of *prpf31* and *prpf4* (see Supplementary Material, Table S3 for sequences). Embryos were injected at the one-or two-cell stage with ~0.5 nl of morpholino dissolved in water containing 0.25% Phenol Red. Embryo rearing and fish husbandry were performed as described previously (16). Lysates for western blots were prepared by homogenization of single larvae in 20 ml of a 1 : 1 mixture of Laemmli sample buffer and buffer B (100 mM NaH2PO4,10 mM Tris pH 8.0, 8 M urea). For rescue experiments, single clutches of embryos were divided into four groups. The first was left uninjected and the second was injected with a lethal concentration of MO (7 mg/ml for *prpf31*-MO, 2 mg/ml for *prpf4*-MO). Groups 3 and 4 were co-injected with a lethal dose of MO together with in vitro transcribed wild-type or mutant mRNA (final concentration 100 ng/ ml). mRNA was capped co-transcriptionally using the mMessage Machine SP6 kit (Ambion) and purified using RNeasy Mini columns (Qiagen, Germany). Translation of injected mRNA was monitored by Western blotting at 12 hpf. After 4dpf, injected larvae were scored as either lethal, severely deformed (curled body axis, gross head misdevelopment, cardiac edema or combinations thereof) or slightly deformed/not affected. At least three independent experiments were performed for each analysis.

Optokinetic nystagmus

OKN analysis was carried out as described (14). Briefly, single larvae were immobilized in a 3.5 cm Petri dish using 3% methyl cellulose and a moving pattern was presented by a back-illuminated metal grating (128 stripes) rotating at 6 rpm for 10 s to the left and right. Animals were recorded from above and the number of saccades was counted. Eye movements of selected larvae were analyzed using a custom script for the NIH ImageJ program.

***In situ* hybridization and staining of zebrafish larvae**

RNA whole-mount ISHs were carried out as described previously (36). Templates for probe transcription were amplified from cDNA by using specific PCR primers (Supplementary Material, Table S3), cloned into the pCRII vector and transcribed with Sp6 or T7 RNA polymerase in a digoxigenin labelling reaction.

For staining of the cartilage skeleton, larvae were fixed in 4% paraformaldehyde, washed in PBS and bleached for 1 h in 1 ml of 10% H_2O_2 containing one drop of 2 M KOH. After bleaching, specimens were washed in PBS and stained overnight in Alcian-blue (0.1% Alcian-blue, 70% ethanol, 1% HCl). Discoloration was performed in acidic ethanol (5% HCl, 70% ethanol) for at least 5 h. Larvae were dehydrated in increasing concentrations of ethanol and stored in 80% glycerol until photography.

For immunostaining, larvae were fixed in 4% paraformalde hyde at 4°C overnight, washed and incubated with 30% saccharose. Larvae were positioned in Tissue-Tek (SAKURA, Zoeterewoude, The Netherlands), frozen in liquid nitrogen and 8 µm sections were cut in a Jung Frigocut 2800N (Leica). After transfer to SuperFrostPlus

Microscope Slides, blocking was performed using 2% goat serum in PBS. For labelling of rods or double-cone pair photoreceptors, sections were incubated with mouse monoclonal 1D4 anti-rhodopsin antibodies (1 : 200; Abcam, Cambridge, UK) or mouse monoclonal anti-zpr-1 antibodies (1 : 300; Zebrafish International Resource Center, Eugene, USA) in 5% goat serum in PBS containing 0.3% Triton X-100 for 3 h at room temperature. The primary antibodies were visualized by using a Texas Red dye-conjugated goat anti-mouse IgG + IgM (1 : 120; Jackson ImmunoResearch, Baltimore, USA). Slides were mounted in Vectashield Mounting Medium with DAPI (Vector Laboratories, Burlingame, USA).

Microarray analysis of zebrafish morphants

Zebrafish embryos were injected at the one-cell stage with *prpf31* morpholino at a concentration of 2.5 mg/ml. At 3dpf, ~2500 eyes (1250 eyes each for morpholino-injected embryos and non-injected control) were manually dissected and used for total RNA preparation (RNeasy Kit, Qiagen, Singapore). RNAs were reverse-transcribed in the presence of dNTPs mixed with aminoallyl-dUTP (Sigma-Aldrich, USA), followed by coupling with mono-functional NHS-ester Cy3 and Cy5 dyes (Amersham, USA). Samples were hybridized on customized Compugen zebrafish array slides containing 23.232 zebrafish-specific oligonucleotide probes. Fluorescence intensity detection was performed as described earlier (37). The intensity values were normalized (Lowess normalization) and subjected to SAM analysis (www-stat.stanford.edu/~tibs/ SAM/). The cutoff threshold for significant down - regulation was set to an FC of 1.5x and the q-value was below 5%.

RT–PCR analysis

Whole-embryo RNA was extracted with Trizol (Invitrogen) from 20 injected or control embryos. After DNase digestion, RNA was recovered using RNeasy columns (Qiagen). Equal amounts of RNA were used for the subsequent reverse transcription with random hexamer primers. PCR was performed using gene-specific primers (Supplementary Material, Table S3) and analyzed by agarose gel electrophoresis. Ethidium-bromide-stained PCR products were quantified with the NIH ImageJ software package, and mean values from three experiments were calculated.

SUPPLEMENTARY MATERIAL

Supplementary Material is available at HMG online.

ACKNOWLEDGEMENTS

We thank P. Engerer and J. Beck for validating microarray data, R. Lührmann and A. Bindereif for reagents, as well as M. Gessler and A. Chari for critically reading the manuscript.

Conflict of Interest statement. None declared.

FUNDING

This work was supported by DFG grants to U.F. (SFB581 and RVZ-network) and an AcRF grant (T207B3107) from the Ministry of Education, Singapore, to C.W. B.L. and A.H. received fellowships from the German ProRetina foundation and the GK 1048, respectively.

REFERENCES

1. Hartong, D.T., Berson, E.L. and Dryja, T.P. (2006) Retinitis pigmentosa. Lancet, 368, 1795–809.
2. Daiger, S.P., Bowne, S.J. and Sullivan, L.S. (2007) Perspective on genes and mutations causing retinitis pigmentosa. Arch. Ophthalmol., 125, 151–158.
3. Vithana, E.N., Abu-Safieh, L., Allen, M.J., Carey, A., Papaioannou, M., Chakarova, C., Al-Maghtheh, M., Ebenezer, N.D., Willis, C., Moore, A.T. et al. (2001) A human homolog of yeast pre-mRNA splicing gene, PRP31, underlies autosomal dominant retinitis pigmentosa on chromosome 19q13.4 (RP11). Mol. Cell, 8, 375–381.
4. Chakarova, C.F., Hims, M.M., Bolz, H., Abu-Safieh, L., Patel, R.J., Papaioannou, M.G., Inglehearn, C.F., Keen, T.J., Willis, C., Moore, A.T. et al. (2002) Mutations in HPRP3, a third member of pre-mRNA splicing factor genes, implicated in autosomal dominant retinitis pigmentosa. Hum. Mol. Genet., 11, 87-92.
5. Zhao, C., Bellur, D.L., Lu, S., Zhao, F., Grassi, M.A., Bowne, S.J., Sullivan, L.S., Daiger, S.P., Chen, L.J., Pang, C.P. et al. (2009) Autosomal-dominant retinitis pigmentosa caused by a mutation in SNRNP200, a gene required for unwinding of U4/U6 snRNAs. Am. J. Hum. Genet., 85, 617–627.
6. Li, N., Mei, H., MacDonald, I.M., Jiao, X. and Hejtmancik, J.F. (2010) Mutations in ASCC3L1 on 2q11.2 are associated with autosomal dominant retinitis pigmentosa in a Chinese family. Invest. Ophthalmol. Vis. Sci., 51, 1036–1043.
7. Wahl, M.C., Will, C.L. and Lu¨hrmann, R. (2009) The spliceosome: design principles of a dynamic RNP machine. Cell, 136, 701–718.
8. Liu, S., Rauhut, R., Vornlocher, H. and Lu¨hrmann, R. (2006) The network of protein–protein interactions within the human U4/U6.U5 tri-snRNP. RNA, 12, 1418–1430.
9. House, A.E. and Lynch, K.W. (2006) An exonic splicing silencer represses spliceosome assembly after ATP-dependent exon recognition. Nat. Struct. Mol. Biol., 13, 937–944.
10. Bonnal, S., Martı´nez, C., Fo¨rch, P., Bachi, A., Wilm, M. and Valca´rcel, J. (2008) RBM5/Luca-15/H37 regulates Fas alternative splice site pairing after exon definition. Mol. Cell, 32, 81–95.
11. Sharma, S., Kohlstaedt, L.A., Damianov, A., Rio, D.C. and Black, D.L. (2008) Polypyrimidine tract binding protein controls the transition from exon definition to an intron defined spliceosome. Nat. Struct. Mol. Biol., 15, 183–191.
12. Abu-Safieh, L., Vithana, E.N., Mantel, I., Holder, G.E., Pelosini, L., Bird, A.C. and Bhattacharya, S.S. (2006) A large deletion in the adRP gene PRPF31: evidence that haploinsufficiency is the cause of disease. Mol. Vis., 12, 384–388.
13. Weidenhammer, E.M., Singh, M., Ruiz-Noriega, M. and Woolford, J.L.J. (1996) The PRP31 gene encodes a novel protein required for pre-mRNA splicing in Saccharomyces cerevisiae. Nucleic Acids Res., 24, 1164–1170.
14. Neuhauss, S.C.F. (2003) Behavioral genetic approaches to visual system development and function in zebrafish. J. Neurobiol., 54, 148–160.
15. McWhorter, M.L., Monani, U.R., Burghes, A.H.M. and Beattie, C.E. (2003) Knockdown of the survival motor neuron (Smn) protein in zebrafish causes defects in motor axon outgrowth and pathfinding. J. Cell Biol., 162, 919–931.
16. Winkler, C., Eggert, C., Gradl, D., Meister, G., Giegerich, M., Wedlich, D., Laggerbauer, B. and Fischer, U. (2005) Reduced U snRNP assembly causes motor axon degeneration in an animal model for spinal muscular atrophy. Genes Dev., 19, 2320–2330.
17. Larison, K.D. and Bremiller, R. (1990) Early onset of phenotype and cell patterning in the embryonic zebrafish retina. Development, 109, 567–576.

18. Wittkopp, N., Huntzinger, E., Weiler, C., Sauliere, J., Schmidt, S., Sonawane, M. and Izaurralde, E. (2009) Nonsense-mediated mRNA decay effectors are essential for zebrafish embryonic development and survival. Mol. Cell Biol., 29, 3517–3528.
19. Kawashima, T., Pellegrini, M. and Chanfreau, G.F. (2009) Nonsense-mediated mRNA decay mutes the splicing defects of spliceosome component mutations. RNA, 15, 2236–2247.
20. Rivolta, C., McGee, T.L., Rio Frio, T., Jensen, R.V., Berson, E.L. and Dryja, T.P. (2006) Variation in retinitis pigmentosa-11 (PRPF31 or RP11) gene expression between symptomatic and asymptomatic patients with dominant RP11 mutations. Hum. Mutat., 27, 644–653.
21. Ivings, L., Towns, K.V., Matin, M., Taylor, C., Ponchel, F., Grainger, R.J., Ramesar, R.S., Mackey, D.A. and Inglehearn, C.F. (2008) Evaluation of splicing efficiency in lymphoblastoid cell lines from patients with splicing-factor retinitis pigmentosa. Mol. Vis., 14, 2357–2366.
22. Trede, N.S., Medenbach, J., Damianov, A., Hung, L., Weber, G.J., Paw, B.H., Zhou, Y., Hersey, C., Zapata, A., Keefe, M. et al. (2007) Network of coregulated spliceosome components revealed by zebrafish mutant in recycling factor p110. Proc. Natl Acad. Sci. USA, 104, 6608–6613.
23. Banroques, J. and Abelson, J.N. (1989) PRP4: a protein of the yeast U4/U6 small nuclear ribonucleoprotein particle. Mol. Cell Biol., 9, 3710–3719.
24. Bjorn, S.P., Soltyk, A., Beggs, J.D. and Friesen, J.D. (1989) PRP4 (RNA4) from Saccharomyces cerevisiae: its gene product is associated with the U4/U6 small nuclear ribonucleoprotein particle. Mol. Cell Biol., 9, 3698–3709.
25. Horowitz, D.S., Kobayashi, R. and Krainer, A.R. (1997) A new cyclophilin and the human homologues of yeast Prp3 and Prp4 form a complex associated with U4/U6 snRNPs. RNA, 3, 1374–1387.
26. Lauber, J., Plessel, G., Prehn, S., Will, C.L., Fabrizio, P., Groning, K., Lane, W.S. and Luhrmann, R. (1997) The human U4/U6 snRNP contains 60 and 90 kD proteins that are structurally homologous to the yeast splicing factors Prp4p and Prp3p. RNA, 3, 926–941.
27. Bilotta, J., Saszik, S. and Sutherland, S.E. (2001) Rod contributions to the electroretinogram of the dark-adapted developing zebrafish. Dev. Dyn., 222, 564–570.
28. Graziotto, J.J., Inglehearn, C.F., Pack, M.A. and Pierce, E.A. (2008) Decreased levels of the RNA splicing factor Prpf3 in mice and zebrafish do not cause photoreceptor degeneration. Invest. Ophthalmol. Vis. Sci., 49, 3830–3838.
29. Bujakowska, K., Maubaret, C., Chakarova, C.F., Tanimoto, N., Beck, S.C., Fahl, E., Humphries, M.M., Kenna, P.F., Makarov, E., Makarova, O. et al. (2009) Study of gene-targeted mouse models of splicing factor gene Prpf31 implicated in human autosomal dominant retinitis pigmentosa (RP). Invest. Ophthalmol. Vis. Sci., 50, 5927–5933.
30. Vithana, E.N., Abu-Safieh, L., Pelosini, L., Winchester, E., Hornan, D., Bird, A.C., Hunt, D.M., Bustin, S.A. and Bhattacharya, S.S. (2003) Expression of PRPF31 mRNA in patients with autosomal dominant retinitis pigmentosa: a molecular clue for incomplete penetrance? Invest. Ophthalmol. Vis. Sci., 44, 4204–4209.
31. Fitzgibbon, J., Hope, A., Slobodyanyuk, S.J., Bellingham, J., Bowmaker, J.K. and Hunt, D.M. (1995) The rhodopsin-encoding gene of bony fish lacks introns. Gene, 164, 273–277.
32. Boon, K., Grainger, R.J., Ehsani, P., Barrass, J.D., Auchynnikava, T., Inglehearn, C.F. and Beggs, J.D. (2007) prp8 mutations that cause human retinitis pigmentosa lead to a U5 snRNP maturation defect in yeast. Nat. Struct. Mol. Biol., 14, 1077–1083.
33. Huranova, M., Hnilicova, J., Fleischer, B., Cvackova, Z. and Stanek, D. (2009) A mutation linked to retinitis pigmentosa in HPRP31 causes protein instability and impairs its interactions with spliceosomal snRNPs. Hum. Mol. Genet., 18, 2014–2023.
34. Schaffert, N., Hossbach, M., Heintzmann, R., Achsel, T. and Luhrmann, R. (2004) RNAi knockdown of hPrp31 leads to an accumulation of U4/U6 di-snRNPs in Cajal bodies. EMBO J., 23, 3000–3009.
35. Turner, D.L. and Weintraub, H. (1994) Expression of achaete-scute homolog 3 in Xenopus embryos converts ectodermal cells to a neural fate. Genes Dev., 8, 1434–1447.
36. Winkler, C., Schafer, M., Duschl, J., Schartl, M. and Volff, J. (2003) Functional divergence of two zebrafish midkine growth factors following fish-specific gene duplication. Genome Res., 13, 1067–1081.
37. Mathavan, S., Lee, S.G.P., Mak, A., Miller, L.D., Murthy, K.R.K., Govindarajan, K.R., Tong, Y., Wu, Y.L., Lam, S.H., Yang, H. et al. (2005) Transcriptome analysis of zebrafish embryogenesis using microarrays. PLoS Genet., 1, e29

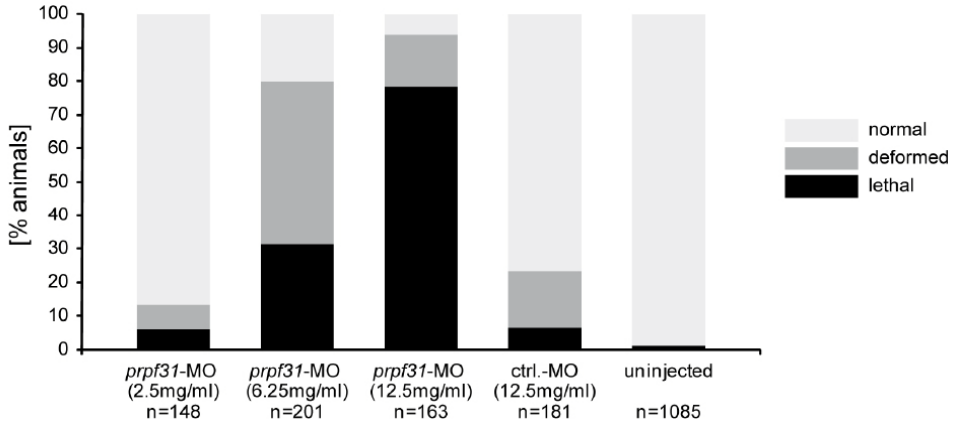

Figure S1. Effect of different concentrations of *prpf31*-MO on zebrafish survival and development. Zebrafish embryos were injected with approx. 0.5 nl of the indicated MO solutions and survival (dark bars) or deformations (grey bars) were scored 4 days later. Uninjected or control-MO injected zebrafish embryos were used as controls. n illustrates the number of embryos injected for each experiment.

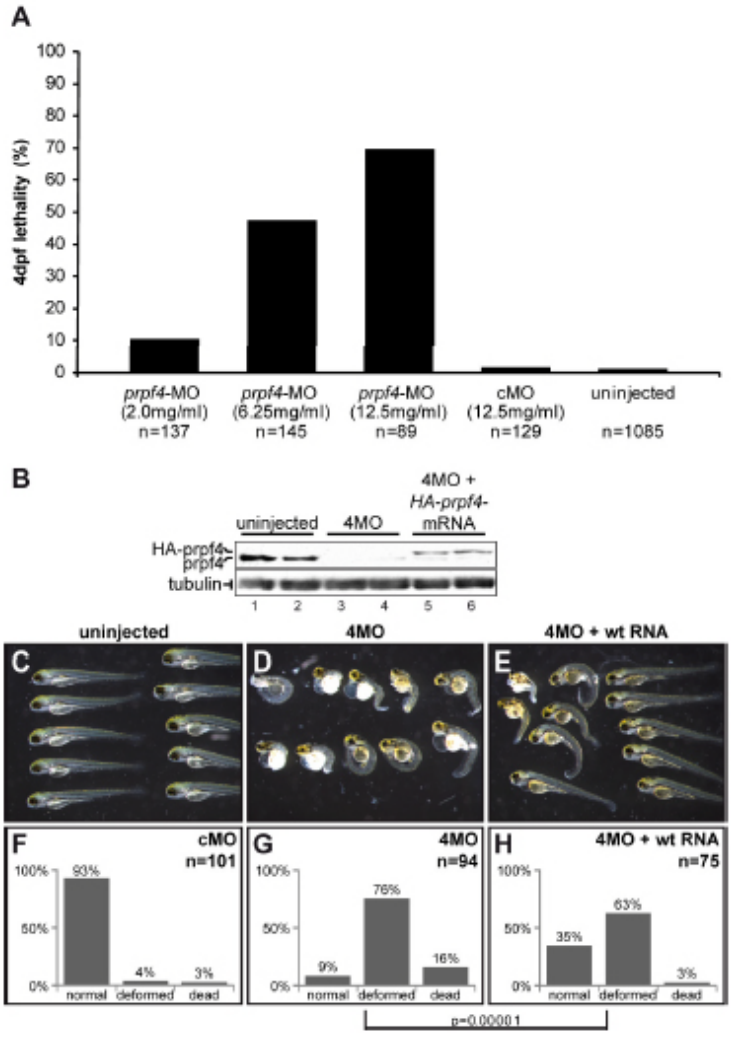

Figure S2. (A) Effect of different concentrations of *prpf4*-MO on zebrafish survival. Zebrafish embryos were injected with approx. 0.5 nl of the indicated MO solutions and survival was scored 4 days later. Uninjected or control-MO injected zebrafish embryos were used as controls. n illustrates the number of embryos injected for each experiment. (B-H) The lethality induced by *prpf4* knockdown can be rescued by co-injection of *prpf4* mRNA. (B) Western blot of single larvae of uninjected, *prpf4* morphant and RNA co-injected fish. Injection of *prpf4*-morpholino alone led to a severe reduction in the expression of the endogenous protein (upper panel, compare lanes 1 and 2 with 3 and 4). Co-injection of 50 pg of *in vitro* transcribed *prpf4* mRNA resulted in the expression of exogenous HA-tagged protein (upper panel, lanes 5 and 6). Tubulin was used as a loading control (lower panel). While control morpholino injected larvae had no visible phenotype (C, F), *prpf4* morphants were severely affected(D, G). Expression of exogenous HA-Prpf4 led to a significant improvement of the phenotype (E, H). Quantification and statistics were performed as described in Figure 1.

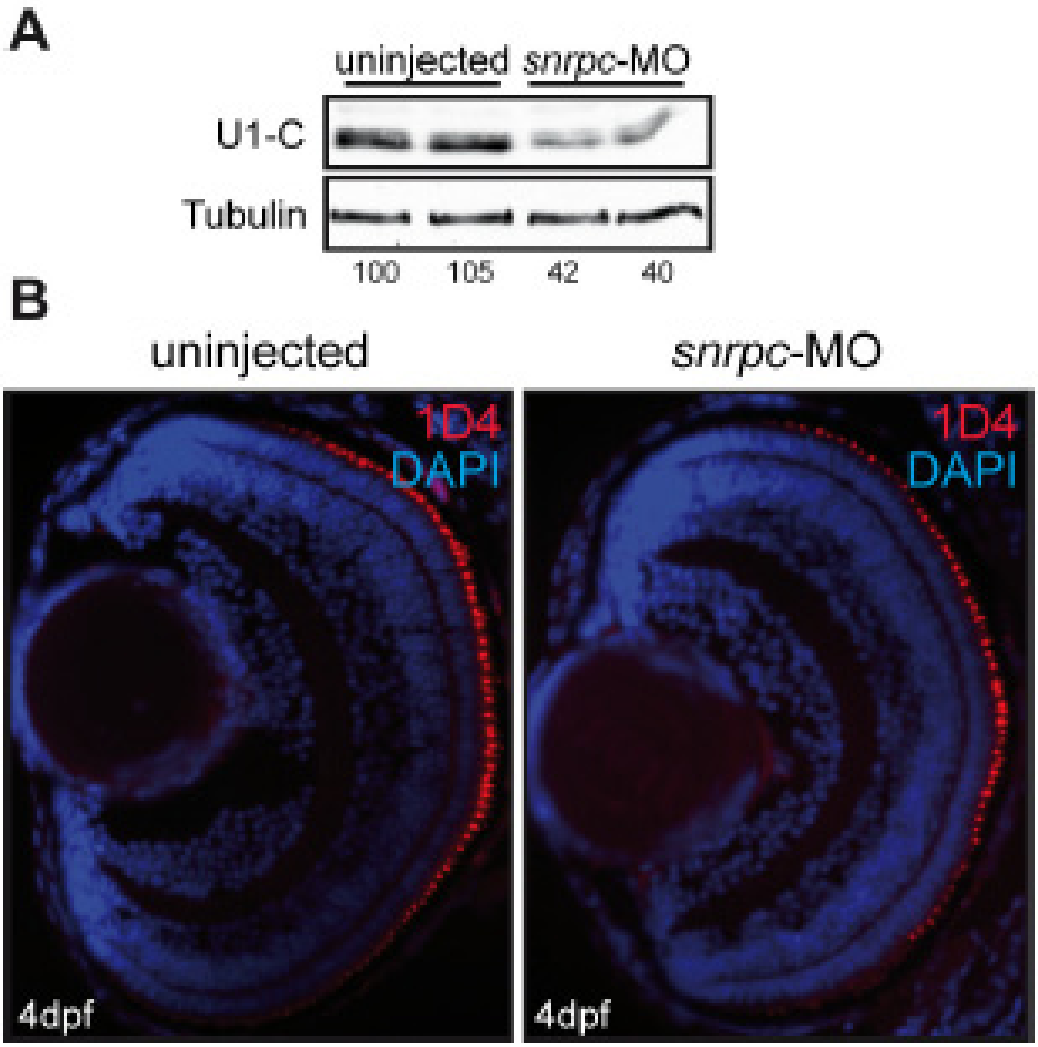

Figure S3. Reduced levels of U1-C protein do not lead to defects in photoreceptor cells. (A) Western blot of uninjected and *U1C* morpholino-injected zebrafish. Protein levels are indicated below the individual lanes. (B) Immunohistochemistry on retinal sections of 4dpf larvae using the 1D4 antibody. DAPI staining (blue) detects the six retinal layers in control (left panel) and U1-C deficient (right panel) animals. Photoreceptor outer segments (red) were not significantly reduced in U1-C morphants.

8.2 Vector maps

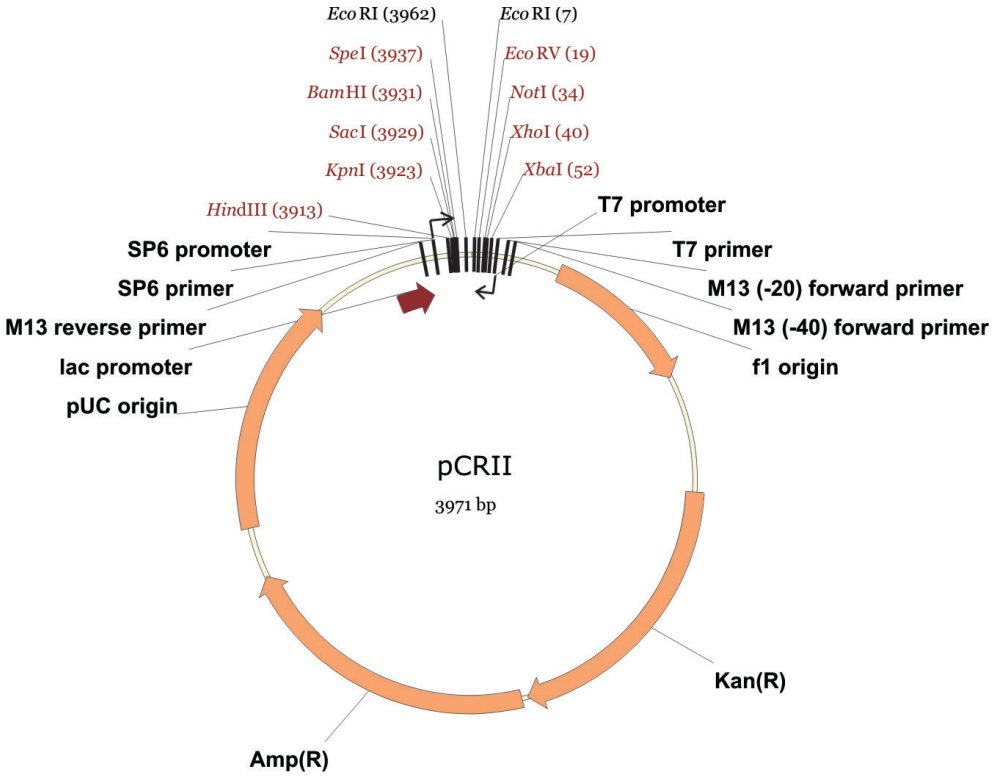

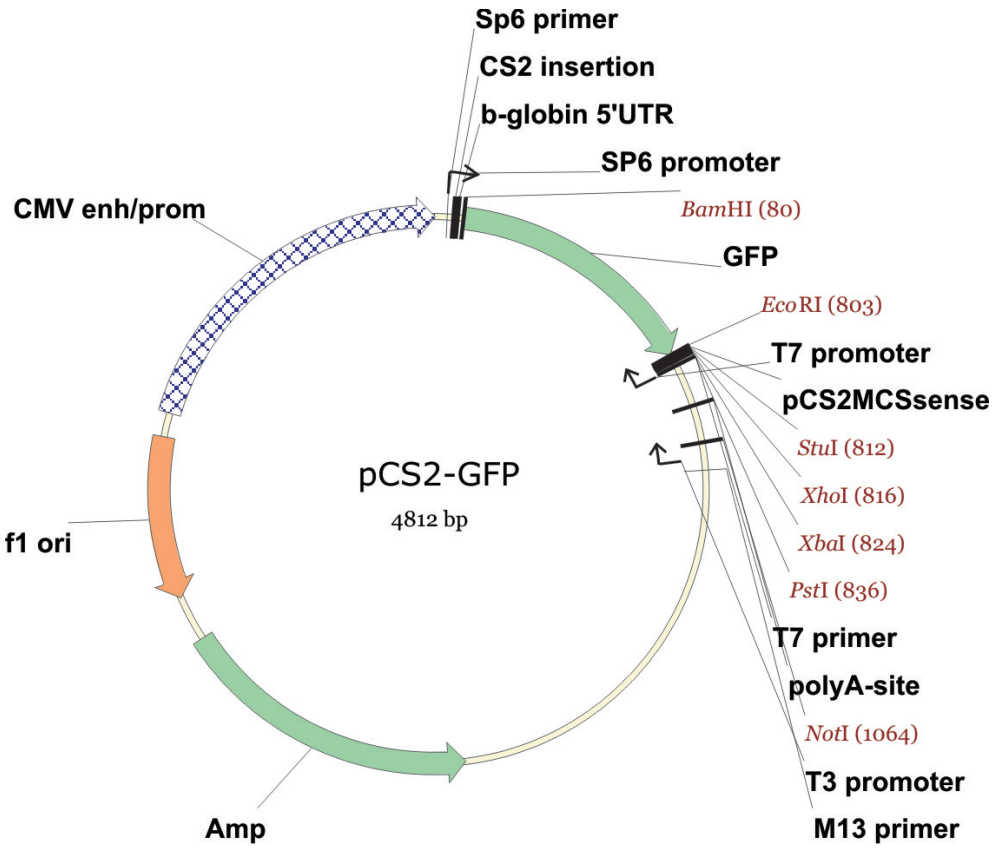

8.3 Abbreviations

RNA	ribonucleic acid
mRNA	messenger RNA
miRNA	microRNA
RNAi	RNA interference
nt	nucleotide
RNP	ribonucleoprotein particle
miRISC	miRNA induced silencing complex
3'UTR	3'-untranslated region
5'UTR	5'-untranslated region
siRNA	small interfering RNA
ORF	open reading frame
pri-miRNA	primary microRNA
pre-miRNA	precursor microRNA
Pol II	RNA polymerase II
RanGTP	Ran guanosine triphosphate
CNS	central nervous system
PNS	peripheral nervous system
RA	retinoic acid
PMN	primary motor neuron
SMN	secondary Motor Neuron
MiP	middle primary motor neuron
RoP	rostral primary motor neuron
CaP	caudal primary motor neuron
ESC	embryonic stem cell
DNA	deoxyribonucleic acid
RE1	repressor element 1
CTD	carboxyl-terminal domain
hpf	hours post fertilization
dpf	day post fertilization
Mo	morpholino
LNA	locked nucleic acid
ml	millilitre
min	minute
M	molar
µg	microgram
RT	room temperature
µl	micro litre
snRNA	small nuclear RNA
cDNA	copy DNA
PCR	polymerase chain reaction
pmol	pico mole
V	volt
H	hour
EtOH	ethanol
MetOH	methanol
mA	milliampere
cm^2	square centimetre
PVDF	polyvinylidene fluoride
NB	Northern blot
WB	Western blot
PFA	paraformaldehyde
DIG	digoxigenin
Flu	fluorescein
NBT	4-nitroblue tetrazolium chloride
BCIP	5-bromo-4-chloro-3-indolyl-phosphate
TUNEL	TdT-mediated dUTP-biotin Nick End labelling
GFP	green fluorescent protein
bp	base pair
rRNA	ribosomal RNA
MBT	midblastula transition
tRNA	transfer RNA

8.4 Erklärung

Hiermit erkläre ich an Eides statt, dass ich die Dissertation

„Functional characterization of the microRNA-26 family in zebrafish neurogenesis“

selbständig angefertigt und keine anderen als die von mir angegebenen Quellen und Hilfsmittel benutzt habe.

Ich erkläre außerdem, dass diese Dissertation weder in gleicher oder anderer Form bereits in einem anderen Prüfungsverfahren vorgelegen hat.

Ich habe früher außer den mit dem Zulassungsgesuch urkundlich vorgelegten Graden keine weiteren akademischen Grade erworben oder zu erwerben versucht.

Würzburg im Januar 2012

Holger Dill

8.5 Lebenslauf

Persönliche Daten

Name:	Holger Dill
Adresse :	Ludwigstraße 21, 97762 Hammelburg
Geburtstag:	07.08.1979 in Würzburg
Familienstand:	ledig

Schulische Ausbildung

1986 – 1990	Grundschule Hammelburg
1990 – 2000	Frobenius-Gymnasium Hammelburg
2000	Allgemeine Hochschulreife

Wehrdienst

2000 – 2001	Grundwehrdienst im Panzerartilleriebataillon 355, Wildflecken

Hochschulstudium

01.10.2001 – 06.02.2007	Studium der Biologie, Julius-Maximilians-Universität Würzburg
24.03.2004	Vordiplom
03.2006 – 01.2007	Diplomarbeit am Institut für Physiologische Chemie 1, Julius-Maximilians-Universität Würzburg
06.02.2007	Diplom
01.2007 – 12.2011	Promotion am Institut für Biochemie, Julius-Maximilians-Universität Würzburg

Teilnahme an wissenschaftlichen Kongressen

14. – 16.09.2006	3rd International PhD Student Symposium – Horizons in Molecular Biology, Göttingen Posterpräsentation
12. – 15.09.2007	4th International PhD Student Symposium – Horizons in Molecular Biology, Göttingen Vortrag
28. – 29.03.2008	4th PRO RETINA Research-Colloquium, Potsdam Posterpräsentation
10. – 13.09.2008	5th International PhD Student Symposium – Horizons in Molecular Biology, Göttingen Posterpräsentation
15. – 19.07.2009	6th European Zebrafish Genetics and Development Meeting, Rom Posterpräsentation
18. – 20.03.2010	EMBL Conference The Complex Life of mRNA – From Synthesis to Decay, Heidelberg
23. – 25.09.2010	8th GfE School, Günzburg

14. – 16.09.2011 Annual Conference of the German Genetics Society, Würzburg
Posterpräsentation

Würzburg im Januar 2012

Holger Dill

8.6 Publications

Thomas Meinhardt, Daniel Lang, Holger Dill and Anke Krüger (2011)
Pushing the Functionality of Diamond Nanoparticles to New Horizons: Orthogonally Functionalized Nanodiamond Using Click Chemistry.
Advanced Functional Materials 21: 494-500

Bastian Linder, Holger Dill, Anja Hirmer, Jan Brocher, Gek Ping Lee, Sinnakaruppan Mathavan, Hanno J. Bolz, Christoph Winkler, Bernhard Laggerbauer and Utz Fischer (2011)
Systemic splicing factor deficiency causes tissue-specific defects: A zebrafish model for Retinitis pigmentosa.
Human Molecular Genetics 20: 368-377

Holger Dill, Bastian Linder, Alexander Fehr and Utz Fischer (2012)
Intronic miR-26b controls neuronal differentiation by repressing its host transcript, *ctdsp2*.
Genes & Development 26: 25-30

Holger Dill, Bastian Linder, Anja Hirmer and Utz Fischer
Analysis of Photoreceptor Degeneration in the Zebrafish *Danio rerio*.
Manuscript in revision

8.7 Danksagung

Ich danke

- Prof. Dr. Utz Fischer für die fachliche Betreuung dieser Arbeit
- Prof. Dr. Dr. Manfred Schartl für seine Tätigkeit als Zweitgutachter dieser Arbeit und für die Erlaubnis die Infrastruktur seines Instituts nutzen zu dürfen
- Prof. Dr. Alexander Buchberger für seine Tätigkeit als dritter Prüfer des Promotionskolloquiums
- Prof. Dr. Christoph Winkler für zahlreiche fachliche Hilfestellungen während der experimentellen Phase dieser Arbeit

- Allen Mitarbeitern des Instituts für Biochemie für die stets angenehme Arbeitsatmosphäre
- Den Diplomanden Anja Hirmer, Alexander Fehr und Bettina Tieg für die konstruktive Mitarbeit an unseren gemeinsamen Projekten
- Thomas Griebel und Claudia Wollny für hilfreiche Kommentare während der Erstellung dieser Arbeit

- Meiner Familie für die Unterstützung während der langen Jahre des Studiums und der Promotion

- Dr. Bettina Kirchmaier dafür, dass du die letzten Jahre, die durchaus sehr nervenaufreibend waren, gemeinsam mit mir durchgestanden hast (auch in einer viel zu kleinen Wohnung und über viele hundert Kilometer der uns trennenden räumlichen Entfernung hinweg)

9 REFERENCES

1. He, X. and M.G. Rosenfeld, *Mechanisms of complex transcriptional regulation: implications for brain development.* Neuron, 1991. **7**(2): p. 183-96.
2. Fire, A., et al., *Potent and specific genetic interference by double-stranded RNA in Caenorhabditis elegans.* Nature, 1998. **391**(6669): p. 806-11.
3. Lee, R.C., R.L. Feinbaum, and V. Ambros, *The C. elegans heterochronic gene lin-4 encodes small RNAs with antisense complementarity to lin-14.* Cell, 1993. **75**(5): p. 843-54.
4. Chen, P.Y. and G. Meister, *microRNA-guided posttranscriptional gene regulation.* Biol Chem, 2005. **386**(12): p. 1205-18.
5. Lim, L.P., et al., *Microarray analysis shows that some microRNAs downregulate large numbers of target mRNAs.* Nature, 2005. **433**(7027): p. 769-73.
6. Meister, G. and T. Tuschl, *Mechanisms of gene silencing by double-stranded RNA.* Nature, 2004. **431**(7006): p. 343-9.
7. Giraldez, A.J., et al., *Zebrafish MiR-430 promotes deadenylation and clearance of maternal mRNAs.* Science, 2006. **312**(5770): p. 75-9.
8. Giraldez, A.J., et al., *MicroRNAs regulate brain morphogenesis in zebrafish.* Science, 2005. **308**(5723): p. 833-8.
9. Woltering, J.M. and A.J. Durston, *MiR-10 represses HoxB1a and HoxB3a in zebrafish.* PLoS One, 2008. **3**(1): p. e1396.
10. He, X., et al., *miR-196 regulates axial patterning and pectoral appendage initiation.* Dev Biol, 2011.
11. Li, N., et al., *Regulation of endoderm formation and left-right asymmetry by miR-92 during early zebrafish development.* Development, 2011. **138**(9): p. 1817-26.
12. Leucht, C., et al., *MicroRNA-9 directs late organizer activity of the midbrain-hindbrain boundary.* Nat Neurosci, 2008. **11**(6): p. 641-8.
13. Li, N., et al., *Dispatched Homolog 2 is targeted by miR-214 through a combination of three weak microRNA recognition sites.* Nucleic Acids Res, 2008. **36**(13): p. 4277-85.
14. Flynt, A.S., et al., *Zebrafish miR-214 modulates Hedgehog signaling to specify muscle cell fate.* Nat Genet, 2007. **39**(2): p. 259-63.
15. Fish, J.E., et al., *miR-126 regulates angiogenic signaling and vascular integrity.* Dev Cell, 2008. **15**(2): p. 272-84.
16. Nicoli, S., et al., *MicroRNA-mediated integration of haemodynamics and Vegf signalling during angiogenesis.* Nature, 2010. **464**(7292): p. 1196-200.
17. Fiedler, J., et al., *MicroRNA-24 Regulates Vascularity After Myocardial Infarction.* Circulation, 2011. **124**(6): p. 720-30.
18. Fish, J.E., et al., *A Slit/miR-218/Robo regulatory loop is required during heart tube formation in zebrafish.* Development, 2011. **138**(7): p. 1409-19.
19. Mishima, Y., et al., *Differential regulation of germline mRNAs in soma and germ cells by zebrafish miR-430.* Curr Biol, 2006. **16**(21): p. 2135-42.
20. Mickoleit, M., T.U. Banisch, and E. Raz, *Regulation of hub mRNA stability and translation by miR430 and the dead end protein promotes preferential expression in zebrafish primordial germ cells.* Dev Dyn, 2011. **240**(3): p. 695-703.
21. Ason, B., et al., *Differences in vertebrate microRNA expression.* Proc Natl Acad Sci U S A, 2006. **103**(39): p. 14385-9.
22. Staton, A.A., H. Knaut, and A.J. Giraldez, *miRNA regulation of Sdf1 chemokine signaling provides genetic robustness to germ cell migration.* Nat Genet, 2011. **43**(3): p. 204-11.
23. Kim, V.N., J. Han, and M.C. Siomi, *Biogenesis of small RNAs in animals.* Nat Rev Mol Cell Biol, 2009. **10**(2): p. 126-39.
24. Hock, J., et al., *Proteomic and functional analysis of Argonaute-containing mRNA-protein complexes in human cells.* EMBO Rep, 2007. **8**(11): p. 1052-60.
25. Meister, G., *miRNAs get an early start on translational silencing.* Cell, 2007. **131**(1): p. 25-8.
26. Bartel, D.P., *MicroRNAs: genomics, biogenesis, mechanism, and function.* Cell, 2004. **116**(2): p. 281-97.

27. Meister, G., et al., *Human Argonaute2 mediates RNA cleavage targeted by miRNAs and siRNAs.* Mol Cell, 2004. **15**(2): p. 185-97.
28. Elbashir, S.M., W. Lendeckel, and T. Tuschl, *RNA interference is mediated by 21- and 22-nucleotide RNAs.* Genes Dev, 2001. **15**(2): p. 188-200.
29. Zdanowicz, A., et al., *Drosophila miR2 primarily targets the m7GpppN cap structure for translational repression.* Mol Cell, 2009. **35**(6): p. 881-8.
30. Liu, J., et al., *MicroRNA-dependent localization of targeted mRNAs to mammalian P-bodies.* Nat Cell Biol, 2005. **7**(7): p. 719-23.
31. Fabian, M.R., et al., *Mammalian miRNA RISC recruits CAF1 and PABP to affect PABP-dependent deadenylation.* Mol Cell, 2009. **35**(6): p. 868-80.
32. Eulalio, A., et al., *Deadenylation is a widespread effect of miRNA regulation.* RNA, 2009. **15**(1): p. 21-32.
33. Rehwinkel, J., et al., *A crucial role for GW182 and the DCP1:DCP2 decapping complex in miRNA-mediated gene silencing.* RNA, 2005. **11**(11): p. 1640-7.
34. Eulalio, A., F. Tritschler, and E. Izaurralde, *The GW182 protein family in animal cells: new insights into domains required for miRNA-mediated gene silencing.* RNA, 2009. **15**(8): p. 1433-42.
35. Kloosterman, W.P., et al., *Substrate requirements for let-7 function in the developing zebrafish embryo.* Nucleic Acids Res, 2004. **32**(21): p. 6284-91.
36. Bartel, D.P., *MicroRNAs: target recognition and regulatory functions.* Cell, 2009. **136**(2): p. 215-33.
37. Lau, N.C., et al., *An abundant class of tiny RNAs with probable regulatory roles in Caenorhabditis elegans.* Science, 2001. **294**(5543): p. 858-62.
38. Lee, R.C. and V. Ambros, *An extensive class of small RNAs in Caenorhabditis elegans.* Science, 2001. **294**(5543): p. 862-4.
39. Lagos-Quintana, M., et al., *Identification of novel genes coding for small expressed RNAs.* Science, 2001. **294**(5543): p. 853-8.
40. Griffiths-Jones, S., *The microRNA Registry.* Nucleic Acids Res, 2004. **32**(Database issue): p. D109-11.
41. Isik, M., H.C. Korswagen, and E. Berezikov, *Expression patterns of intronic microRNAs in Caenorhabditis elegans.* Silence, 2010. **1**(1): p. 5.
42. Lee, Y., et al., *MicroRNA genes are transcribed by RNA polymerase II.* EMBO J, 2004. **23**(20): p. 4051-60.
43. Cai, X., C.H. Hagedorn, and B.R. Cullen, *Human microRNAs are processed from capped, polyadenylated transcripts that can also function as mRNAs.* RNA, 2004. **10**(12): p. 1957-66.
44. Czech, B. and G.J. Hannon, *Small RNA sorting: matchmaking for Argonautes.* Nat Rev Genet, 2011. **12**(1): p. 19-31.
45. Lee, Y., et al., *MicroRNA maturation: stepwise processing and subcellular localization.* EMBO J, 2002. **21**(17): p. 4663-70.
46. Han, J., et al., *Molecular basis for the recognition of primary microRNAs by the Drosha-DGCR8 complex.* Cell, 2006. **125**(5): p. 887-901.
47. Zeng, Y. and B.R. Cullen, *Efficient processing of primary microRNA hairpins by Drosha requires flanking nonstructured RNA sequences.* J Biol Chem, 2005. **280**(30): p. 27595-603.
48. Lee, Y., et al., *The nuclear RNase III Drosha initiates microRNA processing.* Nature, 2003. **425**(6956): p. 415-9.
49. Denli, A.M., et al., *Processing of primary microRNAs by the Microprocessor complex.* Nature, 2004. **432**(7014): p. 231-5.
50. Westholm, J.O. and E.C. Lai, *Mirtrons: microRNA biogenesis via splicing.* Biochimie, 2011. **93**(11): p. 1897-904.
51. Berezikov, E., et al., *Mammalian mirtron genes.* Mol Cell, 2007. **28**(2): p. 328-36.
52. Ruby, J.G., C.H. Jan, and D.P. Bartel, *Intronic microRNA precursors that bypass Drosha processing.* Nature, 2007. **448**(7149): p. 83-6.
53. Lund, E., et al., *Nuclear export of microRNA precursors.* Science, 2004. **303**(5654): p. 95-8.
54. Ketting, R.F., et al., *Dicer functions in RNA interference and in synthesis of small RNA involved in developmental timing in C. elegans.* Genes Dev, 2001. **15**(20): p. 2654-9.
55. Bernstein, E., et al., *Role for a bidentate ribonuclease in the initiation step of RNA interference.* Nature, 2001. **409**(6818): p. 363-6.
56. Hutvagner, G., et al., *A cellular function for the RNA-interference enzyme Dicer in the maturation of the let-7 small temporal RNA.* Science, 2001. **293**(5531): p. 834-8.

57. Packer, A.N., et al., *The bifunctional microRNA miR-9/miR-9* regulates REST and CoREST and is downregulated in Huntington's disease.* J Neurosci, 2008. **28**(53): p. 14341-6.
58. Okamura, K., et al., *The regulatory activity of microRNA* species has substantial influence on microRNA and 3' UTR evolution.* Nat Struct Mol Biol, 2008. **15**(4): p. 354-63.
59. Thomson, J.M., et al., *Extensive post-transcriptional regulation of microRNAs and its implications for cancer.* Genes Dev, 2006. **20**(16): p. 2202-7.
60. Melo, S.A. and M. Esteller, *A precursor microRNA in a cancer cell nucleus: get me out of here!* Cell Cycle, 2011. **10**(6): p. 922-5.
61. Guil, S. and J.F. Caceres, *The multifunctional RNA-binding protein hnRNP A1 is required for processing of miR-18a.* Nat Struct Mol Biol, 2007. **14**(7): p. 591-6.
62. Michlewski, G. and J.F. Caceres, *Antagonistic role of hnRNP A1 and KSRP in the regulation of let-7a biogenesis.* Nat Struct Mol Biol, 2010. **17**(8): p. 1011-8.
63. Michlewski, G., et al., *Posttranscriptional regulation of miRNAs harboring conserved terminal loops.* Mol Cell, 2008. **32**(3): p. 383-93.
64. Brownawell, A.M. and I.G. Macara, *Exportin-5, a novel karyopherin, mediates nuclear export of double-stranded RNA binding proteins.* J Cell Biol, 2002. **156**(1): p. 53-64.
65. Chen, T., A.M. Brownawell, and I.G. Macara, *Nucleocytoplasmic shuttling of JAZ, a new cargo protein for exportin-5.* Mol Cell Biol, 2004. **24**(15): p. 6608-19.
66. Newman, M.A., J.M. Thomson, and S.M. Hammond, *Lin-28 interaction with the Let-7 precursor loop mediates regulated microRNA processing.* RNA, 2008. **14**(8): p. 1539-49.
67. Rybak, A., et al., *A feedback loop comprising lin-28 and let-7 controls pre-let-7 maturation during neural stem-cell commitment.* Nat Cell Biol, 2008. **10**(8): p. 987-93.
68. Heo, I., et al., *TUT4 in concert with Lin28 suppresses microRNA biogenesis through pre-microRNA uridylation.* Cell, 2009. **138**(4): p. 696-708.
69. Trabucchi, M., et al., *The RNA-binding protein KSRP promotes the biogenesis of a subset of microRNAs.* Nature, 2009. **459**(7249): p. 1010-4.
70. Jones, M.R., et al., *Zcchc11-dependent uridylation of microRNA directs cytokine expression.* Nat Cell Biol, 2009. **11**(9): p. 1157-63.
71. Katoh, T., et al., *Selective stabilization of mammalian microRNAs by 3' adenylation mediated by the cytoplasmic poly(A) polymerase GLD-2.* Genes Dev, 2009. **23**(4): p. 433-8.
72. Strahle, U. and P. Blader, *Early neurogenesis in the zebrafish embryo.* FASEB J, 1994. **8**(10): p. 692-8.
73. Lowery, L.A. and H. Sive, *Strategies of vertebrate neurulation and a re-evaluation of teleost neural tube formation.* Mech Dev, 2004. **121**(10): p. 1189-97.
74. Blader, P. and U. Strahle, *Zebrafish developmental genetics and central nervous system development.* Hum Mol Genet, 2000. **9**(6): p. 945-51.
75. Lewis, K.E. and J.S. Eisen, *From cells to circuits: development of the zebrafish spinal cord.* Prog Neurobiol, 2003. **69**(6): p. 419-49.
76. Mendelson, B., *Development of reticulospinal neurons of the zebrafish. I. Time of origin.* J Comp Neurol, 1986. **251**(2): p. 160-71.
77. Jessell, T.M., *Neuronal specification in the spinal cord: inductive signals and transcriptional codes.* Nat Rev Genet, 2000. **1**(1): p. 20-9.
78. Appel, B., *Zebrafish neural induction and patterning.* Dev Dyn, 2000. **219**(2): p. 155-68.
79. Tiso, N., et al., *Differential expression and regulation of olig genes in zebrafish.* J Comp Neurol, 2009. **515**(3): p. 378-96.
80. Lu, Q.R., et al., *Common developmental requirement for Olig function indicates a motor neuron/oligodendrocyte connection.* Cell, 2002. **109**(1): p. 75-86.
81. Rowitch, D.H., et al., *An 'oligarchy' rules neural development.* Trends Neurosci, 2002. **25**(8): p. 417-22.
82. Park, H.C., J. Shin, and B. Appel, *Spatial and temporal regulation of ventral spinal cord precursor specification by Hedgehog signaling.* Development, 2004. **131**(23): p. 5959-69.
83. Park, H.C., et al., *olig2 is required for zebrafish primary motor neuron and oligodendrocyte development.* Dev Biol, 2002. **248**(2): p. 356-68.
84. Jakovcevski, I. and N. Zecevic, *Olig transcription factors are expressed in oligodendrocyte and neuronal cells in human fetal CNS.* J Neurosci, 2005. **25**(44): p. 10064-73.
85. Myers, P.Z., J.S. Eisen, and M. Westerfield, *Development and axonal outgrowth of identified motoneurons in the zebrafish.* J Neurosci, 1986. **6**(8): p. 2278-89.

86. Ericson, J., et al., *Early stages of motor neuron differentiation revealed by expression of homeobox gene Islet-1.* Science, 1992. **256**(5063): p. 1555-60.
87. Hutchinson, S.A. and J.S. Eisen, *Islet1 and Islet2 have equivalent abilities to promote motoneuron formation and to specify motoneuron subtype identity.* Development, 2006. **133**(11): p. 2137-47.
88. Hutchinson, S.A., et al., *Nkx6 proteins specify one zebrafish primary motoneuron subtype by regulating late islet1 expression.* Development, 2007. **134**(9): p. 1671-7.
89. Beattie, C.E., et al., *Temporal separation in the specification of primary and secondary motoneurons in zebrafish.* Dev Biol, 1997. **187**(2): p. 171-82.
90. Sato-Maeda, M., M. Obinata, and W. Shoji, *Position fine-tuning of caudal primary motoneurons in the zebrafish spinal cord.* Development, 2008. **135**(2): p. 323-32.
91. Emery, B., *Regulation of oligodendrocyte differentiation and myelination.* Science, 2010. **330**(6005): p. 779-82.
92. Buckley, C.E., et al., *Temporal dynamics of myelination in the zebrafish spinal cord.* Glia, 2010. **58**(7): p. 802-12.
93. Richardson, W.D., et al., *NG2-glia as multipotent neural stem cells: fact or fantasy?* Neuron, 2011. **70**(4): p. 661-73.
94. Li, H., et al., *Olig1 and Sox10 interact synergistically to drive myelin basic protein transcription in oligodendrocytes.* J Neurosci, 2007. **27**(52): p. 14375-82.
95. Soldati, C., et al., *REST Couples Loss of Pluripotency with Neural Induction and Neural Differentiation.* Stem Cells, 2011.
96. Schoenherr, C.J. and D.J. Anderson, *Silencing is golden: negative regulation in the control of neuronal gene transcription.* Curr Opin Neurobiol, 1995. **5**(5): p. 566-71.
97. Kraner, S.D., et al., *Silencing the type II sodium channel gene: a model for neural-specific gene regulation.* Neuron, 1992. **9**(1): p. 37-44.
98. Mori, N., et al., *A common silencer element in the SCG10 and type II Na+ channel genes binds a factor present in nonneuronal cells but not in neuronal cells.* Neuron, 1992. **9**(1): p. 45-54.
99. Schoenherr, C.J. and D.J. Anderson, *The neuron-restrictive silencer factor (NRSF): a coordinate repressor of multiple neuron-specific genes.* Science, 1995. **267**(5202): p. 1360-3.
100. Chen, Z.F., A.J. Paquette, and D.J. Anderson, *NRSF/REST is required in vivo for repression of multiple neuronal target genes during embryogenesis.* Nat Genet, 1998. **20**(2): p. 136-42.
101. Chong, J.A., et al., *REST: a mammalian silencer protein that restricts sodium channel gene expression to neurons.* Cell, 1995. **80**(6): p. 949-57.
102. Schoenherr, C.J., A.J. Paquette, and D.J. Anderson, *Identification of potential target genes for the neuron-restrictive silencer factor.* Proc Natl Acad Sci U S A, 1996. **93**(18): p. 9881-6.
103. Naruse, Y., et al., *Neural restrictive silencer factor recruits mSin3 and histone deacetylase complex to repress neuron-specific target genes.* Proc Natl Acad Sci U S A, 1999. **96**(24): p. 13691-6.
104. Hakimi, M.A., et al., *A core-BRAF35 complex containing histone deacetylase mediates repression of neuronal-specific genes.* Proc Natl Acad Sci U S A, 2002. **99**(11): p. 7420-5.
105. Lunyak, V.V., et al., *Corepressor-dependent silencing of chromosomal regions encoding neuronal genes.* Science, 2002. **298**(5599): p. 1747-52.
106. Nan, X., et al., *Transcriptional repression by the methyl-CpG-binding protein MeCP2 involves a histone deacetylase complex.* Nature, 1998. **393**(6683): p. 386-9.
107. Jones, P.L., et al., *Methylated DNA and MeCP2 recruit histone deacetylase to repress transcription.* Nat Genet, 1998. **19**(2): p. 187-91.
108. Andres, M.E., et al., *CoREST: a functional corepressor required for regulation of neural-specific gene expression.* Proc Natl Acad Sci U S A, 1999. **96**(17): p. 9873-8.
109. Lee, M.G., et al., *An essential role for CoREST in nucleosomal histone 3 lysine 4 demethylation.* Nature, 2005. **437**(7057): p. 432-5.
110. Yeo, M., et al., *Small CTD phosphatases function in silencing neuronal gene expression.* Science, 2005. **307**(5709): p. 596-600.
111. Oelgeschlager, T., *Regulation of RNA polymerase II activity by CTD phosphorylation and cell cycle control.* J Cell Physiol, 2002. **190**(2): p. 160-9.
112. Egloff, S. and S. Murphy, *Cracking the RNA polymerase II CTD code.* Trends Genet, 2008. **24**(6): p. 280-8.
113. Thompson, J., et al., *Small carboxyl-terminal domain phosphatase 2 attenuates androgen-dependent transcription.* EMBO J, 2006. **25**(12): p. 2757-67.

114. Yeo, M., et al., *A novel RNA polymerase II C-terminal domain phosphatase that preferentially dephosphorylates serine 5.* J Biol Chem, 2003. **278**(28): p. 26078-85.
115. Visvanathan, J., et al., *The microRNA miR-124 antagonizes the anti-neural REST/SCP1 pathway during embryonic CNS development.* Genes Dev, 2007. **21**(7): p. 744-9.
116. Palm, K., et al., *Neuronal expression of zinc finger transcription factor REST/NRSF/XBR gene.* J Neurosci, 1998. **18**(4): p. 1280-96.
117. Conaco, C., et al., *Reciprocal actions of REST and a microRNA promote neuronal identity.* Proc Natl Acad Sci U S A, 2006. **103**(7): p. 2422-7.
118. Ballas, N., et al., *REST and its corepressors mediate plasticity of neuronal gene chromatin throughout neurogenesis.* Cell, 2005. **121**(4): p. 645-57.
119. Singh, A., et al., *Retinoic acid induces REST degradation and neuronal differentiation by modulating the expression of SCF(beta-TRCP) in neuroblastoma cells.* Cancer, 2011. **117**(22): p. 5189-202.
120. Yu, H.B., et al., *Coassembly of REST and its cofactors at sites of gene repression in embryonic stem cells.* Genome Res, 2011. **21**(8): p. 1284-93.
121. Xie, X.H. and J. Wu, *Comparative sequence analysis reveals an intricate network among REST, CREB and miRNA in mediating neuronal gene expression.* Genome Biology, 2006. **7**(9).
122. Klein, M.E., et al., *Homeostatic regulation of MeCP2 expression by a CREB-induced microRNA.* Nat Neurosci, 2007. **10**(12): p. 1513-4.
123. Yoo, A.S., et al., *MicroRNA-mediated conversion of human fibroblasts to neurons.* Nature, 2011. **476**(7359): p. 228-31.
124. Chi, S.W., et al., *Argonaute HITS-CLIP decodes microRNA-mRNA interaction maps.* Nature, 2009. **460**(7254): p. 479-86.
125. Qureshi, I.A. and M.F. Mehler, *Regulation of non-coding RNA networks in the nervous system--what's the REST of the story?* Neurosci Lett, 2009. **466**(2): p. 73-80.
126. Kim, Y.K. and V.N. Kim, *Processing of intronic microRNAs.* EMBO J, 2007. **26**(3): p. 775-83.
127. Chang, T.C., et al., *Widespread microRNA repression by Myc contributes to tumorigenesis.* Nat Genet, 2008. **40**(1): p. 43-50.
128. Zhu, Y., et al., *MicroRNA-26a/b and their host genes cooperate to inhibit the G1/S transition by activating the pRb protein.* Nucleic Acids Res, 2011.
129. Monteys, A.M., et al., *Structure and activity of putative intronic miRNAs promoters.* RNA, 2010.
130. Bak, M., et al., *MicroRNA expression in the adult mouse central nervous system.* RNA, 2008. **14**(3): p. 432-44.
131. Radfar, M.H., W. Wong, and Q. Morris, *Computational prediction of intronic microRNA targets using host gene expression reveals novel regulatory mechanisms.* PLoS One, 2011. **6**(6): p. e19312.
132. Xu, N., et al., *MicroRNA-145 regulates OCT4, SOX2, and KLF4 and represses pluripotency in human embryonic stem cells.* Cell, 2009. **137**(4): p. 647-58.
133. Houbaviy, H.B., M.F. Murray, and P.A. Sharp, *Embryonic stem cell-specific MicroRNAs.* Dev Cell, 2003. **5**(2): p. 351-8.
134. Rosa, A., F.M. Spagnoli, and A.H. Brivanlou, *The miR-430/427/302 family controls mesendodermal fate specification via species-specific target selection.* Dev Cell, 2009. **16**(4): p. 517-27.
135. Huang, B., et al., *MicroRNA expression profiling during neural differentiation of mouse embryonic carcinoma P19 cells.* Acta Biochim Biophys Sin (Shanghai), 2009. **41**(3): p. 231-6.
136. Dostie, J., et al., *Numerous microRNPs in neuronal cells containing novel microRNAs.* RNA, 2003. **9**(2): p. 180-6.
137. Smirnova, L., et al., *Regulation of miRNA expression during neural cell specification.* Eur J Neurosci, 2005. **21**(6): p. 1469-77.
138. Watanabe, T., et al., *Stage-specific expression of microRNAs during Xenopus development.* FEBS Lett, 2005. **579**(2): p. 318-24.
139. Wienholds, E., et al., *MicroRNA expression in zebrafish embryonic development.* Science, 2005. **309**(5732): p. 310-1.
140. Chen, P.Y., et al., *The developmental miRNA profiles of zebrafish as determined by small RNA cloning.* Genes Dev, 2005. **19**(11): p. 1288-93.
141. Wienholds, E., et al., *The microRNA-producing enzyme Dicer1 is essential for zebrafish development.* Nat Genet, 2003. **35**(3): p. 217-8.
142. Lagos-Quintana, M., et al., *Identification of tissue-specific microRNAs from mouse.* Curr Biol, 2002. **12**(9): p. 735-9.

143. Zhang, Z., et al., *MicroRNAs regulate pituitary development, and microRNA 26b specifically targets lymphoid enhancer factor 1 (Lef-1), which modulates pituitary transcription factor 1 (Pit-1) expression.* J Biol Chem, 2010. **285**(45): p. 34718-28.
144. Wong, C.F. and R.L. Tellam, *MicroRNA-26a targets the histone methyltransferase Enhancer of Zeste homolog 2 during myogenesis.* J Biol Chem, 2008. **283**(15): p. 9836-43.
145. Lu, J., et al., *MiR-26a Inhibits Cell Growth and Tumorigenesis of Nasopharyngeal Carcinoma through Repression of EZH2.* Cancer Res, 2011. **71**(1): p. 225-233.
146. Sander, S., et al., *MYC stimulates EZH2 expression by repression of its negative regulator miR-26a.* Blood, 2008. **112**(10): p. 4202-12.
147. Kota, J., et al., *Therapeutic microRNA delivery suppresses tumorigenesis in a murine liver cancer model.* Cell, 2009. **137**(6): p. 1005-17.
148. Ji, Y., et al., *MiRNA-26b regulates the expression of cyclooxygenase-2 in desferrioxamine-treated CNE cells.* FEBS Lett, 2010. **584**(5): p. 961-7.
149. Beitzinger, M., et al., *Identification of human microRNA targets from isolated argonaute protein complexes.* RNA Biol, 2007. **4**(2): p. 76-84.
150. Koensgen, D., et al., *Expression analysis and RNA localization of PAI-RBP1 (SERBP1) in epithelial ovarian cancer: association with tumor progression.* Gynecol Oncol, 2007. **107**(2): p. 266-73.
151. Gennarino, V.A., et al., *MicroRNA target prediction by expression analysis of host genes.* Genome Res, 2009. **19**(3): p. 481-90.
152. Liu, X.X., et al., *MicroRNA-26b is underexpressed in human breast cancer and induces cell apoptosis by targeting SLC7A11.* FEBS Lett, 2011. **585**(9): p. 1363-7.
153. Hu, G., et al., *MTDH activation by 8q22 genomic gain promotes chemoresistance and metastasis of poor-prognosis breast cancer.* Cancer Cell, 2009. **15**(1): p. 9-20.
154. Huse, J.T., et al., *The PTEN-regulating microRNA miR-26a is amplified in high-grade glioma and facilitates gliomagenesis in vivo.* Genes Dev, 2009. **23**(11): p. 1327-37.
155. Lewis, B.P., et al., *Prediction of mammalian microRNA targets.* Cell, 2003. **115**(7): p. 787-98.
156. Leeper, N.J., et al., *MicroRNA-26a is a novel regulator of vascular smooth muscle cell function.* J Cell Physiol, 2011. **226**(4): p. 1035-43.
157. Canalis, E., A.N. Economides, and E. Gazzerro, *Bone morphogenetic proteins, their antagonists, and the skeleton.* Endocr Rev, 2003. **24**(2): p. 218-35.
158. Lopez, P., et al., *Gene control in germinal differentiation: RNF6, a transcription regulatory protein in the mouse sertoli cell.* Mol Cell Biol, 2002. **22**(10): p. 3488-96.
159. Meng, A., et al., *Promoter analysis in living zebrafish embryos identifies a cis-acting motif required for neuronal expression of GATA-2.* Proc Natl Acad Sci U S A, 1997. **94**(12): p. 6267-72.
160. Kimmel, C.B., et al., *Stages of embryonic development of the zebrafish.* Dev Dyn, 1995. **203**(3): p. 253-310.
161. Rupp, R.A., L. Snider, and H. Weintraub, *Xenopus embryos regulate the nuclear localization of XMyoD.* Genes Dev, 1994. **8**(11): p. 1311-23.
162. van Houten, V., et al., *Labeling efficiency of oligonucleotides by T4 polynucleotide kinase depends on 5'-nucleotide.* Anal Biochem, 1998. **265**(2): p. 386-9.
163. Salles, F.J., W.G. Richards, and S. Strickland, *Assaying the polyadenylation state of mRNAs.* Methods, 1999. **17**(1): p. 38-45.
164. Rehmsmeier, M., et al., *Fast and effective prediction of microRNA/target duplexes.* RNA, 2004. **10**(10): p. 1507-17.
165. Rehmsmeier, M., *Prediction of microRNA targets.* Methods Mol Biol, 2006. **342**: p. 87-99.
166. Leuschner, P.J. and J. Martinez, *In vitro analysis of microRNA processing using recombinant Dicer and cytoplasmic extracts of HeLa cells.* Methods, 2007. **43**(2): p. 105-9.
167. Fehr, A., *Funktionelle Analyse der MicroRNA-Familie 26 während der neuronalen Entwicklung des Zebrafisches (Danio rerio)*. 2009, Department of Biochemistry: Wuerzburg.
168. Siomi, H. and M.C. Siomi, *Posttranscriptional regulation of microRNA biogenesis in animals.* Mol Cell, 2010. **38**(3): p. 323-32.
169. Jones-Villeneuve, E.M., et al., *Retinoic acid induces embryonal carcinoma cells to differentiate into neurons and glial cells.* J Cell Biol, 1982. **94**(2): p. 253-62.
170. McBurney, M.W., *P19 embryonal carcinoma cells.* Int J Dev Biol, 1993. **37**(1): p. 135-40.
171. Kloosterman, W.P., et al., *Targeted inhibition of miRNA maturation with morpholinos reveals a role for miR-375 in pancreatic islet development.* PLoS Biol, 2007. **5**(8): p. e203.

172. Fanarraga, M.L., J. Avila, and J.C. Zabala, *Expression of unphosphorylated class III beta-tubulin isotype in neuroepithelial cells demonstrates neuroblast commitment and differentiation.* Eur J Neurosci, 1999. **11**(2): p. 517-27.
173. Katsetos, C.D., et al., *Class III beta-tubulin isotype: a key cytoskeletal protein at the crossroads of developmental neurobiology and tumor neuropathology.* J Child Neurol, 2003. **18**(12): p. 851-66; discussion 867.
174. Shkumatava, A., et al., *Coherent but overlapping expression of microRNAs and their targets during vertebrate development.* Genes Dev, 2009. **23**(4): p. 466-81.
175. Thisse, B., et al., *Spatial and temporal expression of the zebrafish genome by large-scale in situ hybridization screening.* Methods Cell Biol, 2004. **77**: p. 505-19.
176. Pineda, R.H., et al., *Knockdown of Nav1.6a Na+ channels affects zebrafish motoneuron development.* Development, 2006. **133**(19): p. 3827-36.
177. Saint-Amant, L. and P. Drapeau, *Time course of the development of motor behaviors in the zebrafish embryo.* J Neurobiol, 1998. **37**(4): p. 622-32.
178. Grimson, A., et al., *MicroRNA targeting specificity in mammals: determinants beyond seed pairing.* Mol Cell, 2007. **27**(1): p. 91-105.
179. Lund, E., et al., *Deadenylation of maternal mRNAs mediated by miR-427 in Xenopus laevis embryos.* RNA, 2009. **15**(12): p. 2351-63.
180. Tsang, J., J. Zhu, and A. van Oudenaarden, *MicroRNA-mediated feedback and feedforward loops are recurrent network motifs in mammals.* Mol Cell, 2007. **26**(5): p. 753-67.
181. Martello, G., et al., *MicroRNA control of Nodal signalling.* Nature, 2007. **449**(7159): p. 183-8.
182. Obernosterer, G., et al., *Post-transcriptional regulation of microRNA expression.* RNA, 2006. **12**(7): p. 1161-7.
183. Hwang, H.W., E.A. Wentzel, and J.T. Mendell, *A hexanucleotide element directs microRNA nuclear import.* Science, 2007. **315**(5808): p. 97-100.
184. Herranz, H. and S.M. Cohen, *MicroRNAs and gene regulatory networks: managing the impact of noise in biological systems.* Genes Dev, 2010. **24**(13): p. 1339-44.
185. Han, J., A.M. Denli, and F.H. Gage, *The enemy within: intronic miR-26b represses its host gene, ctdsp2, to regulate neurogenesis.* Genes Dev, 2012. **26**(1): p. 6-10.
186. Zhao, X.F., et al., *Treatment with small interfering RNA affects the microRNA pathway and causes unspecific defects in zebrafish embryos.* FEBS J, 2008. **275**(9): p. 2177-84.
187. Fjose, A. and X.F. Zhao, *Exploring microRNA functions in zebrafish.* N Biotechnol, 2010. **27**(3): p. 250-5.
188. Fjose, A. and X.F. Zhao, *Inhibition of the microRNA pathway in zebrafish by siRNA.* Methods Mol Biol, 2010. **629**: p. 239-55.
189. Robu, M.E., et al., *p53 activation by knockdown technologies.* PLoS Genet, 2007. **3**(5): p. e78.
190. Zhao, X., et al., *MicroRNA-mediated control of oligodendrocyte differentiation.* Neuron, 2010. **65**(5): p. 612-26.
191. Lau, P., et al., *Identification of dynamically regulated microRNA and mRNA networks in developing oligodendrocytes.* J Neurosci, 2008. **28**(45): p. 11720-30.
192. Letzen, B.S., et al., *MicroRNA expression profiling of oligodendrocyte differentiation from human embryonic stem cells.* PLoS One, 2010. **5**(5): p. e10480.
193. Bueno, M.J. and M. Malumbres, *MicroRNAs and the cell cycle.* Biochim Biophys Acta, 2011. **1812**(5): p. 592-601.
194. Liu, X., et al., *MicroRNA profiling and head and neck cancer.* Comp Funct Genomics, 2009: p. 837514.
195. Wong, T.S., et al., *Mature miR-184 as Potential Oncogenic microRNA of Squamous Cell Carcinoma of Tongue.* Clin Cancer Res, 2008. **14**(9): p. 2588-92.
196. Heinzelmann, J., et al., *Specific miRNA signatures are associated with metastasis and poor prognosis in clear cell renal cell carcinoma.* World J Urol, 2011. **29**(3): p. 367-73.
197. Chen, L., et al., *Tumor-specific Expression of MicroRNA-26a Suppresses Human Hepatocellular Carcinoma Growth via Cyclin-dependent and -independent Pathways.* Mol Ther, 2011.
198. Kim, H., et al., *Integrative genome analysis reveals an oncomir/oncogene cluster regulating glioblastoma survivorship.* Proc Natl Acad Sci U S A, 2010. **107**(5): p. 2183-8.
199. Salvatori, B., et al., *Critical Role of c-Myc in Acute Myeloid Leukemia Involving Direct Regulation of miR-26a and Histone Methyltransferase EZH2.* Genes Cancer, 2011. **2**(5): p. 585-92.
200. Barik, S., *An intronic microRNA silences genes that are functionally antagonistic to its host gene.* Nucleic Acids Res, 2008. **36**(16): p. 5232-41.

201. Small, E.M., et al., *MicroRNA-218 regulates vascular patterning by modulation of Slit-Robo signaling.* Circ Res, 2010. **107**(11): p. 1336-44.
202. van Rooij, E., et al., *A family of microRNAs encoded by myosin genes governs myosin expression and muscle performance.* Dev Cell, 2009. **17**(5): p. 662-73.
203. Zhou, D., et al., *Genome-wide computational analyses of microRNAs and their targets from Canis familiaris.* Comput Biol Chem, 2008. **32**(1): p. 60-5.
204. Raj, A. and A. van Oudenaarden, *Nature, nurture, or chance: stochastic gene expression and its consequences.* Cell, 2008. **135**(2): p. 216-26.
205. Yeo, M., et al., *Novel repression of Kcc2 transcription by REST-RE-1 controls developmental switch in neuronal chloride.* J Neurosci, 2009. **29**(46): p. 14652-62.
206. Shimojo, M., *RE1-silencing transcription factor (REST) and REST-interacting LIM domain protein (RILP) affect P19CL6 differentiation.* Genes Cells, 2011. **16**(1): p. 90-100.
207. Westbrook, T.F., et al., *A genetic screen for candidate tumor suppressors identifies REST.* Cell, 2005. **121**(6): p. 837-48.
208. Kuwabara, T., et al., *A small modulatory dsRNA specifies the fate of adult neural stem cells.* Cell, 2004. **116**(6): p. 779-93.
209. Yamasaki, Y., et al., *Robust specification of sensory neurons by dual functions of charlatan, a Drosophila NRSF/REST-like repressor of extramacrochaetae and hairy.* Genes Cells, 2011. **16**(8): p. 896-909.
210. Cunliffe, V.T., *Histone deacetylase 1 is required to repress Notch target gene expression during zebrafish neurogenesis and to maintain the production of motoneurones in response to hedgehog signalling.* Development, 2004. **131**(12): p. 2983-95.
211. Cunliffe, V.T. and P. Casaccia-Bonnefil, *Histone deacetylase 1 is essential for oligodendrocyte specification in the zebrafish CNS.* Mech Dev, 2006. **123**(1): p. 24-30.
212. Sapkota, G., et al., *Dephosphorylation of the linker regions of Smad1 and Smad2/3 by small C-terminal domain phosphatases has distinct outcomes for bone morphogenetic protein and transforming growth factor-beta pathways.* J Biol Chem, 2006. **281**(52): p. 40412-9.
213. Wrighton, K.H., et al., *Small C-terminal domain phosphatases dephosphorylate the regulatory linker regions of Smad2 and Smad3 to enhance transforming growth factor-beta signaling.* J Biol Chem, 2006. **281**(50): p. 38365-75.
214. Kokabu, S., et al., *Suppression of BMP-Smad signaling axis-induced osteoblastic differentiation by small C-terminal domain phosphatase 1, a Smad phosphatase.* Mol Endocrinol, 2011. **25**(3): p. 474-81.
215. Knockaert, M., et al., *Unique players in the BMP pathway: small C-terminal domain phosphatases dephosphorylate Smad1 to attenuate BMP signaling.* Proc Natl Acad Sci U S A, 2006. **103**(32): p. 11940-5.
216. Ma, Y.L., et al., *Human embryonic stem cells and metastatic colorectal cancer cells shared the common endogenous human microRNA-26b.* J Cell Mol Med, 2011. **15**(9): p. 1941-54.
217. Kedde, M., et al., *RNA-binding protein Dnd1 inhibits microRNA access to target mRNA.* Cell, 2007. **131**(7): p. 1273-86.
218. Koebernick, K., et al., *Elr-type proteins protect Xenopus Dead end mRNA from miR-18-mediated clearance in the soma.* Proc Natl Acad Sci U S A, 2010. **107**(37): p. 16148-53.
219. Chen, D., et al., *Plant siRNAs from introns mediate DNA methylation of host genes.* RNA, 2011. **17**(6): p. 1012-24.
220. Lee, E.J., et al., *Systematic evaluation of microRNA processing patterns in tissues, cell lines, and tumors.* RNA, 2008. **14**(1): p. 35-42.
221. Anthony, K. and J.M. Gallo, *Aberrant RNA processing events in neurological disorders.* Brain Res, 2010. **1338**: p. 67-77.
222. Berson, E.L., *Retinitis pigmentosa: unfolding its mystery.* Proc Natl Acad Sci U S A, 1996. **93**(10): p. 4526-8.
223. Hartong, D.T., E.L. Berson, and T.P. Dryja, *Retinitis pigmentosa.* Lancet, 2006. **368**(9549): p. 1795-809.
224. Daiger, S.P., S.J. Bowne, and L.S. Sullivan, *Perspective on genes and mutations causing retinitis pigmentosa.* Arch Ophthalmol, 2007. **125**(2): p. 151-8.
225. Chakarova, C.F., et al., *Mutations in HPRP3, a third member of pre-mRNA splicing factor genes, implicated in autosomal dominant retinitis pigmentosa.* Hum Mol Genet, 2002. **11**(1): p. 87-92.
226. McKie, A.B., et al., *Mutations in the pre-mRNA splicing factor gene PRPC8 in autosomal dominant retinitis pigmentosa (RP13).* Hum Mol Genet, 2001. **10**(15): p. 1555-62.

227. Vithana, E.N., et al., *A human homolog of yeast pre-mRNA splicing gene, PRP31, underlies autosomal dominant retinitis pigmentosa on chromosome 19q13.4 (RP11).* Mol Cell, 2001. **8**(2): p. 375-81.
228. Liu, S., et al., *The network of protein-protein interactions within the human U4/U6.U5 tri-snRNP.* RNA, 2006. **12**(7): p. 1418-30.
229. Wahl, M.C., C.L. Will, and R. Luhrmann, *The spliceosome: design principles of a dynamic RNP machine.* Cell, 2009. **136**(4): p. 701-18.
230. Ray, P., et al., *The splicing factor Prp31 is essential for photoreceptor development in Drosophila.* Protein Cell, 2010. **1**(3): p. 267-74.
231. Graziotto, J.J., et al., *Three gene-targeted mouse models of RNA splicing factor RP show late-onset RPE and retinal degeneration.* Invest Ophthalmol Vis Sci, 2011. **52**(1): p. 190-8.
232. Tanackovic, G., et al., *PRPF mutations are associated with generalized defects in spliceosome formation and pre-mRNA splicing in patients with retinitis pigmentosa.* Hum Mol Genet. **20**(11): p. 2116-30.
233. Nasevicius, A. and S.C. Ekker, *Effective targeted gene 'knockdown' in zebrafish.* Nat Genet, 2000. **26**(2): p. 216-20.
234. Bilotta, J. and S. Saszik, *The zebrafish as a model visual system.* Int J Dev Neurosci, 2001. **19**(7): p. 621-9.
235. Leung, Y.F. and J.E. Dowling, *Gene expression profiling of zebrafish embryonic retina.* Zebrafish, 2005. **2**(4): p. 269-83.
236. Graziotto, J.J., et al., *Decreased levels of the RNA splicing factor Prpf3 in mice and zebrafish do not cause photoreceptor degeneration.* Invest Ophthalmol Vis Sci, 2008. **49**(9): p. 3830-8.
237. Winkler, C., et al., *Reduced U snRNP assembly causes motor axon degeneration in an animal model for spinal muscular atrophy.* Genes Dev, 2005. **19**(19): p. 2320-30.
238. Linder, B., et al., *Systemic splicing factor deficiency causes tissue-specific defects: a zebrafish model for retinitis pigmentosa.* Hum Mol Genet, 2011. **20**(2): p. 368-77.
239. Dill, H., *Functional analysis of PRP8 and PRP31 in a zebrafish model for Retinitis pigmentosa*. 2007, Department of Physiological Chemistry 1: Wuerzburg.
240. Yin, J., et al., *Mutant Prpf31 causes pre-mRNA splicing defects and rod photoreceptor cell degeneration in a zebrafish model for Retinitis pigmentosa.* Mol Neurodegener. **6**: p. 56.